Titre: Title:	Infinite-Dimensional Modelling and Control of a MEMS Deformable Mirror with Applications in Adaptive Optics
Auteur: Author:	Amir Badkoubeh-Hazave
Date:	2015
Type:	Mémoire ou thèse / Dissertation or Thesis
Référence: Citation:	Badkoubeh-Hazave, A. (2015). Infinite-Dimensional Modelling and Control of a MEMS Deformable Mirror with Applications in Adaptive Optics [Thèse de doctorat, École Polytechnique de Montréal]. PolyPublie. https://publications.polymtl.ca/1922/

Document en libre accès dans PolyPublie
Open Access document in PolyPublie

URL de PolyPublie: PolyPublie URL:	https://publications.polymtl.ca/1922/
Directeurs de recherche: Advisors:	Guchuan Zhu
Programme: Program:	génie électrique

UNIVERSITÉ DE MONTRÉAL

INFINITE-DIMENSIONAL MODELLING AND CONTROL OF A MEMS
DEFORMABLE MIRROR WITH APPLICATIONS IN ADAPTIVE OPTICS

AMIR BADKOUBEH-HAZAVE
DÉPARTEMENT DE GÉNIE ÉLECTRIQUE
ÉCOLE POLYTECHNIQUE DE MONTRÉAL

UNIVERSITÉ DE MONTRÉAL

ÉCOLE POLYTECHNIQUE DE MONTRÉAL

Cette thèse intitulée :

INFINITE-DIMENSIONAL MODELLING AND CONTROL OF A MEMS
DEFORMABLE MIRROR WITH APPLICATIONS IN ADAPTIVE OPTICS

présentée par : BADKOUBEH-HAZAVE Amir
en vue de l'obtention du diplôme de : Philosophiæ Doctor
a été dûment acceptée par le jury d'examen constitué de :

M. SAYDY Lahcen, Ph. D., président
M. ZHU Guchuan, Ph. D., membre et directeur de recherche
M. DELFOUR Michel, Ph. D., membre
M. PARANJAPE Aditya, Ph. D., membre externe

DEDICATION

You are not a drop in the ocean.
You are the entire ocean, in a drop. . . .
Rumi

ACKNOWLEDGEMENTS

RÉSUMÉ

Le contrôle de déformation est un problème émergent dans les micro structures intelligentes. Une des applications type est le contrôle de la déformation de miroirs dans l'optique adaptative dans laquelle on oriente la face du miroir selon une géométrie précise en utilisant une gamme de micro-vérins afin d'éliminer la distortion lumineuse. Dans cette thèse, le problème de la conception du contrôle du suivi est considéré directement avec les modèles décrits par des équations aux dérivées partielles définies dans l'espace de dimension infinie. L'architecture du contrôleur proposée se base sur la stabilisation par retour des variables et le suivi des trajectoires utilisant la théorie des systèmes différentiellement plats. La combinaison de la commande par rétroaction et la planification des trajectoires permet de réduire la complexité de la structure du contrôleur pour que ce dernier puisse être implémentée dans les microsystèmes avec les techniques disponibles de nos jours. Pour aboutir à une architecture implémentable dans les applications en temps réel, la fonction de Green est considérée comme une fonction de test pour concevoir le contrôleur et pour représenter les trajectoires de référence dans la planification de mouvements.

ABSTRACT

Deformation control is an emerging problem for micro-smart structures. One of its exciting applications is the control of deformable mirrors in adaptive optics systems, in which the mirror face-sheet is steered to a desired shape using an array of micro-actuators in order to remove light distortions. This technology is an enabling key for the forthcoming extremely large ground-based telescopes. Large-scale deformable mirrors typically exhibit complex dynamical behaviors mostly due to micro-actuators distributed in the domain of the system which in particular complicates control design.

A model of this device may be described by a fourth-order in space/second-order in time partial differential equation for the mirror face-sheet with Dirac delta functions located in the domain of the system to represent the micro-actuators. Most of control design methods dealing with partial differential equations are performed on lumped models, which often leads to high-dimensional and complex feedback control structures. Furthermore, control designs achieved based on partial differential equation models correspond to boundary control problems.

In this thesis, a tracking control scheme is designed directly based on the infinite-dimensional model of the system. The control scheme is introduced based on establishing a relationship between the original nonhomogeneous model and a target system in a standard boundary control form. Thereby, the existing boundary control methods may be applicable. For the control design, we apply the tool of differential flatness to a partial differential equation system controlled by multiple actuators, which is essentially a multiple-input multiple-output partial differential equation problem. To avoid early lumping in the motion planning, we use the properties of the Green's function of the system to represent the reference trajectories. A finite set of these functions is considered to establish a one-to-one map between the input space and output space. This allows an implementable scheme for real-time applications. Since pure feedforward control is only applicable for perfectly known, and stable systems, feedback control is required to account for instability, model uncertainties, and disturbances. Hence, a stabilizing feedback is designed to stabilize the system around the reference trajectories. The combination of differential flatness for motion planning and stabilizing feedback provides a systematic control scheme suitable for the real-time applications of large-scale deformable mirrors.

TABLE OF CONTENTS

LIST OF FIGURES

LIST OF SYMBOLS AND ABBREVIATIONS

AO	Adaptive Optics
ARE	Algebraic Riccati Equation
DM	Deformable Mirror
DOF	Degree of Freedom
FFT	Fast Fourier Transform
LQR	Linear-Quadratic Regulator
MEMS	Microelectromechanical Systems
MIMO	Multiple-Input Multiple-Output
ODE	Ordinary Differential Equation
PDE	Partial Differential Equation
RBF	Radial-Based Functions
1D	One-Dimensional
2D	Two-Dimensional
C_0-semigroup	Strongly Continuous Semigroup
$\mathbb{R}$	The field of all real numbers
$\mathbb{C}$	The filed of all complex numbers
$\mathbb{R}^n$	The $n-$dimentional Euclidean space
Ω	A nonempty open subset of $\mathbb{R}^n$
$\partial\Omega$	The boundary of Ω
$\bar{\Omega}$	The closure of Ω
$L(X, Z)$	Set of continuous linear map L between two Hilbert spaces Z and X
H	A Hilbert space
$L^p(\Omega)$	p-integrable functions
$C^m(\Omega)$	The space of m-times boundedly continuously differentiable function from Ω into H
$H^m(\Omega)$	The Sobolev space of order m
w_x	The derivatives of $w(x, t)$ with respect to x
w_t	The derivatives of $w(x, t)$ with respect to t
$S(t)$	C_0-semigroup
$\mathcal{D}(A)$	Domain of the operator A
$\Sigma(A, B)$	The dynamic system with the system matrix A and the input operator B
$\delta(x, \xi)$	Dirac delta function, or impulse function concentrated at the point ξ

$G(x, \xi)$ Green's function

$\varphi(x, \xi)$ Blob function centered at the point ξ

$\tilde{G}(x, \xi)$ Regularized Green's function

CHAPTER 1

INTRODUCTION

We begin this chapter by introducing the deformable mirrors in the context of adaptive optics, AO, and the necessity to deal with the infinite-dimensional control of this device in this context. In Section 1.3 we review the pertinent control methods in this realm. Section 1.4 explains the challenges associated with partial differential equation, PDE, based control designs for the deformable mirrors. Then, Section 1.5, and 1.6 outline the motivation, objectives, and our treatment strategy in this research work. The original contributions of this work are also summarized in Section 1.6. We conclude this chapter by mentioning the organization of this thesis in Section 1.7.

1.1 Deformable Mirrors in the Context of Adaptive Optics systems

Deformable mirrors are key elements for enhancing the performance of optical systems and have been used in many different applications including: free space laser communications [105], [100], retinal imaging [33], biological microscopy [96], and ground-based telescopes [20, 31]. However, despite many similarities, each of these applications has unique features which requires specific insights into the system and specialized techniques. In this research, we mainly focus on the application of deformable mirrors in ground-based telescopes.

The deformable mirrors in this context are intended to remove the distortion of light due to earth atmosphere turbulence. Because atmospheric turbulence is a dynamic phenomenon, the adaptive optics system needs to be sufficiently fast. The sampling times in this application can amount to 0.5 [ms]. Given this sampling time, the high frequency modes of the deformable mirrors can be excited, and thus these devices cannot be considered as static systems [83, 44]. Hence, the control methods developed in other applications based on static models of a deformable mirror, the so-called open-loop control, cannot meet this requirement [108, 98, 21, 85, 100, 36, 32].

On the other hand, the design methods for dynamic control of this device leading to a control structure that requires a considerable number of on-chip sensors for the implementation of closed-loop control are not applicable to microsystems with currently available technologies [44, 6, 59, 83, 77].

Another vital issue is the precision. The high resolution performance of an adaptive optics system is strongly tied to the precise control of its deformable mirror. The displacement

range of a deformable mirrors surface is in micro-meters, and thus an acceptable tracking error should be at least ten times smaller than this range. According to this level of precision, the controller must be developed based on a very precise and a high resolution model [22, 23, 38, 86, 99, 107].

1.2 Finite- versus Infinite-Dimensional Model

Most ordinary differential equation systems describing physical phenomenon are finite-dimensional approximations of distributed parameter systems. Hence, for very high resolution control applications the study of distributed parameter systems, such as control of systems governed by partial differential equations, are of intrinsic interest.

One of the major issues related to approximating a system in finite-dimensional space is that the neglected dynamics might lead to unexpected excitation of truncated modes, and conversely the truncated modes might undesirably contribute to feedback data. In either case, the performance of the closed-loop system may be deteriorated, or, at some points, the system may even be destabilized [14, 81]. Furthermore, the increase of modeling accuracy will lead to high-dimensional and complex feedback control structures, requiring a considerable number of on-chip sensors for the implementation. This raises serious technological challenges for the design, fabrication, and operation of microsystems. Therefore, it is of great interest to directly deal with the control of the exact PDE models.

However, even treatment of some very basic problems of partial differential equation systems, such as heat equations and wave equations, demands a rich background on mathematical foundations, such as functional analysis. For instance, a small alteration on the boundary values could drastically alter the nature of the problem. As a result, the study of partial differential equation systems in the context of infinite-dimensional space has been treated differently on a case-by-case basis and remains an open field for engineering applications.

In this research, we consider the partial differential equation model of a deformable mirror actuated with Microelectromechanical systems, MEMS. In this work, we refer to this device as MEMS-actuated deformable mirror, or deformable mirror for short. In the model, the dynamics of small transversal displacement of the membrane surface may be described by a fourth-order in space and second-order in time partial differential equation, called Timoshenko thin plate equation [101, 106, 48]. The MEMS actuators are considered as pointwise actuators represented by Dirac delta functions located in the domain of the system.

By exploiting the symmetry of the domain, the problem of a 2-dimensional plate equation can be reduced to the Cartesian product of two decoupled 1-dimensional systems of Euler-Bernoulli beam equations [16, 17]. Hence, the main focus of the control design will be on

tracking control of an Euler-bernoulli PDE with in-domain Dirac delta functions as control inputs.

1.3   PDE-Based Tracking Control of Euler-Bernoulli Beams

One of the most popular methods for the tracking control of PDEs is to approximate the PDE by a system of lumped ordinary differential equations, ODE, through the spatial discretization of differential operator [18, 15, 19, 24, 67, 66, 84]. Subsequently, various control methods developed for ODE systems can be directly applied. The problems associated with the approximation of the model mentioned earlier may arise in these methods. Regardless of implementation aspects, we formally review the steps in designs based on a lumped ODE model of a PDE system in Chapter 3.

Moreover, many methods originally developed for nonlinear control of finite-dimensional systems are successfully generalized to control infinite-dimensional systems. This, for instance, includes Lyapunov-based techniques, [71, 68, 5], backstepping [57, 56, 58, 55], and differential flatness for inversion-based trajectory planning and feed-forward control [40, 82, 81, 97, 64]. Furthermore, tracking control is a result of combinations of these approaches [78].

The feedback stabilization of an Euler- Bernoulli beam has been considered in many different sources (see, e.g., [5, 26, 25]). For instance, feedback stabilization using a backstepping approach is considered in [79, 56] which provides a systematic approach for the design of exponentially stabilizing state feedback controllers. Stabilization by strain and shear force boundary feedback using dissipative concepts is addressed in Chapter 4 of [71]. Stabilization of Euler-Bernoulli beams using one in-domain point-wise feedback force has been examined in [5, 4, 3, 25].

The problem of trajectory planning, i.e. the design of an open-loop control to realize prescribed spatial-temporal output paths, using differential flatness which is originally developed for the control of finite-dimensional nonlinear systems, [57, 41, 42, 97, 76, 64], has further been successfully extended to a variety of infinite-dimensional systems (see e.g., [82, 79, 97, 76, 64, 65]).

Differential flatness implies that the system states and the control inputs can be parameterized in terms of a flat, or a so-called basic output, and its time-derivatives up to a certain problem dependent order. By prescribing appropriate trajectories for the flat output, the full-state and input trajectories can be directly evaluated without integration of any differential equation. This implies that a system is differentially flat if the flat output has the same number of components as the number of system inputs, [42, 41, 39, 64, 65]. This is the key

concept in generalizing differential flatness for multi-input multi-output PDEs.

The underlying idea of flatness, i.e. the existence of a one-to-one correspondence between trajectories of systems, has also been adapted successfully to some PDE systems (see, e.g., [52, 65, 73, 79, 90, 94, 74]).

In differential flatness designs, the system states and system inputs can be parameterized by the flat output in terms of infinite power series representations of the system. Then, series coefficients can be obtained by solving recursive equations on time-derivatives of the basic output, which has to be chosen from a certain smooth function, namely Gevrey function. Recent works on the flatness concept has mainly dealt with its extension to trajectory planning for boundary controlled PDE systems in a single spatial coordinate [82, 80]. Tracking control using a combination of flatness and backstepping for parabolic and bi-harmonic PDEs with actuators located on the boundary to stabilize the system along prescribed trajectories has been addressed in [78, 79]. It is, however, very challenging to apply this tool to systems controlled by multiple in-domain actuators.

1.4   The Main Challenge in PDE-Based Deformation Control of Micro-Mirrors

In standard PDE systems, unbounded control operators are typically located on the boundaries of the system, whereas in the PDE model of deformable mirrors the unbounded control operators are distributed in the domain of the system. This makes PDE-based control designs of deformable mirrors drastically different from the standard boundary controlled PDE designs. Particularly, finding a one-to-one correspondence between the control space and the system's state space is not obvious since the dimension of the control space is finite, while that of the state space is infinite.

1.5   Motivation and Objective

The main motivation of this work is to develop a high-precision and real-time applicable control structure for large-scale deformable mirrors in order to reduce the complexity introduced by closed-loop control at the level of every actuator.

To meet this end, the objective of this dissertation is to develop a control law directly based on the partial differential equation model of the system to archive high-precision performance. To mitigate the complexity of the controller, we consider a combination of feedback stabilization and feed-forward motion planing controllers. Minimizing the requirement of sensory data in order to steer the surface mirror asymptotically along reference trajectories is also the other objective of this control design. To achieve real-time implementation, an inversion-based trajectory planing is performed based on the Green's functions of the system

that can be calculated *a priori.*

1.6   Treatment Approach and the Contributions

The problem posed above will be tackled as follows. First, we introduce a dynamic model for a MEMS-actuated deformable mirror described by a set of partial differential equations with unbounded control operators in the domain of the system. Then, we introduce the control scheme based on establishing a relationship between the original nonhomogeneous model and a target system in a standard boundary control form. Then, an asymptotic tracking control is achieved by combining feedback stabilization and feed-forward motion planing allowing the system to follow prescribed output trajectories.

To facilitate the motion planing and real-time implementation of the scheme, the Green's functions of the system employed in the design. A finite set of these functions is considered to establish a one-to-one map between the input space and output space.

The original contributions of the present work are as follows:

First, this work addresses a scheme for control of deformable mirrors that requires only to close few feedback control loops, typically one for 1-dimensional devices. Consequently, the implementation and operation of such devices will be drastically simplified.

Second, the design is directly preformed with the partial differential equation model of the system. Hence, there are no neglected dynamics to sacrifice the performance. The only truncation is required at the level of controller implementation.

Third, we extend the tool of flat systems for tracking control of a PDE system controlled by multiple in-domain actuators, which is essentially a multiple-input multiple-output (MIMO) problem. To the best of the author's knowledge, design scheme without requiring early truncations for tracking control of this type of PDE systems have not yet been reported In the open literature.

Finally, to enable this extension, we introduce a Green's function-based control design. A finite set of Green's functions of the system is used to establish a one-to-one map between the input and the output of the system. Using the Green's functions also enables a simple and computationally tractable implementation of the proposed control scheme. As the static Green's function used in trajectory planning can be computed *a priori*, the developed scheme facilitates real-time implementations. This will have an important impact on the operation of large-scale deformable mirrors.

The other contributions of this research work are also reported in the following journal and refereed conference papers:

The work reported in [13] explains the problem of dynamic control of a MEMS deformable

mirror in the context of adaptive optics. This paper also demonstrates the essential steps for PDE control designs based on the early lumped system.

The paper [8] deals with the application of differential flat systems on a simple model of heat propagation along a bar, which is the same model used throughout Chapter 2 to demonstrate the properties of infinite-dimensional linear systems.

The paper [7, 9, 10, 11, 12] address the tracking control design directly on in-domain controlled Euler-Bernoulli beam equations, which form the main results of Chapter 4.

1.7   Dissertation Organization

The rest of this dissertation is organized as follow:

Chapter 2 outlines the required background on infinite-dimensional systems control theory. Hence, we just refer to the theorems and definitions from this chapter in the design represented in Chapter 4. Thus, the design chapter which explains the original work of this thesis will be succinct.

Chapter 3 presents a background of adaptive optics systems and how the problem can be posed as a tracking control problem. In this chapter, we also present a dynamic model of the deformable mirror. At the end of this chapter, we carry out a case study to show typical steps in the designs based on a finite-dimensional approximation of the model.

Chapter 4 presents the main results of this thesis: the control design based on an infinite-dimensional model of the considered system. This chapter entails two designs. In the first design, we formally establish a map between the in-domain controlled system and a boundary controlled system. The developed map holds for some special test functions which means the approach is valid in a very weak sense. To rectify this caveat, we solve the problem by using the technique of lifting to transform the target system, which is controlled by boundary actuators, to an inhomogeneous PDE driven by sufficiently smooth functions generated by applying blob functions to approximate the delta functions.

Chapter 5 discusses the numerical implementation of the model and presents the simulation results of the designs from Chapter 4.

We conclude this dissertation in Chapter 6 by providing a summary, drawing conclusions based on the results, and suggestions for future developments.

CHAPTER 2

A SYNOPSIS OF INFINITE-DIMENSIONAL LINEAR SYSTEMS CONTROL THEORY

Many problems arising in control systems are described in infinite-dimensional spaces. For example, systems governed by partial differential equations and delay systems are infinite-dimensional. In this thesis, we are interested in tracking control of a partial differential equation model of the system understudy directly in infinite-dimensional space. Hence, this chapter is devoted to providing a background on infinite-dimensional systems.

In this chapter, we first introduce the concept of strongly continuous semigroup, or C_0-semigroup for short, the generators of a C_0-semigroup, and the solution of PDEs. Then, we introduce the prerequisites theorems for the stability, well-posedness, and controllability analysis of PDE systems in an abstract form. In Section 2.9, we introduce the well-known form of boundary control for PDE systems. Through an example on an Euler-Bernoulli beam equation, we demonstrate the two concepts of boundary control and in-domain control can be exchangeable by introducing a proper map. Our coverage in this chapter is driven not by a desire to achieve generality, but rather to gather the prerequisites for the control design and tools for theoretical studies of the system understudy presented in the following chapters.

2.1 Linear Systems on Infinite-dimensional Spaces

From the state space theory of linear time-invariant systems, we know that ordinary differential equations can be written in the following abstract form:

$$\dot{x}(t) = Ax(t) + Bu(t), \quad x(0) = x_0 \tag{2.1a}$$

$$y(t) = Cx(t), \tag{2.1b}$$

where $x(t) \in \mathbb{R}^n$ is the system state, $u(t) \in \mathbb{R}^m$ is the input, and $y \in \mathbb{R}^p$ is the output. The matrix $A \in \mathbb{R}^{n \times n}$ is the system matrix, $B \in \mathbb{R}^{m \times n}$ is the input operator, and $C \in \mathbb{R}^{p \times n}$ is the output operator. From the theory of ordinary differential equations, the state evolution of this system can be represented as:

$$x(t) = e^{At}x_0 + \int_0^t e^{A(t-\tau)}Bu(\tau)d\tau, \quad t > 0, \tag{2.2}$$

where e^{At} is the matrix exponential defined as:

$$e^{At} = \sum_{n=0}^{\infty} \frac{A^n t^n}{n!}. \tag{2.3}$$

However, there are many cases where the system is defined in infinite-dimensional spaces. In this section, we show how systems described by partial differential equations can be written in the same form by using the concept of operators in infinite-dimensional state spaces. Nonetheless, "In contrast of finite-dimensional systems, presenting the properties of infinite-dimensional systems such as well-posedness, controllability, stability, etc. in a general framework of abstract form is far from being the end of the story," as pointed out in [27].

Since the question of existence and uniqueness of solutions to partial differential equations is more difficult than that for ordinary differential equations, we focus first on homogeneous partial differential equations. Thus, we begin by introducing the solution operator, and then we show how to rewrite a partial differential equation as an abstract differential equation in the form of (2.1). Then, we present the notion of input-output map and stability analysis for inhomogeneous systems. We conclude this chapter by introducing the well-known form of boundary control PDEs, well-posedness, and controllability for PDE systems.

2.2 Strongly Continuous Semigroups

To show the importance of continuous semigroups for generalizing the concept of the matrix exponential e^{At} and the concept of a solution on abstract spaces to infinite dimensional equations, we start with the following example from [29].

Example 2.1 *Consider a metal bar of length L with following initial conditions and boundary values [29]:*

$$\frac{\partial w(x,t)}{\partial t} = \frac{\partial^2 w(x,t)}{\partial x^2} \tag{2.4a}$$

$$w(x,0) = w_0(x) \tag{2.4b}$$

$$\frac{\partial w(0,t)}{\partial x} = 0 = \frac{\partial w(L,t)}{\partial x}, \tag{2.4c}$$

where $w(x,t)$ represents the temperature at the position $x \in [0,L]$ at time $t \geq 0$ and $w_0(x)$ represents the initial temperature profile. The boundary conditions state the isolated bar that is no heat flow at the boundaries.

In order to find a solution to (2.4), we try out a solution of the form $w(x,t) = f(t)g(x)$; this method of solution is called separation of variables [63]. Substituting this form of solution

in (2.4) and using the boundary conditions, we obtain:

$$f(t)g(x) = \alpha_n e^{(-n^2\pi^2 t)} \cos(n\pi x), \tag{2.5}$$

where $\alpha_n \in \mathbb{R}$ or $\mathbb{C}$ and $n \in \mathbb{N}$. By the linearity of the PDE (2.4), we have:

$$w_N(x,t) = \sum_{n=0}^{N} \alpha_n e^{(-n^2\pi^2 t)} \cos(n\pi x). \tag{2.6}$$

The function in (2.6) satisfies the PDE and the boundary conditions, but does not verify the initial conditions.

The corresponding initial condition derived from (2.6) $w_N(x,0) = \sum_{n=0}^{N} a_n \cos(n\pi x)$ is a Fourier polynomial. Note that every function q in $L^2(0,L)$, the space of square-integrable functions in $(0,L)$, can be represented by its Fourier series [29]:

$$q(\xi) = \sum_{n=0}^{\infty} \alpha_n \cos(n\pi\xi). \tag{2.7}$$

This series converges in L^2 for:

$$\alpha_0 = \int_0^1 q(\xi)d\xi, \tag{2.8}$$

and

$$\alpha_n = 2\int_0^1 q(\xi)\cos(n\pi\xi)d\xi, \quad n = 1, 2, \cdots . \tag{2.9}$$

If $w_0 \in L^2(0,1)$, then we can find α_n as the corresponding Fourier coefficients and

$$w_N(x,t) = \sum_{n=0}^{N} \alpha_n e^{(-n^2\phi^2 t)} \cos(n\pi x). \tag{2.10}$$

The the solution to (2.4) $w(\cdot, t)$ is an element in $L^2(0,1)$ since $e^{-n^2\pi^2 t} \leq 1$ for $t \geq 0$. It also satisfies the initial conditions by construction. However, as interchanging infinite summation and differentiation is not always possible, it is not clear whether this function satisfies the PDE (2.4) in this example. Nevertheless, the mapping $w_0 \mapsto w(\cdot, t)$ defines an operator, which would assign to an initial condition its corresponding solution at time t, provided w is the solution [29].

This example motivates the generalization of the concept of the matrix exponential e^{At} on abstract space and show the necessity for clarifying the concept of solution to infinite-dimensional equations on abstract spaces.

We denote by X a real or complex separable Hilbert space, with inner product $\langle \cdot, \cdot \rangle_X$ and norm $\| \cdot \|_X = \sqrt{\langle \cdot, \cdot \rangle_X}$. By $L(x)$ we denote the class of linear bounded operators from X to X.

Definition 2.1 *[29] Let X be a Hilbert space. $S(t)_{t>0}$ is called a strongly continuous semigroup, or for short C_0-semigroup, if the following holds:*

1. *For all $t \geq 0$, $S(t)$ is a bounded linear operator on X, i.e., $S(t) \in L(X)$;*

2. *$S(0) = I$;*

3. *$S(t + \tau) = S(t)S(\tau)$ for all $t, \tau > 0$;*

4. *For all $x_0 \in X$, we have that $\|S(t)x_0 - x_0\|_X$ converges to zero, when $t \to 0$, i.e., $t \mapsto S(t)$ is strongly continuous at zero.*

X is called the state space, and the elements of X are called states. A trivial example of a strongly continuous semigroup is the matrix exponential. That is, let A be an $n \times n$ matrix, the matrix-valued function $S(t) = e^{At}$ defines a C_0-semigroup on the Hilbert space $\mathbb{R}^n$.

Example 2.2 *[49] Let $\{\phi_n, n \geq 1\}$ be an orthogonal basis of the separable Hilbert space X, and let $\{\lambda_n, n \geq 1\}$ be a sequence of complex numbers. Then,*

$$S(t)x = \sum_{n=1}^{\infty} e^{\lambda_n t} \langle x, \phi_n \rangle \phi_n \tag{2.11}$$

is a bounded linear operator if and only if $\{e^{Re(\lambda_n)t}, n \geq 1\}$ is a bounded sequence in $\mathbb{R}$.

Under this assumption, we have

$$\|S(t)\| \leq e^{\omega t}, \quad \omega \in \mathbb{R}. \tag{2.12}$$

Furthermore,

$$S(t + s)x = \sum_{n=1}^{\infty} e^{\lambda_n(t+s)} \langle x, \phi_n \rangle \phi_n, \tag{2.13}$$

which can be written as:

$$S(t)S(s)x = \sum_{n=1}^{\infty} e^{\lambda_n t} \langle S(s)x, \phi_n \rangle \phi_n = \sum_{n=1}^{\infty} e^{\lambda_n t} e^{\lambda_n s} \langle S(s)x, \phi_n \rangle \phi_n = S(t + s)x. \tag{2.14}$$

Clearly $S(0) = I$, and the strong continuity follows from the following calculation:

$$\|S(t)x - x\|^2 \;=\; \sum_{n=1}^{\infty} |e^{\lambda_n t} - 1| |\langle x, \phi_n \rangle|^2 \tag{2.15}$$

$$= \sum_{n=1}^{N} |e^{\lambda_n t} - 1| |\langle x, \phi_n \rangle|^2 + \sum_{n=N+1}^{\infty} |e^{\lambda_n t} - 1| |\langle x, \phi_n \rangle|^2 \tag{2.16}$$

$$\leq \sup_{1 \leq n \leq N} |e^{\lambda_n t} - 1|^2 \sum_{n=1}^{N} |\langle x, \phi_n \rangle|^2 + k \sum_{n=N+1}^{\infty} |\langle x, \phi_n \rangle|^2. \tag{2.17}$$

For any $\epsilon > 0$ there exist an $N \in \mathbb{R}$ such that

$$\sum_{n=N+1}^{\infty} |\langle x, \phi_n \rangle|^2 < \frac{\epsilon}{2k}, \tag{2.18}$$

and we can choose $t_0 \leq 1$ such that $\sup_{1 \leq n \leq N} |e^{\lambda_n t_0} - 1|^2 \leq \frac{\epsilon}{2\|x\|^2}$. Thus, for $t \in [0, t_0]$ we have:

$$\|S(t)x - x\|^2 \leq \frac{\epsilon}{2\|x\|^2} \sum_{n=1}^{N} |\langle x, \phi_n \rangle|^2 + k \frac{\epsilon}{2k} \leq \epsilon, \tag{2.19}$$

which shows that $S(t)_{t \geq 0}$ is strongly continuous. Thus, (2.11) defines a C_0-semigroup if and only if $\{e^{Re(\lambda_n)t}, n \geq 1\}$ is a bounded sequence in $\mathbb{R}$ which is the case for $t > 0$ if and only if $\sup_{n \geq 1} Re\lambda_n < \infty$.

As mentioned before, any exponential of a matrix defines a strong continuous semigroup. In fact, semigroups share many properties with theses exponential functions.

Theorem 2.1 *[29] A strongly continuous semigroup $S(t)_{t \geq 0}$ on the Hilbert space X has the following properties:*

1. *$\| S(t) \|$ is bounded on every finite sub-interval of $[0, \infty)$;*

2. *The mapping $t \mapsto S(t)$ is strongly continuous on the interval $[0, \infty)$;*

3. *For all $x \in X$ we have that $\frac{1}{t} \int_0^t S(s)x\,ds \to x$ as $t \to 0$;*

4. *If $\omega_0 = \inf_{t>0}(\frac{1}{t} \log \| S(t) \|)$, $t \to 0$ then $\omega_0 < \infty$;*

5. *For every $\omega > \omega_0$, there exists a constant M_ω such that for every $t \leq 0$ we have $\| S(t) \| \leq M_\omega e^{\omega t}$.*

The constant ω_0 is called the growth bound of the semigroup.

2.3 Infinitesimal Generators

If A is an $n \times n$ matrix, then the semigroup $(e^{At})_{t \geq 0}$ is directly linked to A via

$$A = \left(\frac{d}{dt} e^{At} \right) |_{t=0}. \tag{2.20}$$

Next we associate in a similar way an operator A to a C_0-semigroup $S(t)_{t \geq 0}$.

Definition 2.2 *[29] Let $S(t)_{t \geq 0}$ be a C_0-semigroup on Hilbert space X. If the following limit exists*

$$\lim_{t \to 0} \frac{S(t)x_0 - x_0}{t}, \tag{2.21}$$

then we say that x_0 is an element of the domain of A, or $x_0 \in D(A)$, and we define Ax_0 as

$$Ax_0 = \lim_{t \to 0} \frac{S(t)x_0 - x_0}{t}. \tag{2.22}$$

We call A the infinitesimal generator of the strongly continuous semigroup $S(t)_{t \geq 0}$.

The following theorem shows that for every $x_0 \in D(A)$ the function $t \mapsto S(t)x_0$ is differentiable. In fact, this theorem link a strongly continuous semigroup uniquely to an abstract differential equation.

Theorem 2.2 *, [29], Let $S(t)_{t \geq 0}$ be a strongly continuous semigroup on Hilbert space X with infinitesimal generator A. Then, the following results hold:*

1. *For $x_0 \in D(A)$ and $t \geq 0$ we have $S(t)x_0 \in D(A)$;*

2. *$\frac{d}{dt}(S(t)x_0) = AS(t)x_0$ for $x_0 \in D(A), t \geq 0$;*

3. *$\frac{d^n}{dt^n}(S(t)x_0) = A^n S(t)x_0 = S(t)A^n x_0$ for $x_0 \in D(A^n), t \geq 0$;*

4. *$S(t)x_0 - x_0 = \int_0^t S(s)Ax_0 ds$ for $x_0 \in D(A)$;*

5. *$\int_0^t S(s)x_0 ds \in D(A)$ and $A \int_0^t S(s)x_0 ds = S(t)x - x$ for all $x \in X$, and $D(A)$ is dense in X.*

This theorem implies in particular that for every $x_0 \in D(A)$ the function x defined by $x(t) = S(t)x_0$ satisfies the abstract differential equation $\dot{x} = Ax(t)$. It implies though that every strongly continuous semigroup has a unique generator. It is not hard to show that every generator belongs to a unique semigroup.

2.4 Abstract Differential Equations

Theorem 2.2 shows that for $x_0 \in D(A)$ the function $x(t) = S(t)x_0$ is a solution to the abstract differential equation

$$\dot{x}(t) = Ax(t), \quad x(0) = x_0 \tag{2.23}$$

Definition 2.3 *[49] A differentiable function $x : [0, \infty) \to X$ is called a classical solution of (2.23) if for all $t \geq 0$ we have $x(t) \in D(A)$ and Equation (2.23) is satisfied.*

It is not hard to show that the classic solution is uniquely determined for $x_0 \in D(A)$.

Definition 2.4 *[49] A continuous function $x : [0, \infty) \to X$ is called a mild or weak solution of (2.23) if $\int_0^t x(s)ds \in D(A)$, $x(0) = x_0$ and*

$$x(t) - x(0) = A \int_0^t x(\tau)d\tau, \text{ for all } t \geq 0. \tag{2.24}$$

Furthermore, the mild solution is also uniquely determined.

Finally, we return to the PDE of Example 2.1. We constructed a C_0-semigroup and showed that the semigroup solves an abstract differential equation. A natural question is how this abstract differential equation is related to the PDE (2.4). The mild solution x of (2.4) takes at every time t values in an Hilbert space X. For the PDE (2.4) we chose $X = L^2(0, 1)$. Thus, $x(t)$ is a function of $\xi \in [0, 1]$. Writing down the abstract differential equation using both variables, we obtain:

$$\frac{\partial w(x, t)}{\partial t} = Aw(x, t). \tag{2.25}$$

Comparing this with (2.23) A must be equal to $\frac{\partial^2 w(x,t)}{\partial x^2}$. Since for $x_0 \in D(A)$ the mild solution is a classical solution, the boundary condition must be a part of the domain of A. Hence, the operator A associated to the PDE (2.4) is given by:

$$Aw = \frac{d^2 w}{dx^2}, \tag{2.26}$$

with

$$D(A) = \{w \in L^2(0, 1) | w, \frac{dw}{dx} \text{ are absolutely continuous,} \tag{2.27}$$

$$\frac{d^2 w}{dx^2} \in L^2(0, 1) \text{ and } \frac{dw(0, t)}{dx} = 0 = \frac{dw(L, t)}{dx}\}.$$

2.5 Contraction Semigroup

We realized from the previous sections that every C_0-semigroup possesses an infinitesimal generator. In this section, we are interested in other implication that is which operator A generates a C_0-semigroup. In physical problems, one usually does not start with a semigroup, but with a PDE. This section answers the question how to get from a PDE to an operator A and from the operator A to the semigroup.

The answer to this question is given by Hille-Yosida Theorem [19], which provides the necessary and sufficient condition for A to be the infinitesimal generator of a semigroup. However, in practice often an equivalent theorem which is called the Lumer-Phillips Theorem is used [30, 71]. This theorem gives the answer in a special case, namely contraction semigroups. Hence, we limit our investigation of which operator A generates a C_0-semigroup to this special case.

Definition 2.5 *[29] Let $(S(t))_{t \geq 0}$ be a C_0-semigroup on the Hilbert space X. $(S(t))_{t \geq 0}$ is called contraction semigroup, if $\|S(t)z\| \leq \|z\|$ for every $t \geq 0$.*

Definition 2.6 *[29] A linear operator $A : D(A) \subset X \mapsto X$ is called dissipative, if*

$$\operatorname{Re}\langle Ax, x \rangle \leq 0, \quad x \in D(A). \tag{2.28}$$

Definition 2.7 *[29] A linear operator $A : D(A) \subset X \mapsto X$ is called closed dissipative operator, if the range of $\alpha I - A$, $ran(\alpha I - A)$ is closed for all $\alpha > 0$.*

Theorem 2.3 *(Lumer-Phillips's Theorem) [29] Let A be a linear operator with domain $D(A)$ on a Hilbert space X. Then A is the infinitesimal generator of a contraction semigroup $(S(t)_{t \leq 0})$ on X if and only if A is dissipative and $ran(I - A) = X$.*

The following theorem gives another simple characterization of generators of contraction semigroups.

Theorem 2.4 *[29] Let A be a linear, densely defined, and closed operator on a Hilbert space X. Then A is the infinitesimal generator of a contraction semigroup $(S(t)_{t \leq 0})$ on X if and only if A and the adjoint of A, denoted by A^* and defined later in Definition 2.8, are dissipative.*

Remark 2.1 *Instead of assuming that A^* is dissipative, it is sufficient to assume that A^* has no eigenvalues on the positive real axis.*

Next we apply this theorem to Example 2.1 [49].

Example 2.3 *For the heated bar in Example 2.1, We obtained the following operator:*

$$Ah = \frac{\partial^2 h}{\partial^2 \xi} \text{ with,} \tag{2.29a}$$

$$\mathcal{D}(A) = \left\{ h \in L^2(0,1), \frac{\partial^2 h}{\partial^2 \xi} \in L^2(0,1), \frac{\partial h}{\partial \xi}(0) = 0 = \frac{\partial h}{\partial \xi}(1) \right\}. \tag{2.29b}$$

Next we show that A generates a contraction semigroup on $L^2(0,1)$. A is dissipative, as

$$\langle h, Ah \rangle + \langle h, Ah \rangle = \int_0^1 h(\xi) \overline{\frac{\partial^2 h}{\partial^2 \xi}(\xi)} + \frac{\partial^2 h}{\partial^2 \xi}(\xi) \overline{h(\xi)} d\xi$$

$$= \left(h(\xi) \overline{\frac{\partial h}{\partial \xi}(\xi)} + \frac{\partial h}{\partial \xi}(\xi) h(\xi) \right) \Big|_0^1 - 2 \int_0^1 \frac{\partial h}{\partial \xi}(\xi) \overline{\frac{\partial h}{\partial \xi}(\xi)}$$

$$= 0 - 2 \int_0^1 \left\| \frac{\partial h}{\partial \xi}(\xi) \right\|^2 d\xi \leq 0, \tag{2.30a}$$

where we have used the boundary conditions. It remains to show that the range of $(I - A)$ equals $L^2(0,1)$, i.e., for every $f \in L^2(0,1)$ we have to find an $h \in \mathcal{D}(A)$ such that $(I - A)h = f$. Let $f \in L^2(0,1)$ and define

$$h(\xi) = \alpha \cosh(\xi) - \int_0^\xi \sinh(\xi - \tau) f(\tau) d\tau, \tag{2.31}$$

where

$$\alpha = \frac{1}{\sinh(1)} \int_0^1 \cosh(1 - \tau) f(\tau) d\tau. \tag{2.32}$$

Now directly we can see that h is an element of $L^2(0,1)$ and is absolutely continuous. Furthermore, its derivative is given by

$$\frac{dh}{d\xi} = \alpha \sinh(\xi) - \int_0^\xi \cosh(\xi - \tau) f(\tau) d\tau. \tag{2.33}$$

This function is also absolutely continuous and satisfies the boundary conditions. Furthermore,

$$\frac{d^2 h}{d\xi^2} = \alpha \cosh(\xi) - f(\xi) - \int_0^\xi \sinh(\xi - \tau) f(\tau) d\tau = -f(\xi) + h(\xi). \tag{2.34}$$

Thus $h \in \mathcal{D}(A)$ and $(I - A)h = f$. This proves that for every $f \in L^2(0,1)$ there exists an $h \in \mathcal{D}(A)$ such that $(I - A)h = f$. Thus, according to the Lumer-Phillips's theorem, A generates a contraction semigroup.

Now it remains to find out what is the form of this semigroup. There are two ways of approaching this question. First, we can directly solve the PDE to which operator A is

associated. For instance, in Example 2.1, we can directly solve the PDE, e.g., by using the separation of variables method [63, 91].

Another way is starting from the operator A and solving the eigenfunction equation. For instance in Example 2.1, we can solve the eigenfunction equation, $A\phi_n = \lambda_n \phi_n$, which yields:

$$\phi_n(x) = \begin{cases} 1, & \lambda_0 = 0; \\ \sqrt{2}\cos(n\pi x), & \lambda_n = -n^2\pi^2, n \in N. \end{cases} \tag{2.35}$$

Therefore, the solution to $\dot{z}(t) = Az(t)$, with $z(0) = \phi_n$, is given by:

$$z(t) = e^{\lambda_n t}\phi_n, \tag{2.36}$$

which must be equal to $S(t)\phi_n$. Sine $\{\phi_n, n \in N \cup \{0\}\}$ is an orthonormal basis, we know that

$$z_0 = \sum_{n=0}^{\infty} \langle z_0, \phi_n \rangle \phi_n. \tag{2.37}$$

Hence

$$S(t)z_0 = S(t)\left(\sum_{n=0}^{\infty} \langle z_0, \phi_n \rangle \phi_n\right) = \sum_{n=0}^{\infty} \langle z_0, \phi_n \rangle S(t)\phi_n = \sum_{n=0}^{\infty} \langle z_0, \phi_n \rangle e^{\lambda_n t}\phi_n. \tag{2.38}$$

Thus, we found that the semigroup evaluated at z_0 is equal to this infinite sum.

Remark 2.2 (2.38) *is a formal form of a semigroup. If we write down each elements such that for the inner product and λ, the final equation becomes a tedious expression.*

2.6 Semigroups and Solutions of PDEs

We have shown thus far that for any $z_0 \in \mathcal{D}(A)$, the solution $z(t) := S(t)z_0$ is the solution to

$$\dot{z}(t) = Az(t), \quad z(0) = z_0. \tag{2.39}$$

However, for a general z_0, $Az(t)$ has no meaning nor does $\dot{z}(t)$. To generalize the definition of a solution for a general z_0, we have to first introduce the adjoint of A.

Definition 2.8 *[49] Let A be a densely defined operator with domain $\mathcal{D}(A)$. The domain of A^*, $\mathcal{D}(A^*)$, is defined as consisting of those $w \in X$ for which there exists a $z \in X$ such that*

$$\langle w, Az \rangle = \langle v, z \rangle \quad \forall z \in \mathcal{D}(A). \tag{2.40}$$

If $w \in \mathcal{D}(A^*)$, then A^* is defined as

$$A^*w = v. \tag{2.41}$$

A^* is called the adjoint of A.

Definition 2.9 *The operator A is called positive, if A is self-adjoint, $A = A^*$.*

Now we can define the concept of weak solutions.

Proposition 1 *[49] Let $z_0 \in X$, and define $z(t) = S(t)z_0$. Then for every $w \in \mathcal{D}(A^*)$, the following holds*

$$\frac{d}{dt}\langle w, z(t) \rangle = \langle A^*w, z(t) \rangle. \tag{2.42}$$

This implies that $z(t) := S(t)z_0$ is a weak solution of $\dot{z}(t) = Az(t)$, $z(0) = z_0$.

This is exactly the concept of the weak or mild solution in PDEs.

2.7 Stability

One of the most important aspects of systems theory is the stability, which is strictly related to the design of feedback controls. For infinite-dimensional systems there are different notions of stability such as strong stability, polynomial stability, and exponential stability. We restrict the discourse of this section to the exponential stability and show that the strong stability is weaker than the exponential stability.

Definition 2.10 *Exponential stability: [27] The C_0-semigroup $(S(t)_{t \geq 1})$ on the Hilbert space X is exponentially stable if there exists positive constants M and α such that*

$$\| S(t) \| \leq Me^{-\alpha t} \text{ for } t > 0. \tag{2.43}$$

The constant α is called the decay rate, and the supremum over all possible values of α is the stability margin of $S(t)$; this is minus its growth bound as introduced in Theorem 2.1.

If $S(t)$ is exponentially stable, then the solution to the abstract Cauchy problem

$$\dot{x}(t) = Ax(t), \ t \geq 0, \ x(0) = x_0, \tag{2.44}$$

tends to zero exponentially.

Definition 2.11 *Strong stability: [27] The C_0-semigroup $(S(t)_{t \geq 1})$ on the Hilbert space X is strongly stable if for all $z_0 \in X$*

$$\lim_{t \to +\infty} S(t)z_0 = 0. \tag{2.45}$$

It is evident that the exponential stability always implies the strong stability, but the converse is not true.

The following theorem sorts conditions that guarantee the exponentially stability for infinite-dimensional systems.

Theorem 2.5 *[29] Suppose that A is the infinitesimal generator of the C_0-semigroup $S(t)$ on the Hilbert space X. Then the following statements are equivalent*
— *$S(t)$ is exponentially stable.*
— *For all $z_0 \in X$ we have that $S(t)z_0 \in L^2((0, \infty); X)$.*
— *There exists a positive operator $P \in L(X)$, such that*

$$\langle Ax, Px \rangle + \langle Px, Ax \rangle \leq -\langle x, x \rangle, \text{ for all } x \in D(A). \tag{2.46}$$

Equation (2.46) is called a Lyapunov equation. This Lyapunov equation is being written differently in different literature.

One of the important concepts in finite-dimensional system theory is the relationship between the stability of the system and no poles in the right half plane. Indeed, for finite-dimensional systems, one usually examines the exponential stability via the spectrum of the operator. However, there are examples of unstable semigroups for which the infinitesimal generator A has no spectrum in the set $\{s \in \mathbb{C} \mid \mathrm{Re}(s) \geq 0\}$. Hence, in general, we cannot conclude the stability by only looking at the spectrum of A.

Example 2.4 *Consider a $n \times n$ Jordan matrix with minus half on the diagonal and all ones on the upper diagonal:*

$$A = \begin{pmatrix} -1/2 & 1 & 0 & \cdots & 0 \\ 0 & \ddots & \ddots & & \vdots \\ \vdots & & \ddots & & 1 \\ 0 & \ldots & & 0 & -1/2 \end{pmatrix} \tag{2.47}$$

The exponential of this matrix is given by:

$$\begin{pmatrix} e^{-\frac{t}{2}} & te^{-\frac{t}{2}} & \cdots & \frac{t^{n-1}}{(n-1)!}e^{-\frac{t}{2}} \\ 0 & \ddots & \ddots & \vdots \\ \vdots & \ddots & \ddots & te^{-\frac{t}{2}} \\ 0 & \ldots & 0 & e^{-\frac{t}{2}} \end{pmatrix} \tag{2.48}$$

It clearly shows that all the eigenvalues of this operator are in the left hand-side.

Applying a vector all consisting of one, the first row will be:

$$e^{A_n t} \begin{pmatrix} 1 \\ \vdots \\ 1 \end{pmatrix} = \begin{pmatrix} e^{-t/2}(1 + t + \frac{t^2}{2!} + \cdots + \frac{t^{n-1}}{(n-1)!}) \\ 0 \\ \vdots \end{pmatrix} = \begin{pmatrix} e^{-t/2}e^t \\ 0 \\ \vdots \end{pmatrix} \quad (2.49)$$

For a large value of n the series approximates the Taylor series of e^t. Hence, it is exponentially growing. This counter example shows that even though all the spectrums of this semigroup are non-negative, the system may not be stable. Although this is not a rigorous proof, it is one of the counter examples showing that the eigenvalues or the spectrums of A do not determine the growth of the semigroup.

To determine the exponential stability of infinite-dimensional systems, we can resort to the following theorem.

Theorem 2.6 *[29] The semigroup $S(t)$ is exponentially stable if and only if*

$$\sup_{\{s \in C | \mathrm{Re}(s) > 0\}} \| (sI - A)^{-1} \| < \infty. \quad (2.50)$$

This theorem shows not only the resolvent should exist but also it should be bounded. This theorem is the natural generalization of no poles in the right hand plane for finite-dimensional systems.

2.8   Inhomogeneous Abstract Differential Equations and Stabilization

In the previous sections, we studied homogenous infinite-dimensional systems. However, for control theoretical questions, it is important to add an input to the differential equation. We add an input to the system and define input-output dynamics very similar to those exist in finite-dimensional system theory in the state-space form :

$$\dot{z}(t) = Az(t) + Bu(t), \quad z(0) = z_0 \quad (2.51a)$$

$$y(t) = Cz(t) + Du(t). \quad (2.51b)$$

First we define what we mean by a solution to the dynamic system (2.51). We denote the dynamic system (2.51a) by $\Sigma(A, B)$, and assume that

— A generates a C_0-semigroup $(S(t))_{t \geq 0}$ on the Hilbert space X.

— $B \in L(U, X)$.

To find the form of the solution, we multiply the differential equation (2.51a) by $S(t_1 - t)$, and bring z to the left-hand side to obtain:

$$S(t_1 - t)\dot{z}(t) - S(t_1 - t)Az(t) = S(t_1 - t)Bu(t). \tag{2.52}$$

The left-hand side equals

$$\frac{d}{dt}[S(t_1 - t)z(t)] = S(t_1 - t)Bu(t). \tag{2.53}$$

Hence,

$$\int_0^{t_1} S(t_1 - t)Bu(t)dt = [S(t_1 - t)z(t)]_0^{t_1} = z(t_1) - S(t_1)z(0). \tag{2.54}$$

The existence of the solution to (2.51a) in the form of (2.54) is given in the following theorem.

Theorem 2.7 *[27] Consider the abstract differential equation*

$$\dot{z}(t) = Az(t) + Bu(t), \quad z(0) = z_0 \tag{2.55}$$

where A generates the C_0-semigroup $(S(t))_{t\geq 0}$ on Hilbert space X, let $t \in [0, \tau]$ $B \in L(U, X)$, and $u \in C^1((0, \tau); U)$. Then a (weak) solution to (2.55) is given by

$$z(t) = S(t)z_0 + \int_0^t S(t - \tau)Bu(\tau)d\tau. \tag{2.56}$$

If u is continuously differentiable and $z_0 \in D(A)$, then it is the classical solution.

For an inhomogeneous system, the stabilization problem amounts to finding a feedback, $u = Fz$ which stabilizes the system $\Sigma(A, B)$. In other words, the operator $A + BF$ generates a stable semigroup.

2.9 Boundary Controlled PDEs

Essentially, there exist two types of PDE control schemes depending on how the control action is involved in the system: in-domain control with the actuators located in the interior of the system, and boundary control with the actuators located only on the boundaries. Boundary control of PDEs received more attention than the in-domain control [58]. In the traditional developed area of PDEs, boundary control is considered to be more realistic. For example, in case of fluid flow, actuation is normally expected at the walls of the flow. Moreover, because the actuators and sensors are exercised at spatial points, the input and

output operators are unbounded. As a result, considering unbounded operators in the domain of the system may introduce severe mathematical difficulties. Therefore, boundary points are much more suitable to place the actuators and sensors.

Nonetheless, evolution of micro-devices such as MEMS has brought about many realistic applications for the in-domain PDE control. One of the best examples is the MEMS deformable mirror control.

There is an extensive literature on boundary control of PDE [58, 19]. Typically one can find a thorough chapter on boundary control in most of the books in the field of PDE systems. In this section, we show that in a certain sense these two forms, namely boundary and in-domain control, might be made interchangeable using a proper map.

First, we explain the idea behind this reformulation through an example from [26, 71]. This example shows that the problem of boundary control and interior control is nothing but a matter of mathematical formulation. We construct our argument through the example of a flexible arm with a revolute joint and strain force feedback as a single point input in the domain of the system.

Example 2.5 *Consider a simplified linear dynamic model for the transversal vibration of a flexible arm given by, [26, 71, 72]:*

$$y_{tt}(x,t) + y_{xxxx}(x,t) = -kxy_{xxt}, \quad x \in (0,1), t > 0, \tag{2.57a}$$

$$y(0,t) = y_{xx}(0,t) = 0, \tag{2.57b}$$

$$y_{xx}(1,t) = y_{xxx}(1,t) = 0, \tag{2.57c}$$

$$y(x,0) = y_0(x), y_t(x,0) = y_1(x), \quad x \in (0,1), \tag{2.57d}$$

where $y(x,t)$ denotes the transverse displacement of the arm at time t and position x along the arm length direction. The feedback control y_{xxt} is the velocity of the bending strain and can be directly implemented using a motor driver of velocity reference type. This is a in-domain control form in which the control is a singular point in the domain of the system. To transfer this system to a standard boundary form, a new variable is introduced as follows:

$$y(x,t) = w_{xx}(1-x,t). \tag{2.58}$$

Using this change of variables, (2.57) can be transferred into the following boundary control

form:

$$w_{tt}(x,t) + w_{xxxx}(x,t) = 0, \quad x \in (0,1), t > 0, \tag{2.59a}$$

$$w(0,t) = w_x(0,t) = 0, \tag{2.59b}$$

$$w_{xx}(1,t) = 0, \tag{2.59c}$$

$$w_{xx}(1,t) = kw_t(t,1), \tag{2.59d}$$

Hence via a simple manipulation, we can reformulate this PDE with in-domain control into a PDE with boundary control. However, the price to pay is that y has to be smooth, here at least of $\mathbb{C}^2$. This issue illustrates an important aspect of working with PDEs that of defining the proper space for the system.

Another example in this regards can be found in [19], Chapter 4, in which a general Hyperbolic boundary PDE is transferred into a in-domain form, and the notion of space and dual space for both system is explained.

2.10   Well-Posedness

A PDE is called well-posed, in the sense of Hadamard [27], if:
— a solution exists;
— the solution is unique;
— the solution depends continuously on the data, the initial conditions, and the boundary conditions.

Existence and uniqueness involve boundary conditions. Hence, the study of well-posedness varies from one PDE to the other. We just conclude this section with Theorem 2.8 which is an essential theorem to prove the well-posedness of PDE systems with unbounded input operators. Before that, we first introduce the definition of admissible control operators.

Definition 2.12 *[27] The control operator B in abstract system (2.51a), $\Sigma(A, B)$, is called admissible for $S(t)$ on X if $\forall T > 0$ and $\forall z \in \mathcal{D}(A^*)$, there exists a constant $C_T > 0$ such that*

$$\int_0^T \|B^* S(t) z(t)\|_U^2 \, dt \leq C_T \|z\|_X^2, \tag{2.60}$$

where $B^* \in \mathcal{L}(\mathcal{D}(A^*); U)$ is the adjoint of B.

An operator B satisfying the admissibility condition defined above is also called regular for $S(t)$ on X.

Theorem 2.8 *[27] The inhomogeneous abstract system (2.51a), $\Sigma(A, B)$, is well-posed if A is skew-adjoint, i.e. $S^* = -S$, and B is admissible for the space.*

2.11   Controllability

In contrast to the case of linear finite-dimensional control systems, there are many types of controllability for infinite-dimensional system. Four essential types of controllability in this regards are: *exact controllability, approximate controllability, trajectory controllability, and null controllability* [27].

We are interested in the exact controllability. The exact controllability property is the possibility to steer the state of the system from any initial data to any target by choosing the control as a function of time in an appropriate way. The exact controllability implies the other types of controllability. However, the converse is not true in general.

There is no general framework for controllability assessment of infinite-dimensional system. However, it should be noted that for linear system (2.51a) with bounded control operator B in Hilbert spaces, many profound results are already known in earlier literatures [51, 50].

Theorem 4.15 of [29] states that if A generates a C_0-semigroup in a Hilbert space and B is a bounded operator and the control space is finite dimensional, then the linear system (2.51a) is not exactly controllable in $[0; t]$ for any finite $t > 0$. On the other hand, the following useful theorem provides an essential property for systems in which B is unbounded:

Theorem 2.9 *[50] System* (2.51a) *is exactly controllable in* $[0; t]$ *for any finite* $t > 0$ *if* A *generates a stable C_0-semigroup and B is unbounded but admissible.*

Hence, the controllability for the linear system $\Sigma(A, B)$ with unbounded operator B can be derived from well-posedness and stability analysis. We refer to [51] for recent consideration on this respect, and [47, 46] for the controllability of Euler-Bernoulli beams with unbounded input.

CHAPTER 3

ADAPTIVE OPTICS SYSTEMS

3.1 Introduction

Adaptive Optics (AO) is a technology used in optic systems to correct wavefront aberrations and the loss of image quality. One of the very exciting applications of this technology is in extremely large ground-based telescopes that are currently under development in Europe and North America [31]. The goal of this chapter is to present an overview of the AO technique in the context of ground-based telescopes, and then formulate the problem as a control problem to be treated in the sequel. This chapter examines the following topics: the structure of adaptive optics systems in ground-based telescopes; deformable mirrors modelling; and a finite-dimensional approximation solution for deformation control of this device.

3.2 Adaptive Optics

The term adaptive optics (AO) refers to optical systems that adapt in real time to compensate distortions of light introduced along the propagation path from the source point to the receiver [36]. This definition opens up two fertile areas of research: first, identifying the distortion and defining the reference shape; second, real time compensation for the distorting effect. The present research is focused on investigating the latter problem as a real time control problem.

Among the most important applications of AO we can find free space laser communications [105], [100], retinal imaging [33, 37], biological microscopy [96] , optical fabrication [34], and ground-based telescopes [87]. However, despite many similarities, each particular application has unique features which require its own insight to the system and specialized techniques. Hence, this research work is mainly focused on the application of AO in ground-based telescopes.

In the context of ground-based telescopes, as shown in Fig 3.1, AO is used to correct aberrations of celestial light due to turbulence of earth atmosphere to achive a crisp image rather than a hazy one. Figure 3.2 shows a typical setup of AO in astronomical telescopes.
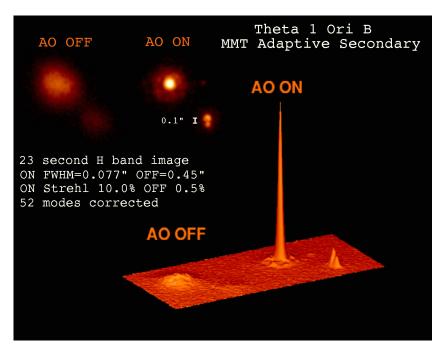
Figure 3.1 A typical example of how AO systems can make very sharp images. Photo Credit: Laird Close, CAAO, Steward Observatory (lclose@as.arizona.edu)
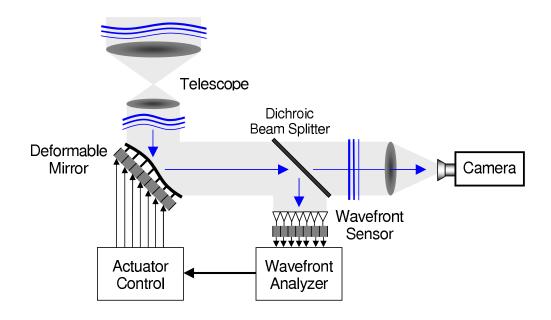
Figure 3.2 Illustration of AO principle in the context of astronomical telescope.
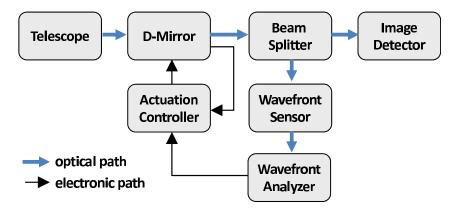
Figure 3.3 Schematic representation of open-loop AO with closed-loop DM control.

3.3 Structure of Adaptive Optics Systems

A typical AO system consists of the following components: a deformable mirror to correct the aberrated wavefronts; a wavefront sensor to measure the aberrations; a light source to drive the sensor; and a wavefront reconstructor, which receives sensor measurements and generates the reference shape for the deformable mirror. This structure is depicted in Fig 3.3.

The deformable mirror is the key element of this system. Thus, the high resolution performance of an adaptive optics system highly depends on the precise control of this device.

One of the prerequisites towards a precise control of deformable mirrors is a very accurate model of this device to describe the response of the mirror to the inputs. Moreover, since atmospheric turbulence is a dynamic phenomenon, the compensation needs to be sufficiently fast. Technically speaking, the expected closed-loop system bandwidth should be beyond 1 kHz. In view of such sampling frequencies, the deformable mirror can no longer be considered as a static system, since high frequency resonance modes can be exited as well, see e.g. [45]. In the next section, we develop a dynamic model that describes both transient and steady state behaviour of a typical deformable mirror actuated by microelectromechanical systems (MEMS).

3.4 MEMS-Actuated Deformable Mirror Modelling

The current commercially available MEMS-based deformable mirrors consist of a thin flexible membrane coated with highly reflective material. Actuators attached beneath the mirror face-sheet steer the mirror from an initial state to a prescribed shape. Arguably, the off-the-shelves DM for AO applications can be categorized based on two features: membrane

mirror and technology of actuators.

In terms of membrane mirror, DMs are divided into two commonplace categories: continuous face-sheet mirrors and segmented mirrors. Figure 3.4 shows the cross sectional schematics of the main components of the continuous (left) and segmented (right) deformable mirror from Boston Micro Machine (BMC).
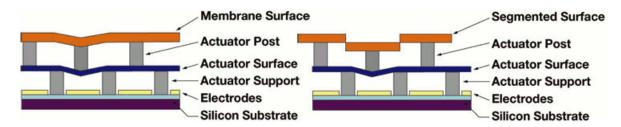
Figure 3.4 Cross sectional schematics of the main components of BMC's continuous (left) and segmented (right) MEMS deformable mirrors. Picture courtesy of Michael Feinberg, BMM, (mrf@bostonmicromachines.com).

Continuous membrane mirrors have optimal fill factor and no diffraction effects. Hence, this type of mirrors are used when high power dissipation is an issue, e.g., laser micromachining, and when high-order corrections are needed, e.g., astronomy. However, they have limited deformation range, are slower than segmented mirrors, and suffer from crosstalk [31, 36]. Therefore, more elaborated control algorithms are required to overcome these drawbacks.

In terms of actuators, two ubiquitous technologies are: piezo-stack DMs and Micro Electro Mechanical System (MEMS) DMs. MEMS-DMs are the most popular one because of their simple structural geometry, flexible operation, and easy fabrication from standard and well-understood materials [54]. Electrostatic actuation is also the dominant scheme used for MEMS deformable mirrors in adaptive optics applications [109, 32, 75, 111, 95].

In this work, we use a relatively simple model for MEMS-actuated continuous facesheet DM displacement based on the thin plate theory [102]. Henceforward, we use the term DM to refer to this type of deformable mirrors, unless otherwise mentioned.

The considered DM, as shown in Fig. 3.5, consists of two coupled mechanical subsystems: a continuous flexible membrane facesheet and an array of N by N micro-actuators connected to the facesheet via rigid posts, all integrated together on a common silicon substrate using micro fabrication technology.

When the DM is in static equilibrium, forces due to the actuators acting on the mirror are balanced by restoring forces due to flexure of the membrane. If the rigid posts are relatively small, the membrane is of uniform thickness, and the displacement is small relatively to the
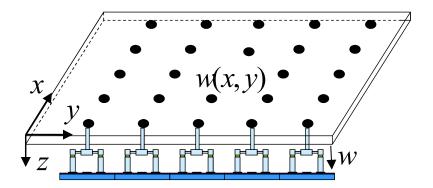
Figure 3.5 Schematic representation of the MEMS-DM. The downward displacement corresponds to positive direction.

Equation (3.1) describes the steady-state behavior of the DM. In open loop DM control, the coefficient p_{ij} is computed by inverting the solution of this equation empirically or theoretically, and is called the influence function [32, 107].

To deal with the dynamic control problem, we need to take into account the transient behavior of the system as well. The transient behavior of the mirror can be captured in the model by adding the second time derivatives of the displacement as in wave propagation equations. Hence, the dynamic of the membrane mirror can be presented as follow:

$$\sigma d \frac{\partial w^2(x,y)}{\partial^2 t} + D\nabla^4 w(x,y) = \sum_{i=1}^{n_x} \sum_{j=1}^{n_y} p_{ij}\delta((x,y) - (x_i, y_j)), \quad (3.2)$$

where σ and d denote the mass density and the thickness of the plate, respectively.

For each actuators, we employ an algebraic model:

$$z_{ij} = f(p_{ij}, V_{ij}), \quad i = 1, \cdots, n_x, \ j = 1, \cdots, n_y, \quad (3.3)$$

where z_{ij} denotes vertical deflection of the actuator at (x_i, y_j); p_{ij} as mentioned denotes the load on the facesheet; V_{ij} denotes the "command voltage" applied to the actuator at (x_i, y_j), and f is a function describing the relationship between the voltage and load of the MEMS actuator to the vertical displacement and usually considered a nonlinear ordinary differential

equation (see, e.g., [75, 111]). Since the actuators are firmly attached to the membrane facesheet, coupling conditions will be:

$$w(x_i, y_j) = z_{ij}, \quad i = 1, \cdots, n_x, \ j = 1, \cdots, n_y. \tag{3.4}$$

As a result, the governing model for this device may be represented by the partial differential equation (3.2) coupled with $n_x \times n_y$ nonlinear ordinary differential equations of the MEMS actuators. This is not a easy model to start our control design. Hence, we address some simplifying assumptions, in the following section, to reduce the complexity of the model.

3.5 Simplifying Assumptions on the Model

To reduce the complexity of the model, we start with the MEMS actuators of the system. The dynamics of MEMS actuators which represent the relationship between input voltages and vertical displacements as represented in (3.3) are highly nonlinear (see, e.g., [75, 111]). However, if we assume that the actuators are operating in a stable domain [95], and also their dynamics is sufficiently faster than that of the membrane mirror, then we can ignore the nonlinear dynamics of the actuators. Furthermore, since the focus of this research work is on the shape control of deformable mirrors, considering Dirac delta functions to describe the behaviour of the actuators in the domain of the PDE system is a reasonable assumption. This assumption is sufficient for our control development, especially because the dimension of the rigid posts is much smaller than that of the membrane mirror. Hence, they can be considered as point-wise actuators. As a result, the coupled PDE-ODE model of the device can be reduced to a PDE system with in-domain point-wise control inputs represented by Dirac delta functions.

Mathematically speaking, in order to have this model controllable, the system should have a unique solution. To address this issue, we have to associate a set of proper boundary conditions to the model. The boundary conditions have to describe the physical behaviour of the structure. We assume the membrane mirror is suspended at two ends and supported at two other ends. Note that this suspended-supported boundary conditions are standard conditions for plate and beam equations that facilitate well-posedness and controllability studies of the model and also describe well the structure of a large-scale deformable mirror. These boundary conditions describe a rectangle segment of the membrane mirror which is terminated with the frame at two sides, and two other sides are suspended on holding rigid posts. We prove the well-posedness and the controllability of the model based on this set of boundary conditions in Chapter 4.

Furthermore, DM deflection is typically measured relative to a "bias" deflection, obtained

when a bias voltage is applied simultaneously to all the actuators. We take this physical property into account by assigning initial conditions to the displacement and the rate of displacement of membrane mirror.

Moreover, by assuming a fully symmetric distribution of the actuators in x-y plane, the plate equation of the large-scale deformable mirror model (3.1) can be reduced to the Cartesian product of two decoupled 1-dimensional systems of Euler-Bernoulli beam equations [16, 17]. Hence, considering this assumption, we limit the control design to one row of actuators located along the x-axis and suppose that the mass of the device is normalized to one unit.

3.6 Lumped Model and Finite-Dimensional Control Design

In this section, we present a simple simulation study based on a finite-dimensional approximation of the model. In this study, a finite element approximation of the model is considered on space which results in a set of lumped ordinary differential equations. Then, a linear-quadratic tracking, LQT, scheme is applied to develop the control law for tracking reference trajectories. This design formally shows the essential steps in control designs based on lumped model. The results of this section has been published in [13].

3.6.1 Control Design of Lumped System

For this design, we consider the beam equation model of the system with one row of actuators located along the x-axis as:

$$w_{tt}(t, x) + Dw_{xxxx}(t, x) = -\sum_{i=1}^{n_x} p_i \delta(x - x_i). \tag{3.5}$$

where w_{tt} and w_{xxxx} represent the second time derivatives and the fourth space derivatives of $w(x, t)$. The goal of the control design is to find p_i to steer the beam along reference trajectories. Note that the open-loop approaches for deformable mirrors aim at finding a static p_i, the so-called influence functions. However, in closed-loop control schemes, p_i is computed dynamically.

To carry out the control design, we discretize w_{xxxx} on space. More specifically, we approximate the fourth time space derivatives of w based on a linear combination of the actuators as stencil points. Then, we may apply an optimal quadratic tracking control to drive the quasi-ODE system resulting from space discretization. Assuming that $w(t, x)$ is sufficiently smooth in space, i.e., at least n times continuously differentiable, the Taylor

series expansion of w at each point x_i in the stencil about $\bar{x}$ obtains as:

$$w(t, x_i) = w(t, \bar{x}) + (x_i - \bar{x})w'(t, \bar{x}) + \cdots + \frac{(x_i - \bar{x})^k}{k!} w^{(k)}(t, \bar{x}) + \cdots , \quad i = 1, \cdots, n. \quad (3.6)$$

Our aim is to find a linear combination of stencil points that agree with $w_{xxxx}(t, x)$ up to a certain order. Therefore, we write:

$$c_{i1}w(t, x_1) + c_{i2}w(t, x_2) + \cdots + c_{in}w(t, x_n) = w_{xxxx}(t, x_i) + O(h^p), \quad (3.7)$$

where $O(h^p)$ is the error of the pth order approximation and h is the mesh width, equal to the absolute distance between two adjacent actuators. The coefficients c_{ij} may be obtained from the following algebraic equation [69]:

$$\frac{1}{(i-1)} \sum_{j=1}^{n_x} c_{ij}(x_j - \bar{x})^{(i-1)} = \begin{cases} 1, & \text{if } i - 1 = 4 \\ 0, & \text{othewise} \end{cases} \quad i = 1, \cdots, n_x. \quad (3.8)$$

For $n_x > 4$, the bi-harmonic operator can be represented in the following matrix form:

$$A_d = [c_{ij}], \qquad i = 1, \cdots, n_x; j = 1, \cdots, n_x.$$

Substituting this matrix form in (3.5) leads to the following quasi-ODE form:

$$\frac{\partial W^2(t)}{\partial^2 t} + DA_dW(t) = F, \quad (3.9)$$

where $W(t) = [w_1(t), w_2(t), \cdots, w_{n_x}(t)]^T$ and $F = [f_1, f_2, \cdots, f_{n_x}]^T$. F may be obtained from controller synthesis part. Letting W and W_t be the state variables and denoting

$$X^T = [W^T \quad W_t^T],$$

(3.9) can be written in state-space form as:

$$\begin{aligned} \dot{X} &= AX + BU, \\ Y &= CX, \end{aligned} \quad (3.10)$$

where $A = \begin{bmatrix} \mathbf{0} & I_{n_x} \\ -DA & \mathbf{0} \end{bmatrix}$, $B = \begin{bmatrix} \mathbf{0} \\ I_{n_x} \end{bmatrix}$, and $U = F$. In these matrices, $\mathbf{0}$ is the null matrix with appropriate dimension and I_{n_x} represents the identity matrix. Y is the measured output which is defined as face-sheet displacement at actuators' posts. Therefore, $C = [I_{n_x} \quad \mathbf{0}_{n_x}]$.

Now, we can apply LQT scheme to compute the state feedback control law. As our objective is to bring the state X to approach a reference X_{ref}, we impose a new variable $Z(t) = X(t) - X_{ref}$. The LQT problem amounts then to find a control U which would minimize the cost function:

$$J_{LQR} = \int_0^\infty (Z^T Q Z + \rho U^T R U) dt, \qquad (3.11)$$

subject to System (3.10), where Q is an $2n_x \times 2n_x$ symmetric positive-semi-definite matrix, R is an $n_x \times n_x$ symmetric positive-definite matrix, and ρ is a positive constant. The first term in the integral corresponds to the energy of the controlled output and the second one corresponds to the energy of the control signal. Decreasing the energy of the controlled output will require a large control signal and a small control signal will lead to a large controlled output. The role of the constant ρ is to establish a trade-off among these conflicting goals. One static state feedback solution of the LQT problem is:

$$U = -KZ, \qquad (3.12)$$

where K is a $n_x \times 2n_x$ matrix given by:

$$K = \rho R^{-1} B^T P, \qquad (3.13)$$

with P the unique positive-definite solution of the following equation

$$A^T P + PA + Q - \rho P B R^{-1} B^T P = 0,$$

known as the Algebraic Riccati Equation (ARE) [53]. In (3.12) the driving signal that controls the deformation of the beam is computed by system state.

Note that this design requires the measurement of all the state variables. Even with an output-feedback control scheme, a considerable number of measurements are still needed to assure an adequate performance. This is one of the main limitations in the designs based on the lumped model (see, e.g., [14, 81]).

3.6.2 Simulation Study

The simulation study is carried out in the COMSOL software by considering a deformable Poly-Si beam with a length of $2.8 \times 10^{-2} m$ and thickness of $3\mu m$. Consequently, D will be 3.78×10^{-7} for this Poly-Si beam. 8 actuators are uniformly placed along the domain of the system which means in the model we chose $n_x = 8$. The system matrix A can be computed

from (3.8). In order that A could meet the well-posed provision of the bi-harmonic operator, we consider the following boundary conditions:

$$w(0) = 0, \quad w_x(0) = 0, \quad w(L) = 0, \quad w_x(L) = 0.$$

This set of boundary conditions physically means a simply supported beam with slop and deflection set to zero at both ends. Accordingly, we will have:

$$A = \begin{bmatrix} 1 & 0 & 0 & 0 & 0 & 0 & 0 & 0 \\ 250 & -250 & 0 & 0 & 0 & 0 & 0 & 0 \\ 250 & -1000 & 1500 & -1000 & 250 & 0 & 0 & 0 \\ 0 & 2500 & -1000 & 1500 & -1000 & 250 & 0 & 0 \\ 0 & 0 & 250 & -1000 & 1500 & -1000 & 250 & 0 \\ 0 & 0 & 0 & 250 & -1000 & 1500 & -1000 & 250 \\ 0 & 0 & 0 & 0 & 0 & 0 & 250 & 250 \\ 0 & 0 & 0 & 0 & 0 & 0 & 0 & 1 \end{bmatrix}.$$

Since the boundaries of the system are fixed, we do not have control over the two extreme points at both ends. Therefore, we extract the skew part of A and denote it by

$$A_d = \begin{bmatrix} 1500 & -1000 & 250 & 0 \\ -1000 & 1500 & -100 & 250 \\ 2500 & -10000 & 15000 & -10000 \\ 0 & 250 & -1000 & 1500 \end{bmatrix}.$$

To design the controller, we chose $Q = C^T \times C$, $R = B^T \times B$, and $\rho = 1$. The LQT controller gain, K, will be given by:

$$K = \begin{bmatrix} \underline{3.79} & 1.55 & 0.08 & -0.14 & \underline{7.59} & 0.20 & 0.01 & -0.02 \\ 1.55 & \underline{4.28} & 1.53 & 0.08 & 0.20 & \underline{7.65} & 0.20 & 0.01 \\ 0.08 & 1.53 & \underline{4.28} & 1.55 & 0.01 & 0.20 & \underline{7.65} & 0.20 \\ -0.14 & 0.08 & 1.55 & \underline{3.79} & -0.02 & 0.01 & 0.20 & \underline{7.59} \end{bmatrix}.$$

Note that the underlined entries indicate the self effect of the actuators. Obviously, every actuator should have the most significant control on itself.

Figures 3.6 to 3.8 represent the simulation results of closed-loop deformation control. [1] In

---

1. Note that the simulation is preformed with a very beginning version of COMSOL software which just provides outputs in JPEG format. The low quality of the depicted results is mainly due to converting this JPEGs to PDF to be used in the LATEX file.

simulation, The desired shape, as shown in Fig. 3.6, is described by $W = -10^{-6}\sin(\frac{2\pi}{2.8}x)e^x$. It can be seen that the system tracks the reference shape with an acceptable tracking error, shown in Fig. 3.8, and the controller drives the beam to the steady-state mode within a reasonable time (Fig. 3.6). It is worth noting that the simulation is carried out in a normalized coordinate. Therefore, the time scale is also normalized. The maximum amplitude of the control signal is approximately 8×10^{-6} (Fig. 3.7) which is a affordable displacement for a MEMS actuator to operate in a stable region. However, in order to avoid the undesired overshot in actuation, one should consider more sophisticated control techniques, such as constrained quadratic control.

3.6.3 Summary and Discussion

In this chapter, we presented the adaptive optics in the context of ground-based telescopes and introduced a dynamic partial differential equation model for deformable mirrors. A controller is designed based on a finite-dimension approximation of the PDE model. The design formally presented the typical steps in control designs based on approximating PDE models to ordinary differential equations. However, this approach requires at least as many sensors as actuators to implement the closed-loop control which is not implementable with the currently available fabrication technologies of DMs.

In addition, the neglected dynamics due to reducing the system to a finite-dimensional model may deteriorate the performance or even destabilize the system, known as the spillover effect in PDE control systems. Thus, a high order approximation is often required in the design for assuring system stability, which in turn might lead to complex control structures. These issues raise serious technological challenges in the design, fabrication, and operation of microsystems. Therefore, it is of great interest to directly deal with the control of PDE models from both theoretical and practical viewpoints.
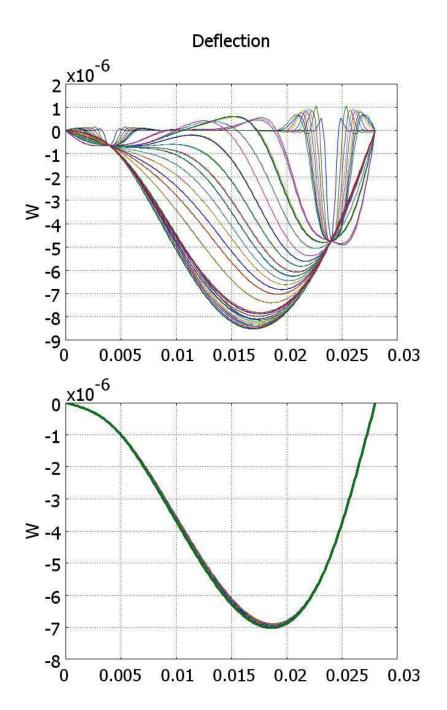
Figure 3.6 Two Snapshots of the beam from the initial state to steady-state; snapshots for $t \in [0\ 0.8]$ presented on the top figure, and for $t \in [0.8\ 1]$ on the bottom.
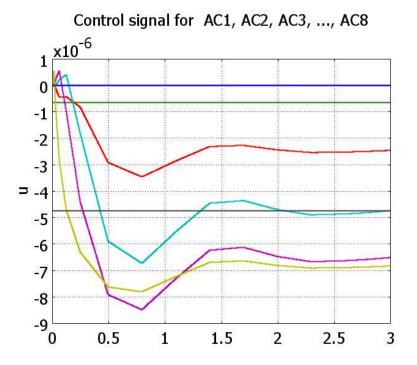
Figure 3.7 Control effort generated on each actuator points, two first and two last actuators are fixed to comply with boundary condition.
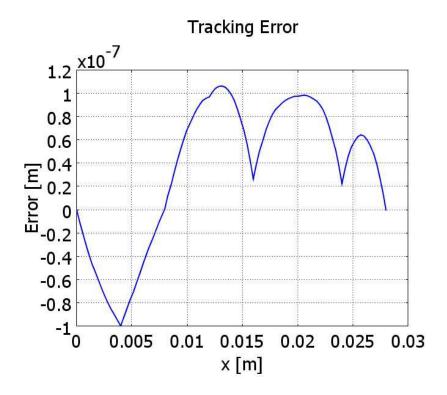

Figure 3.8 The error between the desired and actual trajectory.

CHAPTER 4

CONTROL DESIGN: FLATNESS-BASED DEFORMATION CONTROL OF EULER-BERNOULLI BEAMS WITH IN-DOMAIN ACTUATION

This chapter addresses the main results of this research. In this chapter, we start by presenting an Euler-Bernoulli model of the deformable beam described by a fourth-order partial differential equation, and discussing the well-posedness and controllability of the model. Then, in Section 4.2.3, we develop the Green's function of the system which will be employed later in the control algorithm design. We start the design in Section 4.3 by establishing a formal map between the in-domain controlled system and a standard boundary-controlled model. Based on this map, we develop a control strategy, which is a combination of feedback stabilization and differential flatness-based feed-forward motion planing. This part formally shows a way to deal with the tracking control problem of in-domain controlled PDE systems. However, the map holds only for some special test functions. Thus, since we limit the test functions to some convenient ones, the original PDE is satisfied in a very weak sense, but not in the usual one. To cope with this problem, we develop another design in Section 4.4. In this design instead of trying to establish such an equivalence, we approximate the solution of the original system by that of a target system driven by regularized inputs in the steady state. To do this, we use the technique of lifting to transform the target system, which is controlled by boundary actuators, to an inhomogeneous PDE driven by sufficiently smooth functions generated by applying blobs, used to approximate the Dirac delta functions. This would allow establishing a relationship between the original system and the target system in a usual weak sense. Theorem 4.6 entails this issue. Moreover, the transient behavior, the stability of the closed-loop system, and the regulation error dynamics are addressed in Theorem 4.8 and Corollary 1.

4.1 Notation

For the purpose of clarity, we recall the notations, most of which are defined in Chapter 2.

Let $\mathbb{R}$ be the field of all real numbers. For $n \geq 1$, $\mathbb{R}^n$ denotes the n-dimensional Euclidean space with norm $\|x\|$ and inner product $\langle x, y \rangle$ for all x and y in $\mathbb{R}^n$. Let Ω be a nonempty open subset of $\mathbb{R}^n$. Denoting by $\partial\Omega$ the boundary of Ω, then $\bar{\Omega} = \Omega \cup \partial\Omega$ is the closure of Ω. Given a continuous linear map L between two Hilbert space and letting H be a Hilbert space, $L^p(\Omega)$, $p > 0$, will be the normed linear space of all equivalent classes of Lebesgue-measurable

functions from Ω into H, which are p-integrable or essentially bounded if $p = \infty$. Denote by $C^m(\Omega)$ the space of m-times boundedly continuously differentiable function from Ω into H. For $m \geq 1$, $H^m(\Omega)$ denotes the Hilbert space of all real-valued functions in $L^2(\Omega)$ of which the first m^{th} distributional derivatives belong to $L^2(\Omega)$.

4.2 Basic Properties of the Considered System

4.2.1 System Modeling

In this subsection, we briefly recall the main results from Section 3.4 for a one-dimensional deformable mirror.

As shown in Fig. 4.1, the considered device consists of a continuous flexible beam and an array of N micro-actuators connected to the beam via rigid spots. As the dimension of the spots connecting the actuators to the continuous surface is much smaller than the extent of the beam, the effect of the force generated by actuators at rigid spots is considered as a pointwise control, which can be represented by Dirac delta functions concentrating at rigid spots. The displacement of the beam at the position x and the instant t is denoted by $w(x,t)$. For notational simplicity, we do not show all the variables of functions if there is no ambiguity, e.g., $w = w(x,t)$. The derivatives of w with respect to its variables are denoted by w_x and w_t, respectively. The dynamic transversal displacement of the beam with constant mass density ρ and flexural rigidity EI normalized to one and point actuators located at $\{x_1, x_2, \cdots, x_N\}$, can be described by the following PDE [102, 25]:

$$w_{tt}(x,t) + w_{xxxx}(x,t) = \sum_{i=1}^{N} \alpha_i(t)\delta(x - x_i), \quad x \in \Omega, t > 0, \tag{4.1a}$$

$$w(0,t) = w_x(1,t) = w_{xx}(0,t) = w_{xxx}(1,t) = 0, \tag{4.1b}$$

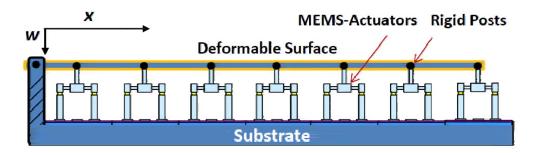$$w(x,0) = h_0(x), w_t(x,0) = h_1(x), \quad x \in \Omega, \tag{4.1c}$$

Figure 4.1 Schematic of the deformable microbeam.

where x is a normalized variable spanned over the domain $\Omega = (0,1)$, $\delta(x - x_i)$ is the Dirac mass concentrated at the point $x_i \in \Omega$, denoting the actuation spots, and $\alpha_i : t \mapsto \mathbb{R}$, $i = 1, \ldots, N$, are the control signals. h_0 and h_1 represent the initial values of the displacement and its time-derivative associated with the beam. The boundary condition (4.1b) means that the beam is simply supported at $x = 0$ and the shear hinged at $x = 1$. Without loss of generality, we assume that $0 < x_1 < x_2 < \cdots < x_N < 1$.

Remark 4.1 *The boundary conditions given in* (4.1b) *capture well the property of the structure that is suspended at the left end and supported by a vertically moving actuator at the right end. Note that for other bending schemes, such as clamped-clamped and clamped-free configurations, the boundary conditions are different, which may lead to different feedback stabilization strategies [25]. Nevertheless, the system architecture and the procedure for feedforward control design remain the same.*

Remark 4.2 *The considered problem can also be modeled as a serially connected beam [25]. Indeed, these two models are equivalent in the sense that they lead to the same abstract linear system in variational form (see, e.g., [92, 25, 60, 62, 61]).*

Remark 4.3 *Electrostatic actuation is one of the dominant schemes used for MEMS deformable mirrors [107, 32]. However, the dynamics of electrostatic MEMS are highly nonlinear and performance enhancement of such devices is a challenging topic (see, e.g., [75, 111]). In this research, we concentrate on shape control of deformable mirrors while ignoring the dynamics of the actuators, which is supposed to be sufficiently faster than the dynamics of the structure. Moreover, we suppose that the actuators are working in the stable operation range [95]. In fact, considering the dynamics of the actuators will lead to a coupled PDE-ODE control problem.*

The control objective is to steer the beam displacement, $w(x, t)$, to follow a desired form described by $w_d(x, t)$ via in-domain pointwise actuation.

The model given in (4.1) is a nonstandard PDE due to the in-domain pointwise actuation, represented by Dirac functions, on the right-hand side of (4.1a). Thus, the classical definition of derivative cannot be applied. Therefore, we will invoke the weak derivative notion of a solution to this model in the weak sense [89].

Specifically, (4.1) does not admit strong solutions in the classic sense for $w \in C^4([0 \ T] \times \Omega \backslash \{x_i\}_{1 \leq i \leq N}) \bigcap C^3([0 \ T] \times \bar{\Omega})$ because of the unbounded Delta dirac functions on the right-hand-side of (4.1a). However, in practice, there exist functions that satisfy this differential equation, except they are not sufficiently smooth. A typical example of this type of situations is the impulse response of a (finite- or infinite-dimensional) system, which is indeed physically

meaningful, although it is only differentiable up to a finite order. Such functions are called weak or generalized solutions to the corresponding differential equation.

The weak solution of a PDE can be defined by means of weak derivative in the theory of distributions [89]. To find the weak derivatives, the system is multiplied by a sufficiently smooth function with a compact support, called test function. Then, integrating over the domain results in a sufficiently smooth function coming from the rough distribution. Applying integration by part and Green's formula, up to a certain problem-dependent order, will enable the definition of the derivatives of distributions. To this end, we start by defining the convergence on $C_0^\infty(\Omega)$.

Definition 4.1 *Let Ω be a domain in $\mathbb{R}(n \geq 1)$. A sequence $\{\varphi_j\}$ of functions belonging to $C_0^\infty(\Omega)$ converges to $\varphi \in C_0^\infty(\Omega)$, if*

(i) there exists $K \subset \Omega$ such that $supp(\varphi_j - \varphi) \subset K$ for every j, and

(ii) $\lim_{j \to \infty} \partial^\alpha \varphi_j(x) = \partial^\alpha \varphi(x)$ uniformly on K for each multi-index α.

The linear space $C_0^\infty(\Omega)$ having the above properties is called fundamental space, denoted by $\mathscr{D}(\Omega)$. The space of all linear continuous functionals on $\mathscr{D}(\Omega)$, denoted by $\mathscr{D}'(\Omega)$, is called the space of (Schwartz) distributions on Ω, which is the dual of $\mathscr{D}(\Omega)$ (see, e.g., Chapter 1 of [2] for more properties of $\mathscr{D}(\Omega)$ and $\mathscr{D}'(\Omega)$).

Denote the set Φ by

$$\Phi = \left\{ \phi \in H^2(0,1); \phi(0) = \phi_x(1) = 0 \right\}. \tag{4.2}$$

In the following definition, we define a weak solution of (4.1).

Definition 4.2 *Let $T > 0$ and $\alpha_i \in L^2(0,T)$ for $i = 1, 2, ..., N$. Let $h_0 \in \Phi$, $h_1 \in L^2(0,1)$. A weak solution to the Cauchy problem (4.1) is a function $w \in C([0,T]; \Phi) \cap C^1([0,T]; L^2(0,1))$, satisfying*

$$w(x,0) = h_0(x), \quad x \in (0,1),$$

such that, for every $v \in C^1([0,T]; \Phi)$, one has for almost every $\tau \in [0,T]$

$$
\int_0^1 w_t(x,\tau)v(x,\tau)\,dx - \int_0^1 h_1(x)v(x,0)\,dx
$$
$$
- \int_0^\tau \int_0^1 w_t(x,t)v_t(x,t)\,dx\,dt
$$
$$
+ \int_0^\tau \int_0^1 w_{xx}(x,t)v_{xx}(x,t)\,dx\,dt
$$
$$
= \sum_{i=1}^N \int_0^\tau \int_0^1 \alpha_i(t)\delta(x - x_i)v(x,t)\,dx\,dt. \tag{4.3}
$$

For every $v \in C^1([0,T]; \Phi)$, the function $w(x,t)$ given by 4.3 is a weak solution for the system. In the next section, we study the uniqueness of this solution through well-posedness analysis of the model.

4.2.2 Well-Posedness and Controllability of the Model

In the investigation of the well-posedness of the considered system, we employ the formulation of Cauchy problem for abstract linear control systems, which enables the application of the framework of semigroup theory [27, 29, 104]. More specifically, in this framework the assessment of well-posedness amounts to showing that if the system is defined on an appropriate Hilbert space, then by Riesz' representation theorem there exists a unique solution to the problem (see, e.g., Page 52 of [89] and Chapter 1 of Part II in [19]).

Let $X = \Phi \times L^2(0,1)$, where Φ is defined in (4.2), be a Hilbert space equipped with appropriate inner product and norm. We define the subspace $\mathcal{D}(A) \subset X$ by:

$$
\mathcal{D}(A) = \left\{ (w,v) \in [\Phi \cap H^4(0,1)] \times \Phi \mid w_{xx}(0,t) = w_{xxx}(1,t) = 0 \right\} \tag{4.4}
$$

with the corresponding operator $A : \mathcal{D}(A) \to X$ defined as:

$$
A \begin{pmatrix} w \\ v \end{pmatrix} = \begin{pmatrix} v \\ -w_{xxxx} \end{pmatrix}, \tag{4.5}
$$

where the derivative with respect to x are calculated in the dual space of $\mathcal{D}(A)$, denoted by $\mathcal{D}'(A)$, with respect to the pivot space X.

Denoted by $S(t)$, $t \in [0, +\infty)$, the semigroup generated by A and by $S^*(t)$ the semigroup generated by A^*, the adjoint of A. It can be shown that $\mathcal{D}'(A^*)$, the dual of $\mathcal{D}(A^*)$ with respect to the space X, satisfies [104]

$$
\mathcal{D}(A^*) \subset X \subset \mathcal{D}'(A^*). \tag{4.6}
$$

Moreover, the control operator $B : \mathbb{R}^N \mapsto \mathcal{D}'(A^*)$ is defined as:

$$Br = \begin{pmatrix} 0 \\ \sum_{i=1}^N r_i \delta(x - x_i) \end{pmatrix}, \quad \forall r \in \mathbb{R}^N. \tag{4.7}$$

With the above notations we can translate System (4.1) into the equivalent Cauchy problem described by an abstract linear control system of the following form:

$$\dot{y} = Ay + Bu, \quad y(0) = y^0, \tag{4.8}$$

where $y = \begin{pmatrix} w & w_t \end{pmatrix}^T \in X$ is the state vector, $u : [0, T] \to U$ is the control signal, $U = \mathbb{R}$ is the control space, and $y^0 = \begin{pmatrix} h_0 & h_1 \end{pmatrix}^T$ is the initial condition.

Note that the control operator B in (4.8) is not continuous nor bounded in classical sense. Hence, we are interested in the set of operators for which all the weak solutions of System (4.8) for $u(t)$ given in $L^2((0, T); U)$ and y^0 given in X are continuous X-valued functions, as defined in Definition 2.12.

We start by giving a formal definition of a solution to (4.8). Let $\tau \in [0, T]$ and $\varphi : [0, \tau] \to X$. We take the inner product in X of (4.8) with φ and perform integration on $[0, \tau]$. Using integration by part together with (4.8), we obtain formally:

$$\langle y(\tau), \varphi(\tau) \rangle_X - \langle y^0, \varphi(0) \rangle_X = \int_0^\tau \langle y(t), \dot{\varphi} + A^* \varphi(t) \rangle_X dt + \int_0^\tau \langle u(t), B^* \varphi(t) \rangle_U dt. \tag{4.9}$$

Taking $\varphi = S^*(\tau - t)z(\tau)$, for $\forall z(\tau) \in X$, we have $\dot{\varphi}(t) + A^* \varphi(t) = 0$, which leads to:

$$\langle y(\tau), z(\tau) \rangle_X - \langle y^0, S^*(\tau)z(\tau) \rangle_X = \int_0^\tau \langle u(t), B^* S^*(\tau - t)z(\tau) \rangle_U dt, \quad \forall \tau \in [0, T], \forall z(\tau) \in X. \tag{4.10}$$

Definition 4.3 *Let $T > 0$, $y^0 \in X$, and $u \in L^2((0, T); U)$. A weak solution to the Cauchy problem (4.8) associated with (4.1) is defined by (4.10) with the regularity $y \in C([0, T]; X)$.*

Based on this definition of solutions, we introduce the following theorem for the well-posedness of the Cauchy problem of abstract linear control systems of the form defined in (4.8) (see Theorem 2.37 in [27], Page 53), and a proposition from [5] that we use later to prove the uniqueness of the solution.

Theorem 4.1 *Let $T > 0$. Then for every $y^0 \in X$ and every $u \in L^2((0, T); U)$, the Cauchy problem (4.8) has a unique solution y if A is a generator of a strongly continuous semigroup $S(t)$ and B is admissible for $S(t)$ on X.*

Theorem 4.2 (Proposition 2.1 [5]) *If $y^0 = (w^0, w^1) \in X$, then for the problem (4.8) we have:*

$$\| \varphi(\xi, \cdot) \|^2_{H^1(0,T)} \leq C \left(\| w^0 \|^2_{H^2(0,1)} + \| w^1 \|^2_{L^2(0,1)} \right), \tag{4.11}$$

where C is a positive constant which depends only on ξ and T.

The following theorem states the well-posedness property of (4.1) presented in the abstract form (4.8).

Theorem 4.3 *Let $T > 0$ and denote $\alpha(t) = (\alpha_i(t), \ldots, \alpha_N(t))$. Then for every $y^0 = (w^0, w^1) \in X$ and every $u(t) = \alpha(t) \in L^2((0,T);U)$, the Cauchy problem (4.8) associated to (4.1) has a unique solution $y \in C([0,T]; X)$ defined by (4.10).*

Proof. Since A is skew-adjoint, by Stone's theorem [27], it generates a strongly continuous semigroup of isometries $S(t)$ on X. Hence, based on Theorem 4.1, it is sufficient to show that the control operator B expressed by (4.7) is admissible for $S(t)$ on X.

According to (4.7), the operator $B^* : \mathcal{D}(A^*) \mapsto \mathbb{R}^N$ is given by:

$$B^* \begin{pmatrix} w \\ v \end{pmatrix} = \sum_{i=1}^{N} v(\xi_i), \quad \forall \begin{pmatrix} w \\ v \end{pmatrix} \in \mathcal{D}(A^*). \tag{4.12}$$

This implies that

$$B^* S^*(t) \begin{pmatrix} w^0 \\ w^1 \end{pmatrix} = \sum_{i=1}^{N} \varphi_t(\xi_i), \quad \forall \begin{pmatrix} w^0 \\ w^1 \end{pmatrix} \in \mathcal{D}(A^*). \tag{4.13}$$

According to Theorem 4.2 and Equation (4.13), we deduce that for all $T > 0$, there exists a constant $C_T > 0$ such that

$$\int_0^T \left\| B^* S^*(t) \begin{pmatrix} w^0 \\ w^1 \end{pmatrix} \right\|^2 dt \leq C_T \left\| \begin{pmatrix} w^0 \\ w^1 \end{pmatrix} \right\|^2_X, \quad \forall \begin{pmatrix} w^0 \\ w^1 \end{pmatrix} \in \mathcal{D}(A^*). \tag{4.14}$$

This implies that the operator B is regular for $S(t)$ on X. From Theorem 4.1, we can conclude then on the existence and the uniqueness of the solution to the Cauchy problem (4.8) associated to System (4.1). $\qquad\square$

Remark 4.4 *The well-posedness of a similar system with only one in-domain input has been shown in [5] (Proposition 3.1). In such a case, $B : \mathbb{R} \mapsto \mathcal{D}'(A^*)$. Therefore, Theorem 4.3 can be seen as a direct extension of this result.*

For the controllability of the system from Chapter 2, we have:

Theorem 4.4 *System (4.8) is exactly controllable in $[0; T]$ for any finite $y^0 \geq 0$ if A gener-ates a stable C_0-semigroup and B is unbounded but admissible.*

Proof. The admissibility of the unbounded operators B is shown in the well-posedenss study. Hence, showing the stability of C_0-semigroup generator A will complete the proof. This issue is addressed in Section 4.4.3. $\qquad \square$

4.2.3 Green's Functions for Euler-Bernoulli Beams

One of the main contribution of this work is to leverage the Green's function in the design. It is shown that a finite set of the Green's functions of the system can be used to approximate desired trajectories. Therefore, an exact invertible and finite-dimensional input to output map can be obtained without invoking any truncations. It also facilitates the real time implementation of the design since the decomposition of desired trajectories can be assessed *a priori*.

This subsection recalls some basic notation, properties, and results related to the Green's function, which will be employed later in control algorithm development. The Green's function is a basic tool in the study of PDEs and there exists a rich literature on this topic (see e.g., [91]). In this research, we are particularly interested in the static Green's function corresponding to the steady-state beam equation, which will be used in our design.

Consider a generic form of steady-state equation corresponding to the beam equation (4.1) with an arbitrary excitation function, $f(x)$:

$$\overline{w}_{xxxx}(x) = f(x), \quad x \in \Omega, \tag{4.15a}$$

$$\overline{w}(0) = \overline{w}_x(1) = \overline{w}_{xx}(0) = \overline{w}_{xxx}(1) = 0. \tag{4.15b}$$

For a point-wise actuation scheme described by System (4.1), the source term is of the form $\sum_{i=1}^{N} \overline{\alpha}_i \delta(x - x_i)$, where $\overline{\alpha}_i$, $i = 1, \cdots, N$, represent the steady-state actuation signals. The static Green's function, or the Green's function for short, corresponding to (4.15), denoted by $G(x, \xi)$, is the solution to such an equation for $f(x) = \delta(x - \xi), x, \xi \in \Omega$, with homogeneous boundary conditions.

The Green's function $G(x, \xi)$ can be calculated by measuring the response of the system at point x for the pressure applied at the point ξ. Therefore, it can be seen as the impulse response of the system, which is an essential and important property for system analysis. Based on the principle of superposition for linear systems, the solution to the steady-state

beam equation (4.15) can be expressed in terms of the Green's function as:

$$\overline{w}(x) = \int_\Omega G(x, \xi) f(\xi) d\xi. \tag{4.16}$$

Obviously, the domain of the Green's function is determined by the original system.

When the actuator makes vertical movement at the point $x = \xi$, based on the continuity condition, the displacement, the rotation, and the bending force from the left and right side of this point are identical. That is $G(x, \xi^-) = G(x, \xi^+)$, $G_x(x, \xi^-) = G_x(x, \xi^+)$, and $G_{xx}(x, \xi^-) = G_{xx}(x, \xi^+)$. Meanwhile, this movement will generate a shear force, represented by the jump $G_{xxx}(x, \xi^+) - G_{xxx}(x, \xi^-) = 1$ [25]. Solving (4.15a) and applying continuity, jump, an boundary conditions (4.15b), we obtain the Green's function for System (4.15), which is given by

$$G(x, \xi) = \begin{cases} \left(-\dfrac{x^3}{6} + x\xi \left(1 - \dfrac{\xi}{2} \right) \right), & 0 \leq x < \xi; \\ \left(-\dfrac{\xi^3}{6} + \xi x \left(1 - \dfrac{x}{2} \right) \right), & \xi \leq x \leq 1. \end{cases} \tag{4.17}$$

The Green's function is used for two different purposes in our design. First, this function is used to construct test functions in the development of a map between the in-domain and boundary data. Secondly, the property given in (4.16) is employed to generate reference trajectories in motion planning. As shown latter in Section 4.3.3, motion planning for the considered 4th-order beam equitation requires that the base functions must have a continuous 3th-order derivative on space at the actuation points (see (4.42d)). However, the Green's function given in (4.17) is only of H^2 over Ω. A solution for overcoming this problem is the use of regularized Green's functions that are sufficiently smooth.

Different from the Green's function that is the response to the Delta dirac input, a regularized Green's function, denoted by $\widetilde{G}$, is generated by using a cutoff function, also called *blob*, as the input to the system. Driving the steady state equation (4.15) by a blob of the following form [28]:

$$\varphi_\delta(x - \xi) = \frac{3\delta}{4((x - \xi)^2 + \delta^2)^{5/2}}, \tag{4.18}$$

where δ is a small scaling parameter, the corresponding regularized Green's function is given by:

$$\widetilde{G}(x, \xi) = \frac{1}{12} \left((x - \xi)^2 + \delta^2 \right)^{3/2} + Ax^3 + Bx^2 + Cx + D, \tag{4.19}$$

where

$$A = \frac{(2(\xi - 1)^2 + 3\delta^2)(\xi - 1)}{4((\xi - 1)^2 + \delta^2)^{3/2}}, \tag{4.20a}$$

$$B = -(\delta^2 + 2\xi^2)/(4(\delta^2 + \xi^2)^{1/2}), \tag{4.20b}$$

$$\begin{aligned} C =& (\delta^2 + 2\xi^2)/(4(\delta^2 + \xi^2)^{(}1/2)) - ((2(\xi - 1)^2 + 2\delta^2) \\ & \times (\xi - 1) + \delta^2(\xi - 1))/(8((\xi - 1)^2 + \delta^2)^{3/2}) \\ & + (((\xi - 1)^2 + \delta^2)^{1/2}(\xi - 1))/4, \end{aligned} \tag{4.20c}$$

$$D = -(\delta^2 + \xi^2)^{3/2}/12. \tag{4.20d}$$

Note that for $\forall \delta > 0$, the blob given in (4.18) satisfies

$$\int_{-\infty}^{\infty} \varphi_\delta(x)dx = 1. \tag{4.21}$$

It can also be shown that the regularized Green's function generated by the blob defined in (4.18) gives an approximation of the Green's function with $O(\delta^2/x^2)$ and $\tilde{G}$ converges to G as $\delta \to 0$ [28].

4.3   The First Design: Mapping In-domain Actuation into Boundary Control

The control scheme presented in this section consists in first mapping the original nonhomogeneous model into a target system in a standard boundary control form. The system has a finite number of actuators which means the control space is of finite dimensions whereas the degree of freedom (DOF) of the system is of infinite dimensions. This underactuated property of the system is solved by splitting reference trajectories into a finite set of sub-trajectories based on an essential property of the Green's functions. The technique of flatness-based trajectory planning can then be readily applied to boundary controls introduced in the formulation of the target system. A standard closed-loop feedback control is used to stabilize the system around the desired trajectories. The combination of feedback stabilization and feedforward motion planning results in an asymptotic tracking control law allowing the system to follow prescribed trajectories.

4.3.1   Mapping In-domain Actuation into Boundary Control

To circumvent the complexity introduced by unbounded in-domain actuators in the model (4.1), we start by introducing a formal map that will transform this nonstandard problem into a standard boundary control form to which existing stabilization and control methods may be applied. To this end, we consider the following target system described by

a homogenous initial-boundary value PDE:

$$u_{tt}(x,t) + u_{xxxx}(x,t) = 0, \quad x \in \Omega, t > 0, \tag{4.22a}$$

$$u(0,t) = u_x(1,t) = u_{xx}(0,t) = 0, \quad t > 0, \tag{4.22b}$$

$$u_{xxx}(1,t) = g(t), \quad t > 0, \tag{4.22c}$$

$$u(x,0) = h_0(x), u_t(x,0) = h_1(x), \quad x \in \Omega, \tag{4.22d}$$

where $g(t)$ is the control placed on the boundary and the other variables are defined in (4.1). Our aim is to find a relationship that maps the effect of the actuation signals appearing on the right-hand side of (4.1a) to the boundary control $g(t)$ in (4.22c), representing a shear force. Note that (4.22) is an abstract mathematical model used in control design, which does not describe the physical system operated by multiple interior actuators.

Our goal is to ensure that Systems (4.1) and (4.22) have an identical weak solution. The weak solution to Systems (4.1) is introduced in Section 4.2. The weak solution to (4.22) can be obtained by repeating the same procedure. We multiply (4.22) by a test function $v \in C^1([0,T]; \Phi)$, where Φ is defined in (4.2). Then, the weak solution in integral form can be derived by integration over $[0,\tau] \times \Omega$, with $\tau \in [0,T]$. We can then obtain the following equations using integration by parts twice on the term $w_{tt}(x,t)v(x,t)$, and Green's formula [48] two times on the term $w_{xxxx}(x,t)v(x,t)$:

$$\langle u_t(x,t), v_t(x,t) \rangle_{(\tau,\Omega)} + \langle u_{xx}(x,t), v_{xx}(x,t) \rangle_{(\tau,\Omega)}$$
$$- \int_\Omega (h_1(x)v(x,0) - u_t(x,\tau)v(x,\tau)$$
$$+ u(x,\tau)v_t(x,\tau)) \, dx + \int_0^\tau \int_{\partial\Omega} v_x(x,t)u_{xxx}(x,t)d\omega dt$$
$$- \int_0^\tau \int_{\partial\Omega} v_{xx}(x,t)u_{xx}(x,t)d\omega dt = 0, \tag{4.23}$$

where

$$\langle f(x,t), g(x,t) \rangle_{(\tau,\Omega)} = \int_0^\tau \int_\Omega f(x,t)g(x,t)dxdt \tag{4.24}$$

denotes a spatio-temporal inner product, and $d\omega$ denotes the integration variable on the boundary where $x = 0$ and $x = 1$ are the boundary points for this system. By applying the

boundary conditions given in (4.22c), and (4.22b), we have:

$$
\begin{aligned}
&\langle u_t(x,t), v_t(x,t)\rangle_{(\tau,\Omega)} + \langle u_{xx}(x,t), v_{xx}(x,t)\rangle_{(\tau,\Omega)} \\
&- \int_\Omega (h_1(x)v(x,0) - u_t(x,\tau)v(x,\tau) \\
&+ u(x,\tau)v_t(x,\tau))\, dx + \int_0^\tau \int_{\partial\Omega} v(x,t)g(t)d\omega dt = 0.
\end{aligned}
\tag{4.25}
$$

Finally, a sufficient condition for which Systems (4.1) and (4.61) have an identical weak solution can be obtained by subtracting (4.25) from (4.3):

$$
\int_{\partial\Omega} v(x,t)g(t)d\omega - \sum_{i=1}^N \int_\Omega \alpha_i(t)v(x,t)\delta(x-x_i)dx = 0.
\tag{4.26}
$$

To find a closed-form expression for $g(t)$, we choose a test function of the form:

$$
v(x) = \sum_{j=1}^N G(x,\xi_j),
\tag{4.27}
$$

where $G(x,\xi_j)$, $j = 1,\cdots,N$, are computed from (4.17).

Note that a wide class of functions can be considered as a candidate for test functions, for example a function formed by the eigenfunctions of the system. The reason that the Green's function is chosen as a test function comes primarily from the fact that it leads to a simple solution while guaranteeing the solvability of the map between the boundary value and the actual actuation signals, as shown below.

By substituting (4.27) into (4.26) and using the basic property of Dirac delta functions, we can rearrange (4.26) in terms of $g(t)$ as

$$
g(t) = \sum_{j=1}^N \frac{\sum_{i=1}^N \alpha_i(t)G(x_i,\xi_j)}{\Gamma(\xi_j)},
\tag{4.28}
$$

where

$$
\Gamma = \sum_{m=1}^N \int_{\partial\Omega} G(x,\xi_j)d\omega.
\tag{4.29}
$$

Hence, the map between the in-domain control signals and the corresponding boundary values can be expressed by:

$$
\begin{pmatrix}
G(x_1,\xi_1) & \cdots & G(x_N,\xi_1) \\
\vdots & \ddots & \vdots \\
G(x_1,\xi_N) & \cdots & G(x_N,\xi_N)
\end{pmatrix}
\begin{pmatrix}
\alpha_1(t) \\
\vdots \\
\alpha_N(t)
\end{pmatrix}
= \Gamma
\begin{pmatrix}
g_1(t) \\
\vdots \\
g_N(t)
\end{pmatrix},
\tag{4.30}
$$

with

$$g(t) = \sum_{j=1}^{N} g_j(t) = \frac{1}{\Gamma} \sum_{j=1}^{N} \sum_{i=1}^{N} G(x_i, \xi_j)\alpha_i(t). \tag{4.31}$$

Clearly, (4.30) and (4.31) bridge the nonhomogeneous PDE system (4.1) with the standard boundary control form (4.22). This will allow the use of existing methods to deal with the PDE controlled on the boundary and then applying the results back to the original in-domain actuation signals by inverting (4.30). Note that (4.30) is a static map whose invertibility can be assessed *a priori*. This shows the simplicity of the proposed approach.

Theorem 4.5 *The map given in* (4.30) *is invertible if the test functions as chosen* $v(x) = \sum_{j=1}^{N} G(x, \xi_j)$, $\xi_j, j = 1, \ldots, N$, *are all distinguished, and* $G(x, \xi_j)$ *is of the form*

$$G(x, \xi_j) = \begin{cases} -\dfrac{x^3}{6} + x\xi_j \left(1 - \dfrac{\xi_j}{2}\right), & 0 \le x < \xi_j; \\ -\dfrac{\xi_j^3}{6} + \xi_j x \left(1 - \dfrac{x}{2}\right), & \xi_j \le x \le 1. \end{cases} \tag{4.32}$$

Note that $G(x, \xi_j)$ given in (4.32) is the static Green's function of the beam equation parameterized by ξ_j. It is easy to check that $G(x, \xi_j)$ is a positive, monotonically increasing function and $G(x, \xi_i) \ne G(x, \xi_j)$, $\forall \xi_i \ne \xi_j$ and $x \in (0, 1]$.

   Proof. First, being the fundamental static solution of the beam equation (4.1) corresponding to the input $\delta(x - \xi_j)$, $G(x, \xi_j)$ is in Φ. We need then to proof that the matrix in the left-hand-side of (4.30) formed by Green's functions corresponding to distinguished ξ_js, denoted by $[G(x_i, \xi_j)]_{N \times N}$, is invertible. If, otherwise, $[G(x_i, \xi_j)]_{N \times N}$ is not invertible, then it is of rank less than N. Without loss of generality, assume that there exist $N - 1$ constants, $k_1, k_2, ..., k_{N-1}$, such that

$$G(x_1, \xi_N) = \sum_{i=1}^{N-1} k_i G(x_1, \xi_i), \tag{4.33a}$$

$$G(x_2, \xi_N) = \sum_{i=1}^{N-1} k_i G(x_2, \xi_i), \tag{4.33b}$$

$$\vdots \tag{4.33c}$$

$$G(x_N, \xi_N) = \sum_{i=1}^{N-1} k_i G(x_N, \xi_i). \tag{4.33d}$$

The above equations show that

$$G(x, \xi_N) = \sum_{i=1}^{N-1} k_i G(x, \xi_i) \tag{4.34}$$

has N different positive solutions $x_1, x_2, \cdots x_N$, $x_i \in (0,1)$, $i = 1, \ldots, N$.

We consider two cases:

(i) If $N > 3$, since $\xi_i, i = 1, \ldots, N$, are distinguished, $G(x, \xi_j)$, $i = 1, \ldots, N$, are all different from each other. Hence

$$G(x, \xi_N) \not\equiv k_1 G(x, \xi_1) + k_2 G(x, \xi_2) + \cdots + k_{N-1} G(x, \xi_{N-1}). \tag{4.35}$$

Note that $G(x, \xi_j), j = 1, \ldots, N$, are of order at most 3, then (4.34) has at most 3 different solutions in $\mathbb{R}$, which is a contradiction.

(ii) If $N \leq 3$, it is easy to check that (4.34) has a solution $x = 0$, and a pair of solutions $x = x^0$ and $x = -x^0$ near the origin 0. By the assumption, (4.34) has N different positive solutions, then it must be $N = 1$, which leads to a contradiction with the non-invertible property of $G(x_1, \xi_1) \neq 0$.

$\square$

Remark 4.5 *Note that the map given in (4.30) holds only for some particular test functions. Thus, since we limit the test functions to some convenient ones, the original PDE is satisfied in a very weak sense, but not in the usual one. This caveat is addressed in the next design presented in Section 4.4.*

4.3.2 Feedback Stabilization

According to the method of energy multiplier, the target system (4.22) is exponentially stable if the following condition holds on the boundary (see, e.g., [25] and Theorem 2.3 of [5]):

$$g(t) = w_{xxx}(1, t) = k_g w_t(1, t), \tag{4.36}$$

where $k_g > 0$ is a real-valued constant.

It can be seen from (4.31) that one of the in-domain control signal can be uniquely defined by the stabilizing feedback (4.36) and the other g_js. For notational simplicity, we assign the stabilizing feedback to g_N and hence:

$$g_N(t) = k_g w_t(1, t) - \sum_{j=1}^{N-1} g_j(t). \tag{4.37}$$

In fact, Equation (4.37) constrains the system trajectory to a stable region, yet the remaining $N - 1$ degrees-of-freedom of the system can be used to implement feed-forward control for tracking reference trajectories.

4.3.3 Decomposition of Reference Trajectories and Formal Series-Based Motion Planning

To design the feed-forward controls g_j, $j = 1, \ldots, N-1$, we use the technique of motion planning developed in [58]. In this technique the formal power series is used to parameterize the system inputs and states by a so-called flat output and its time-derivatives.

Assume that the reference trajectory is of the following form:

$$w_d(x,t) = \sum_{j=1}^{N-1} w_d^j(x,t) = \sum_{j=1}^{N-1} \beta_j \widetilde{G}(x, \xi_j) \phi_j(t), \tag{4.38}$$

where β_j is a constant, $\widetilde{G}(x, \xi_j)$ is the regularized Green's function of System (4.15), and $\phi_j(t)$ is a smooth function evolving through time from zero to one. In order that the reference trajectory given in (4.38) be feasible, $\phi_j(t)$ must respect the physical restrictions on control authority, such as rising time.

The motivation of such a decomposition lies on the fact that the Green's function intrinsically meets boundary conditions and the physical properties of the system. In addition, this form of reference trajectory will not only allow achieving the solvability but also be computationally traceable. The parameter β_j can be derived from (4.38) as shown below.

Based on (4.38), the desired profile in steady-state can be expressed as

$$\overline{w}_d(x) = \sum_{j=1}^{N-1} \beta_j \widetilde{G}(x, \xi_j). \tag{4.39}$$

Taking $N-1$ distinguished points along $\overline{w}_d(x)$ and arranging (4.39) in a matrix form, we get:

$$\begin{pmatrix} \beta_1 \\ \vdots \\ \beta_{N-1} \end{pmatrix} = \begin{pmatrix} \widetilde{G}(x_1, \xi_1) & \cdots & \widetilde{G}(x_{N-1}, \xi_1) \\ \vdots & \ddots & \vdots \\ \widetilde{G}(x_1, \xi_{N-1}) & \cdots & \widetilde{G}(x_{N-1}, \xi_{N-1}) \end{pmatrix}^{-1} \begin{pmatrix} \overline{w}_d(x_1) \\ \vdots \\ \overline{w}_d(x_{N-1}) \end{pmatrix}. \tag{4.40}$$

Similar to the map of (4.30), the invertibility of the square matrix in (4.40) can be verified *a priori*.

Motion planing amounts then to taking $w_d^j(x_k, t) \in C^\infty$ as the desired output of the system at x_k and to generating the full-state trajectory $u^j(x, t)$. The control signal can be directly computed from the full-state trajectory, which should force the output $u^j(x_k, t)$ to track the reference output $w_d^j(x_k, t)$.

Consider a configuration in which the reference output and the actuator are co-located at the same point x_j, for $j = 1, \cdots, N-1$. The system dynamics corresponding to the input

g_j are then of the following form:

$$u_{tt}^j(x,t) + u_{xxxx}^j(x,t) = 0, \tag{4.41a}$$

$$u^j(0,t) = u_x^j(1,t) = u_{xx}^j(0,t) = 0, \tag{4.41b}$$

$$u_{xxx}^j(1,t) = g_j(t). \tag{4.41c}$$

In the presence of stabilizing feedback loop, the motion planing design can be process with zero-initial conditions. We are interested in finding the control signal $g_j(t)$ so that the trajectory of the beam (4.41) at x_j meets the following constrains:

$$u^j(x_j,t) = w_d^j(x_j,t) = \beta_j \widetilde{G}(x_j, \xi_j)\phi_j(t), \tag{4.42a}$$

$$u_x^j(x_j,t) = w_{d,x}^j(x_j,t) = \beta_j \widetilde{G}_x(x_j, \xi_j)\phi_j(t), \tag{4.42b}$$

$$u_{xx}^j(x_j,t) = w_{d,xx}^j(x_j,t) = \beta_j \widetilde{G}_{xx}(x_j, \xi_j)\phi_j(t), \tag{4.42c}$$

$$u_{xxx}^j(x_j,t) = w_{d,xxx}^j(x_j,t) = \beta_j \widetilde{G}_{xxx}(x_j, \xi_j)\phi_j(t). \tag{4.42d}$$

To solve this, we consider the method of formal power series [58]. By using the formal power series to approximate the solution of the system for a excitation at point x_j, the full-state trajectory of the system can be expressed as:

$$u^j(x,t) = \sum_{k=0}^{\infty} a_k(t)\frac{(x-x_j)^k}{k!}, \tag{4.43}$$

weighted by time varying coefficients $a_k(t)$. It can be shown by a direct computation that:

$$a_{k+4}(t) = -\ddot{a}_k(t), \quad \forall k \geq 0, \tag{4.44}$$

with

$$a_0(t) = P_0(x_j)\phi_j(t), a_1(t) = P_1(x_j)\phi_j(t), \tag{4.45}$$

$$a_2(t) = P_2(x_j)\phi_j(t), a_3(t) = P_3(x_j)\phi_j(t), \tag{4.46}$$

where $P_0(x_j)$, $P_1(x_j)$, $P_2(x_j)$, and $P_3(x_j)$ computed from reference trajectory $w_j^d(x,t)$ and its

first, second, and third spatial derivatives are given by:

$$P_0(x_j) = \frac{\delta^3}{12} + \frac{A(x_j)}{6}x_j^3 + \frac{B(x_j)}{2}x_j^2 + C(x_j)x_j + D(x_j), \tag{4.47a}$$

$$P_1(x_j) = \frac{A(x_j)}{2}x_j^2 + B(x_j)x_j + c(x_j), \tag{4.47b}$$

$$P_2(x_j) = \frac{\delta}{4} + A(x_j)x_j + B(x_j), \tag{4.47c}$$

$$P_3(x_j) = A(x_j), \tag{4.47d}$$

where A, B, C, and D are:

$$A = \frac{(2(\xi - 1)^2 + 3\delta^2)(\xi - 1)}{4((\xi - 1)^2 + \delta^2)^{3/2}}, \tag{4.48a}$$

$$B = -(\delta^2 + 2\xi^2)/(4(\delta^2 + \xi^2)^{1/2}), \tag{4.48b}$$

$$C = (\delta^2 + 2\xi^2)/(4(\delta^2 + \xi^2)^{(}1/2)) - ((2(\xi - 1)^2 + 2\delta^2)$$
$$\times (\xi - 1) + \delta^2(\xi - 1))/(8((\xi - 1)^2 + \delta^2)^{3/2})$$
$$+ (((\xi - 1)^2 + \delta^2)^{1/2}(\xi - 1))/4, \tag{4.48c}$$

$$D = -(\delta^2 + \xi^2)^{3/2}/12. \tag{4.48d}$$

Therefore,

$$a_{4k} = (-1)^k a_0^{(2k)} = (-1)^k P_0(x_j)\phi_j^{(2k)}(t), \tag{4.49a}$$

$$a_{4k+1} = (-1)^k P_1(x_j)\phi_j^{(2k)}(t), \tag{4.49b}$$

$$a_{4k+2} = (-1)^k P_2(x_j)\phi_j^{(2k)}(t), \tag{4.49c}$$

$$a_{4k+3} = (-1)^k P_3(x_j)\phi_j^{(2k)}(t). \tag{4.49d}$$

The full-state trajectory becomes:

$$u^j(x,t) = \sum_{k=0}^{\infty}\sum_{n=0}^{3} \frac{(-1)^k P_n(x - x_j)^{4k+n}}{(4k + n)!}\phi_j^{(2k)}(t). \tag{4.50}$$

The corresponding input can be computed from (4.41c), which is of the form:

$$
\begin{aligned}
g_j(t) &= \sum_{k=0}^{\infty} \sum_{n=0}^{3} \frac{(-1)^k P_n (4k+n)(4k+n-1)(4k+n-2)}{(4k+n)!} \\
&\quad \times (1-x_j)^{4k+n-3} \phi_j^{(2k)}(t) \\
&= P_3 \phi_j(t) + \sum_{k=1}^{\infty} \sum_{n=0}^{3} \frac{(-1)^k P_n (1-x_j)^{4(k-1)+n+1}}{(4(k-1)+n+1)!} \phi_j^{(2k)}(t) \\
&= P_3 \phi_j(t) - \sum_{k=0}^{\infty} \sum_{n=0}^{3} \frac{(-1)^k P_n (1-x_j)^{4k+n+1}}{(4k+n+1)!} \phi_j^{(2(k+1))}(t).
\end{aligned} \tag{4.51}
$$

(4.50) and (4.51) show that the system trajectory $u^j(x,t)$ and the control input $g_j(t)$ can be parameterized in terms of $\phi_j(t)$ and its time derivatives. Therefore, System (4.41) is (differential) flat with $\phi_j(t)$ as basic output [94]. Hence, the system trajectory and the control input can be directly derived from the prescribed flat output via pure algebraic operations.

To ensure the convergence of infinite series (4.50) and (4.51), we choose the following smooth function [94]:

$$
\phi_j(t) = \begin{cases}
0, & \text{if } t \leq 0 \\[2mm]
\dfrac{\displaystyle\int_0^t \exp(-1/(\tau(1-\tau)))^\varepsilon d\tau}{\displaystyle\int_0^T \exp(-1/(\tau(1-\tau)))^\varepsilon d\tau}, & \text{if } t \in (0, T) \\[4mm]
1, & \text{if } t \geq T
\end{cases} \tag{4.52}
$$

which is known as Gevrey function of order $\sigma = 1 + 1/\varepsilon$, $\varepsilon > 0$ [70].

Proposition 2 *If the basic outputs $\phi_j(t)$, $j = 1, \ldots, N-1$, are chosen as Gevrey functions of order $1 < \sigma < 2$, then the infinite series (4.50) and (4.51) are convergent.*

Proof. We prove the convergence of the power series (4.50) using Cauchy-Hadamard Theorem. The convergence of (4.51) then follows easily using the same argument.

Denote in (4.50):

$$
b_k = \sum_{n=0}^{3} \frac{P_n (x - x_j)^{4k+n}}{(4k+n)!} \phi_j^{(2k)}(t). \tag{4.53}
$$

Then, (4.50) converges if $\limsup_{k \to \infty} \sqrt[k]{|b_k|} < 1$.

For a Gevrey function ϕ_j of order σ, we have [94]:

$$
\exists K, M > 0, \forall k \in \mathbb{N}, \forall t \in [t_0, t_1], \left| \phi_j^{(k+1)}(t) \right| \leq M \frac{(k!)^\sigma}{K^k}. \tag{4.54}
$$

Thus, for $0 < x_j < 1$ and $x \in [0,1]$, b_k can be majorized as:

$$|b_k| < \left| \sum_{n=0}^{3} \frac{P_n}{(4k+n)!} \phi_j^{(2k)}(t) \right|$$
$$< \left| \sum_{n=0}^{3} \frac{P_n}{(4k+n)!} M \frac{((2k)!)^\sigma}{K^{2k}} \right|. \qquad (4.55)$$

Therefore:

$$\limsup_{k\to\infty} \sqrt[k]{b_k} = \limsup_{k\to\infty} \sum_{n=0}^{3} \frac{4}{K^2} (MP_n)^{1/k} \frac{((2k)!)^{\sigma/k}}{((4k+n)!)^{1/k}}$$
$$< \limsup_{k\to\infty} \frac{1}{K^2} \frac{(((2k)!)^{1/2k})^{2\sigma}}{(((4k)!)^{1/4k})^4}. \qquad (4.56)$$

Applying Stirling's formaula $\sqrt[k]{k!} \simeq (k/e)$ yields:

$$\limsup_{k\to\infty} \sqrt[k]{b_k} \le \frac{4e^{4-2\sigma}}{K^2} \limsup_{k\to\infty} \frac{(2k)^{2\sigma}}{(4k)^4}. \qquad (4.57)$$

Since

$$\limsup_{k\to\infty} \frac{(2k)^{2\sigma}}{(4k)^4} = \begin{cases} 0, & \sigma < 2; \\ \frac{1}{16}, & \sigma = 2; \\ \infty, & \sigma > 2, \end{cases} \qquad (4.58)$$

we can conclude by Cauchy-Hadamard Theorem that the radius of convergence of (4.50) is infinity for $\sigma < 2$ and $4K^2$ for $\sigma = 2$. The series (4.50) diverges if $\sigma > 2$.

$\square$

Remark 4.6 *In general, the Gevrey bounds are unknown, but can be estimated following the way presented in [35]. Furthermore, a symmetric function in the transient phase can be considered to improve convergency analysis [35].*

Remark 4.7 *For numerical implementations, (4.51) needs to be truncated to finite terms. An upper bound on truncation errors can be directly computed using the property of Gevrey function given in (4.52) [93].*

Finally, substituting $g_1, \ldots, g_{N-1}$ computed from (4.51) together with g_N computed from (4.37) into (4.30), the in-domain actuation signals α_i, $i = 1, \cdots, N$, can be uniquely determined by the pure algebraic solution of (4.30).

4.4 The Second Control Design: In-domain Actuation Design via Boundary Control Using Regularized Input Functions

In this section, we present another design by approximating the solution of the original system by that of a target system in the steady state. Note that the map established in the previous design holds only for some particular test functions. Thus, the original PDE is satisfied in a very weak sense, which might not hold in the usual one, because the test functions are limited to some convenient ones.

To rectify this caveat, in this new design instead of establishing such an equivalence, we approximate the solution of the original system by that of a target system driven by regularized inputs in the steady state. To this end, we use the technique of lifting to transform the target system, which is controlled by boundary actuators, to an inhomogeneous PDE driven by sufficiently smooth functions generated by applying blobs. Using blob functions to approximate the delta functions would allow establishing a relationship between the original system and the target system in a usual weak sense. This matter is entailed in Theorem 4.6.

Moreover, in order to show that the regulation error dynamics converge to zero, we re-design the feedback controller. The stability of the closed-loop system and the convergence of the regulation error dynamics are assessed in Section 4.4.3. Furthermore, transient behavior and the stability of the closed-loop system and regulation error dynamics are addressed in Theorem 4.8 and Collary 1. Note that for clarity of the notation we change the number of in-domain actuators to $N + 1$ in the model. We use N actuators for feedforward motion planning, and dedicate the $(N + 1)^{\text{th}}$ actuator to the feedback stabilization control of the closed-loop system. Hence, the system model becomes:

$$w_{tt}(x,t) + w_{xxxx}(x,t) = \sum_{j=1}^{N+1} \alpha_j(t)\delta(x - x_j), \ x \in (0,1), \ t > 0, \tag{4.59a}$$

$$w(0,t) = w_x(1,t) = w_{xx}(0,t) = w_{xxx}(1,t) = 0, \ t > 0, \tag{4.59b}$$

$$w(x,0) = h_0(x), w_t(x,0) = h_1(x), \ x \in (0,1), \tag{4.59c}$$

where all the variables are defined in (4.1).

Remark 4.8 *A weak solution to*(4.59) *can be defined similar to Definition 4.2 by changing* N *to* $N + 1$.

4.4.1 Relating In-domain Actuation to Boundary Control

For the feedforward motion planning with N actuators located in the domain, we consider the dynamics of the desired trajectory as follow:

$$w_{tt}^d(x,t) + w_{xxxx}^d(x,t) = \sum_{j=1}^{N} \alpha_j(t)\delta(x - x_j), \ x \in (0,1), \ t > 0, \tag{4.60a}$$

$$w^d(0,t) = w_x^d(1,t) = w_{xx}^d(0,t) = w_{xxx}^d(1,t) = 0, \ t > 0, \tag{4.60b}$$

$$w^d(x,0) = w_t^d(x,0) = 0, \ x \in (0,1). \tag{4.60c}$$

The weak solution of (4.60) can be defined in a similar way as Definition 4.2. Note that it is shown later that the initial conditions given in (4.1c) will be captured by the regulation error dynamics. Therefore, feedforward control design can be carried out based on System (4.60) with zero-initial conditions.

Due to the fact that the model given in (4.60) is driven by unbounded inputs, we will apply a sequence of blobs $\varphi(x - x_j)$ to approximate $\delta(x - x_j)$ in the sense of distributions. We will then show that in steady state, $\overline{w}^d$ can be approximated by a sufficiently smooth function. More specifically, we consider first the following boundary controlled PDE:

$$u_{tt}(x,t) + u_{xxxx}(x,t) = 0, \quad x \in (0,1), \ t > 0, \tag{4.61a}$$

$$u(0,t) = u_x(1,t) = u_{xx}(0,t) = 0, \quad t > 0, \tag{4.61b}$$

$$u_{xxx}(1,t) = g(t), \quad t > 0, \tag{4.61c}$$

$$u(x,0) = u_t(x,0) = 0, \quad x \in (0,1), \tag{4.61d}$$

where $g(t) = \sum_{j=1}^{N} g_j(t)$. Without special statements, we assume that $g_j(t) \in C^3([0,+\infty))$ and $g_j(0) = \dot{g}_j(0) = 0$ for $j = 1,2,...,N$. Note that the motivation behind considering (4.61) as a target system is that it allows leveraging the techniques of boundary control for feedforward control design while avoiding early truncations of dynamic model and/or controller structure.

Definition 4.4 Let $T > 0$. A weak solution to the Cauchy problem (4.61) is a function $u \in C([0,T]; \Phi) \cap C^1([0,T]; L^2(0,1))$ satisfying

$$u(x,0) = u_t(x,0) = 0, \quad x \in (0,1),$$

such that, for every $v \in C^1([0,T]; \Phi)$, one has for almost every $\tau \in [0,T]$

$$\int_0^1 u_t(x,\tau)v(x,\tau)\,dx - \int_0^\tau \int_0^1 u_t(x,t)v_t(x,t)\,dx\,dt \qquad (4.62)$$
$$+ \int_0^\tau g(t)v(1,t)\,dt + \int_0^\tau \int_0^1 u_{xx}(x,t)v_{xx}(x,t)\,dx\,dt = 0.$$

Let $\psi(x,t) = u(x,t) - \sum_{j=1}^N g_j(t)H_j(x)$, where $H_j(x)$, $j = 1,2,...,N$, are defined in $[0,1]$ satisfying

$$H_{jxxxx}(x) = \varphi(x - x_j), \qquad (4.63a)$$
$$H_j(0) = H_{jx}(1) = H_{jxx}(0) = 0, H_{jxxx}(1) = 1, \qquad (4.63b)$$

with $\varphi(x) \in L^2(\mathbb{R})$. Then by lifting, (4.61) can be transformed into the following one with zero boundary conditions

$$\psi_{tt}(x,t) + \psi_{xxxx}(x,t) = -\sum_{j=1}^N \ddot{g}_j(t)H_j(x) - \sum_{j=1}^N g_j(t)H_{jxxxx}(x), \ x \in (0,1), \ t > 0, \qquad (4.64a)$$
$$\psi(0,t) = \psi_x(1,t) = \psi_{xx}(0,t) = \psi_{xxx}(1,t) = 0, \qquad (4.64b)$$
$$\psi(x,0) = \psi_t(x,0) = 0, \ \ x \in (0,1). \qquad (4.64c)$$

In order to relate (4.60) to (4.61), we first establish a relationship between (4.60) and (4.64), especially in steady state. Let $\alpha_j(t) = -g_j(t)$ and suppose that $\lim_{t\to\infty} \alpha_j(t) = \overline{\alpha}_j$ and $\lim_{t\to\infty} g_j(t) = \overline{g}_j$ for $j = 1, \ldots, N$. We have then in steady state:

$$\overline{\psi}_{xxxx}(x) = -\sum_{j=1}^N \overline{g}_j H_{jxxxx}(x) = \sum_{j=1}^N \overline{\alpha}_j \varphi(x - x_j), \ x \in (0,1), t > 0, \qquad (4.65a)$$
$$\overline{\psi}(0) = \overline{\psi}_x(1) = \overline{\psi}_{xx}(0) = \overline{\psi}_{xxx}(1) = 0. \qquad (4.65b)$$

For $j = 1,2,...,N$, given a sequence of blobs $\{\varphi_m(x - x_j)\}$, we seek a sequence of functions $\{H_j^m(x)\}$ such that

$$H_{jxxxx}^m(x) = \varphi_m(x - x_j) \qquad (4.66)$$

with $H_j^m(x)$ satisfying (4.63b) and $\varphi_m(x - x_j) \to \delta(x - x_j)$ in $\mathscr{D}'(0,1)$ as $m \to +\infty$. Therefore, considering (4.65) and the steady-state model of (4.60), we have $\overline{\psi}_m \to \overline{w}^d$ in $C^1([0,1])$ as $m \to +\infty$ (see Theorem 4.6). Hence, to find the feedforward control law, we may consider the systems (4.64) and (4.65).

Lemma 1 *[1] Let $\varphi_m(x) \in L^2(\mathbb{R})$ be defined by*

$$\varphi_m(x) = \frac{1}{\pi} \frac{\sin mx}{x}. \tag{4.67}$$

Then $\varphi_m(x)$ has the following properties:

(i) $\int_{-\infty}^{+\infty} \varphi_m(x)\,dx = \int_{-\infty}^{+\infty} \frac{1}{\pi} \frac{\sin mx}{x}\,dx = 1.$

(ii) $\varphi_m(x) \to \delta(x)$ *in* $\mathscr{D}'(\mathbb{R})$ *as* $m \to \infty.$

By taking φ_m given in (4.67) as the input to (4.66), we get

$$H_j^m(x) = \frac{1}{6}x^3 - \frac{1}{2}x + \int_0^x \int_1^z \int_0^y \int_1^t \varphi_m(s - x_j)\mathrm{d}s\mathrm{d}t\mathrm{d}y\mathrm{d}z.$$

Theorem 4.6 *Let $\varphi_m(x)$ be defined as in Lemma 1. Assume that $\alpha_j(t) = -g_j(t)$ tends to $\overline{\alpha}_j = -\overline{g}_j$ as $t \to \infty$ for all $j = 1, 2, ..., N$. Denote by $\overline{\psi}_j^m$ and by $\overline{w}_j^d$ the steady-state solutions of System (4.60) and System (4.64), respectively. Then $\overline{\psi}_j^m \to \overline{w}_j^d$ in $C^1([0, 1])$ as $m \to +\infty$ for $j = 1, 2, ..., N$.*

Proof. In the steady state, we have

$$\overline{\psi}_{jxxxx}^m(x) = -\overline{g}_j H_{jxxxx}^m(x) = \overline{\alpha}_j \varphi_m(x - x_j), \tag{4.68a}$$

$$\overline{\psi}_j^m(0) = \overline{\psi}_{jx}^m(1) = \overline{\psi}_{jxx}^m(0) = \overline{\psi}_{jxxx}^m(1) = 0, \tag{4.68b}$$

and

$$\overline{w}_{jxxxx}^d(x) = \overline{\alpha}_j \delta(x - x_j), \tag{4.69a}$$

$$\overline{w}_j^d(0) = \overline{w}_{jx}^d(1) = \overline{w}_{jxx}^d(0) = \overline{w}_{jxxx}^d(1) = 0. \tag{4.69b}$$

Taking $v(x) \in \mathscr{D}(0, 1)$ as a test function and integrating by parts, we get

$$\int_0^1 \left(\overline{\psi}_{jx}^m(x) - \overline{w}_{jx}^d(x) \right) v_{xxx}(x)\mathrm{d}x = \overline{\alpha}_j \int_0^1 \left(\varphi_m(x - x_j) - \delta(x - x_j) \right) v(x)\mathrm{d}x.$$

Since $\varphi_m(x - x_j) \to \delta(x - x_j)$ in the sense of distributions as $m \to +\infty$ and $v_{xxx} \in \mathscr{D}(0, 1)$, it follows that $\overline{\psi}_{jx}^m \to \overline{w}_{jx}^d$ in the sense of distributions as $m \to +\infty$ for $j = 1, 2, ..., N$. Furthermore, as $\overline{\psi}_{jx}^m \in L^1(0, 1)$ and $\overline{w}_{jx}^d \in L^1(0, 1)$, we have $\overline{\psi}_{jx}^m \to \overline{w}_{jx}^d$ a.e. in $(0, 1)$ (see Lemma 3.31 of [2], page 74). Then by the continuity of $\overline{\psi}_{jx}^m$ and $\overline{w}_{jx}^d$, we conclude that $\overline{\psi}_{jx}^m \to \overline{w}_{jx}^d$ pointwisely in $(0, 1)$. Therefore $\overline{\psi}_j^m \to \overline{w}_j^d$ in $C^1([0, 1])$ as $m \to +\infty$ for $j = 1, 2, ..., N$. $\square$

4.4.2 Well-posedness of Cauchy Problems

Well-posedness analysis is essential to the approach developed in this work. In this subsection, we establish the existence and the uniqueness of weak solutions of equations (4.60), (4.61) and (4.64).

Theorem 4.7 *The following statements hold true:*

(i) Assume $\alpha_j \in L^2(0,T)$ for $j = 1, 2, ..., N+1$. Let $h_0 \in \Phi$, $h_1 \in L^2(0,1)$, and $T > 0$. Then System (4.60) and System (4.61) has a unique weak solution $w \in C([0,T]; \Phi) \cap C^1([0,T]; L^2(0,1))$ and $w^d \in C([0,T]; \Phi) \cap C^1([0,T]; L^2(0,1))$, respectively.

(ii) Let $T > 0$ and $g \in C^2([0,T])$. Then System (4.61) has a unique weak solution $u \in C([0,T]; \Phi) \cap C^1([0,T]; L^2(0,1))$. Furthermore, if $g \in C^3([0,T])$ and $H_j^m(x)$, $j = 1, 2, ..., N$, is defined as in (4.63b), then System (4.64) has a unique solution $\psi_m \in C([0,T]; \Phi) \cap C^1([0,T]; L^2(0,1))$.

Proof. The proof of (i) can be proceeded step by step as in Proposition 3.1 of [5]. We prove the first result of (ii) and the second part can be proceeded in the same way. We assume firstly $g(t) \in C^3([0,T])$ and consider the following system:

$$\nu_{tt}(x,t) + \nu_{xxxx}(x,t) = \left(\frac{1}{2}x - \frac{1}{6}x^3\right)\ddot{g}(t), \ x \in \Omega, t > 0, \tag{4.70a}$$

$$\nu(0,t) = \nu_x(1,t) = \nu_{xx}(0,t) = \nu_{xxx}(1,t) = 0, \tag{4.70b}$$

$$\nu(x,0) = 0, \nu_t(x,0) = 0, \ \ x \in \Omega. \tag{4.70c}$$

Let $X = \Phi \times L^2(0,1)$ and $H_{(0)}^4(0,1) = \{u \in H^4(0,1); u(0) = u_x(1) = u_{xx}(0) = u_{xxx}(1) = 0\}$. Define the inner product on X by $\langle (u_1, v_1), (u_2, v_2) \rangle_X = \int_0^1 (u_{1xx}u_{2xx} + v_1 v_2)\mathrm{d}x$. Define the subspace $\mathcal{D}(A) \subset X$ by $\mathcal{D}(A) = \{(u,v); (u,v) \in H_{(0)}^4(0,1) \times \Phi\}$, with the corresponding operator $A : \mathcal{D}(A) \to X$ defined as:

$$A\begin{pmatrix} u \\ v \end{pmatrix} = \begin{pmatrix} v \\ -u_{xxxx} \end{pmatrix}.$$

One may easily check that $\mathcal{D}(A)$ is dense in X, A is closed, $A^* = -A$, and $\langle Az, z \rangle_X = 0$. Thus, by Stone's theorem, A generates a semigroup of isometries on X. Based on a classical result on perturbations of linear evolution equations (see, e.g., Theorem 1.5, Chapter 6, page 187, [88]) there exists uniquely $z = (z_1, z_2) \in C^1([0,T]; X) \cap C([0,T]; \mathcal{D}(A))$, such that

$$\frac{\mathrm{d}z}{\mathrm{d}t} = Az + \begin{pmatrix} 0 \\ \left(\frac{1}{2}x - \frac{1}{6}x^3\right)\ddot{g}(t) \end{pmatrix}, \ z(\cdot, 0) = (0, \ 0),$$

which implies that (4.70) has a unique solution $\nu = z_1 \in C([0,T]; H_{(0)}^4(0,1)) \cap C^1([0,T]; \Phi)$ in the usual sense. Particularly, $\nu \in C([0,T]; \Phi) \cap C^1([0,T]; L^2(0,1))$ is a weak solution. A direct computation shows that $u = \nu - \left(\frac{1}{2}x - \frac{1}{6}x^3\right) g(t)$ is a solution of (4.61) in the usual sense and, in particular, it is a weak solution.

Now for $g \in C^1([0,T])$, let $g_n \in C^3([0,T])$ such that $g_n \to g$ in $C^1([0,T])$. Consider $u_n = \nu_n - \left(\frac{1}{2}x - \frac{1}{6}x^3\right) g_n(t)$, where ν_n is the solution of (4.70) corresponding to the data $g_n(t)$. Then arguing as above and taking limit as in Chapter 2 of [**?**], we may obtain the existence and the uniqueness of a weak solution of (4.64). □

4.4.3 Feedback Control and Stability of the Inhomogeneous System

The validity of the proposed scheme requires a suitable closed-loop control that guarantees the stability of the original inhomogeneous system. As the $(N+1)^{\text{th}}$ actuator is dedicated to stabilizing control, (4.59) can be written as

$$w_{tt}(x,t) + w_{xxxx}(x,t) - \alpha_{N+1}(t)\delta(x - x_{N+1}) = \sum_{j=1}^{N} \alpha_j(t)\delta(x - x_j), \ x \in (0,1), \ t > 0. \quad (4.71)$$

Suppose further that the feedback control is taken as [5, 25]

$$\alpha_{N+1}(t) = -kw_t\left(x_{N+1}, t\right), \quad (4.72)$$

where k is a positive-valued constant. Then in closed-loop, (4.71) becomes

$$w_{tt}(x,t) + w_{xxxx}(x,t) + kw_t\left(x,t\right)\delta(x - x_{N+1}) = \sum_{j=1}^{N} \alpha_j(t)\delta(x - x_j), \ x \in (0,1), \ t > 0.$$

$$(4.73)$$

Let $\mathcal{D}(A) = \{(w,v); (w,v) \in [H^2(0,1) \cap (H^4(0, x_1) \cup H^4(x_1, x_2) \cup \cdots \cup H^4(x_N, x_{N+1}) \cup H^4(x_{N+1}, 1))] \times H^2(0,1), w(0) = w_x(1) = w_{xx}(0) = w_{xxx}(1) = 0, v(0) = v_x(1) = 0\}$ and X be defined as in the proof of Theorem 4.8. Let $T > 0$ and $\alpha_j \in L^2(0,T)$ for $j = 1, ..., N$. Assume $(h_0, h_1) \in X$. To address the stability of System (4.73) with the boundary conditions (4.1b) and initial conditions (4.1c), we consider the corresponding linear control system under abstract form:

$$\dot{z} = Az + B\alpha, \ t > 0, \quad (4.74a)$$

$$z(0) = z^0 = (h_0, h_1)^T, \quad (4.74b)$$

where $z = (w, v)^T$, $\alpha = (\alpha_1, \cdots, \alpha_N)^T$, $A : \mathcal{D}(A) \to X$ is defined as:

$$A \begin{pmatrix} w \\ v \end{pmatrix} = \begin{pmatrix} v \\ -w_{xxxx} - kv\delta(x - x_{N+1}) \end{pmatrix}, \tag{4.75}$$

with $v = w_t$, and $B : \mathbb{R}^N \to \mathcal{D}'(A^*)$ is defined as:

$$(B\alpha)y = \begin{pmatrix} 0 \\ \sum_{j=1}^N \alpha_j \delta(x - x_j) \end{pmatrix}^T y, \quad \forall \, y \in \mathcal{D}(A^*), \tag{4.76}$$

where A^* is the adjoint of A. It can be directly verified that A is dissipative [5].

Thus, A generates a strongly continuous semigroup $S(t)$ on X. The semigroup $S^*(t)$, generated by A^*, equals to $S(t)$. Note that $B^* : \mathcal{D}(A^*) \to \mathbb{R}^N$ is defined by

$$B^*y = (y_2(x_1), \ldots, y_2(x_N))^T, \forall y = \begin{pmatrix} y_1 \\ y_2 \end{pmatrix} \in \mathcal{D}(A^*). \tag{4.77}$$

Let $U = \mathbb{R}^N$. Then, the solution of the Cauchy problem (4.74) can be defined as follows (see [**?**], Definition 2.36, p53):

$$\langle z(\tau), y^\tau \rangle_X = \langle z^0, S^*(\tau)y^\tau \rangle_X + \int_0^\tau \langle \alpha(t), B^* S^*(\tau - t)y^\tau \rangle_U dt, \, \forall \, \tau \in [0, T], \forall \, y^\tau \in X. \tag{4.78}$$

One may verify, as in Chapter 2 of [**?**], that the solution defined by (4.78) is also a weak solution of (4.73) under the form given in Definition 4.2.

Theorem 4.8 *Assume $\alpha_j \in L^\infty(0, +\infty)$, $j = 1, \ldots, N$. For $x_{N+1} = 1$, there exist positive constants C_1, C_2, and λ such that for any $t \geq 0$, there holds:*

$$\|z(t)\|_X \leq C_1 e^{-\lambda t}\|z^0\|_X + C_2 \max_j \|\alpha_j\|_{L^\infty(0, +\infty)}. \tag{4.79}$$

Proof. The proof generalization of Theorem 2.37 in [**?**] for multiple-output system. First, the admissible property of B can be obtained from the proof of Theorem 4.1. Moreover, $S(t)$ generated by A defined in (4.75) is an exponentially stable C_0-semigroup on X if $x_{N+1} \in (0, 1)$ is a rational number with coprime factorization, in particular for $x_{N+1} = 1$ (see, e.g., [5, 25]), i.e. there exist two positive constants C_1 and λ, such that

$$\|S(t)\| \leq C_1 e^{-\lambda t}, \, \forall \, t \geq 0.$$

As $S(t) = S^*(t)$, then using the same arguments as in the proof of Theorem 2.37 in [**?**], we can conclude that all the constants in (4.79) are independent of t. $\qquad\square$

Now consider the regulation error defined as $e(x,t) = w(x,t) - \overline{w}^d(x)$. Denoting $\Delta\alpha_j(x,t) = \alpha_j(x,t) - \overline{\alpha}_j(x)$, $j = 1, \ldots, N$, then from (4.73), (4.59b), (4.59c), and the steady-state model of (4.60), the regulation error dynamics satisfy

$$e_{tt}(x,t) + e_{xxxx}(x,t) + ke_t(x,t)\,\delta(x - x_{N+1}) = \sum_{j=1}^{N} \Delta\alpha_j(t)\delta(x - x_j), \ \ x \in (0,1), t > 0,$$

$$\tag{4.80a}$$

$$e(0,t) = e_x(1,t) = e_{xx}(0,t) = e_{xxx}(1,t) = 0, \ \ t > 0, \tag{4.80b}$$

$$e(x,0) = e_0(x) = h_0(x) - \overline{w}^d(x),$$

$$e_t(x,0) = e_1(x) = h_1(x), \ \ x \in (0,1). \tag{4.80c}$$

Obviously, the regulation error dynamics are in an identical form as (4.73) with the same type of boundary conditions. We can then consider the solution of System (4.80) defined in the same form given by (4.78) with $z_e = (e, e_t)$ and $z_e^0 = (e_0, e_1)$.

Corollary 1 *Assume that all the conditions in Theorem 4.8 are fulfilled and $z_e^0 \in X$. Then there exist positive constants C_1, C_2, and λ, independent of t, such that for any $t \geq 0$, there holds:*

$$\|z_e(t)\|_X \leq C_1 e^{-\lambda t}\|z_e^0\|_X + C_2 \max_j \|\Delta\alpha_j\|_{L^\infty(0,+\infty)}. \tag{4.81}$$

Moreover, if $\lim_{t\to\infty} \Delta\alpha_j = 0$ for all $j = 1, \ldots, N$, then $\lim_{t\to\infty} e(x,t) = 0$, $\forall x \in (0,1)$.

Remark 4.9 *This stabilization feedback also complete the proof of Theorem 4.4.*

The feedforward control satisfying the conditions for closed-loop stability and regulation error convergence can be obtained through motion planning, as presented in the next section.

4.4.4 Motion Planning and Feedforward Control

According to the principle of superposition for linear systems, we consider in feedforward control design the dynamics of System (4.61) corresponding to the input $g_j(t)$, which are of the following form:

$$u_{jtt}(x,t) + u_{jxxxx}(x,t) = 0, \tag{4.82a}$$

$$u_j(0,t) = u_{jx}(1,t) = u_{jxx}(0,t) = 0, \tag{4.82b}$$

$$u_{jxxx}(1,t) = g_j(t), \tag{4.82c}$$

$$u_j(x,0) = u_{jt}(x,0) = 0. \tag{4.82d}$$

The required control signal $g_j(t)$ should be designed so that the output of System (4.82) follows a prescribed function $u_j^d(x_j, t)$ and that the conditions in Theorem 4.8 and Corollary 1 are fulfilled.

Motion planning becomes then to take $u_j^d(x_j, t)$ as the desired output and to generate the full-state trajectory of the subsystem $u_j(x, t)$, which is carried out in this work using flatness-based motion planning (see, e.g., [43, 78, 79, 81, 94]). To solve this problem, we apply a standard Laplace transform-based procedure. Henceforth, we denote by $\widehat{f}(x, s)$ the Laplace transform of a function $f(x, t)$ with respect to time variable. Then, in the Laplace domain, the transformed equations are given by

$$\widehat{u}_{jxxxx}(x, s) - q^4(s)\widehat{u}_j(x, s) = 0, \tag{4.83a}$$

$$\widehat{u}_j(0, s) = \widehat{u}_{jx}(1, s) = \widehat{u}_{jxx}(0, s) = 0, \tag{4.83b}$$

$$\widehat{u}_j(x_j, s) = \widehat{u}_j^d(x_j, s), \tag{4.83c}$$

where $q^4(s) = -s^2$. The general solution of (4.83a) can be expressed as

$$\widehat{u}_j(x, s) = a_j(s)\widehat{C}_1(x, s) + b_j(s)\widehat{S}_1(x, s) + c_j(s)\widehat{C}_2(x, s) + d_j(s)\widehat{S}_2(x, s), \tag{4.84}$$

where

$$\widehat{C}_1(x, s) = (\cosh(q(s)x) + \cos(q(s)x))/2, \tag{4.85a}$$

$$\widehat{C}_2(x, s) = (\cosh(q(s)x) - \cos(q(s)x))/2q^2(s), \tag{4.85b}$$

$$\widehat{S}_1(x, s) = (\sinh(q(s)x) + \sin(q(s)x))/2q(s), \tag{4.85c}$$

$$\widehat{S}_2(x, s) = (\sinh(q(s)x) - \sin(q(s)x))/2q^3(s) \tag{4.85d}$$

are the basic solutions to (4.83a).

To determine the coefficients $a_j(s)$, $b_j(s)$, $c_j(s)$, and $d_j(s)$, we use the property $\widehat{C}_{1x} = q^4(s)\widehat{S}_2$, $\widehat{C}_{2x} = \widehat{S}_1$, $\widehat{S}_{1x} = \widehat{C}_1$, $\widehat{S}_{2x} = \widehat{C}_2$, and apply the boundary values given in (4.83b) and $\widehat{u}_j(x_j, s) = \widehat{u}_j^d(x_j, s)$. We obtain:

$$a_j = c_j = 0,$$

$$b_j(s)\widehat{S}_1(x_j, s) + d_j(s)\widehat{S}_2(x_j, s) = \widehat{u}_j^d(x_j, s),$$

$$\widehat{u}_{jx}(1, s) = b_j(s)\widehat{C}_1(1, s) + d_j(s)\widehat{C}_2(1, s) = 0.$$

We can write then

$$\widehat{R}(s)\begin{pmatrix} b_j \\ d_j \end{pmatrix} = \begin{pmatrix} \widehat{u}_j^d(x_j, s) \\ 0 \end{pmatrix},$$

where

$$\widehat{R}(s) = \begin{pmatrix} \widehat{S}_1(x_j, s) & \widehat{S}_2(x_j, s) \\ \widehat{C}_1(1, s) & \widehat{C}_2(1, s) \end{pmatrix}.$$

Now b_j and d_j can be computed as

$$\begin{pmatrix} b_j \\ d_j \end{pmatrix} = \widehat{R}^{-1}(s) \begin{pmatrix} \widehat{u}_j^d(x_j, s) \\ 0 \end{pmatrix} = \frac{\text{adj}(\widehat{R}(s))}{\det(\widehat{R}(s))} \begin{pmatrix} \widehat{u}_j^d(x_j, s) \\ 0 \end{pmatrix}.$$

Letting

$$\widehat{u}_j^d(x_j, s) = \det\left(\widehat{R}(s)\right) \widehat{y}_j(s), \tag{4.86}$$

it follows that

$$\widehat{u}_j(x, s) = (\widehat{C}_2(1, s)\widehat{S}_1(x, s) - \widehat{C}_1(1, s)\widehat{S}_2(x, s))\widehat{y}_j(s). \tag{4.87}$$

Note that $\widehat{y}_j(s) \leftrightarrow y_j(t)$ is the so-called basic output, or flat output. In order to transfer the full-state trajectory and the control input from frequency domain to time domain, we use the Taylor expansion of trigonometric and hyperbolic functions in (4.85a)-(4.85d) with respect to x. The full-state trajectory $\widehat{u}_j(x, s)$ in (4.87) can be written in the form

$$\widehat{u}_j(x, s) = \left(\frac{1}{2}x - \frac{1}{6}x^3\right) \widehat{y}_j(s) \tag{4.88}$$
$$+ \sum_{n=1}^{\infty} \left(\sum_{k=0}^{n} \frac{x^{4k+1}}{(4k+1)!(4(n-k)+2)!} - \sum_{k=0}^{n} \frac{x^{4k+3}}{(4k+3)!(4(n-k))!} \right) q^{4n}(s)\widehat{y}_j(s).$$

Thus, in time domain the full-state trajectory with zero initial values is given by

$$u_j(x, t) = \left(\frac{1}{2}x - \frac{1}{6}x^3\right) y_j(t) \tag{4.89}$$
$$+ \sum_{n=1}^{\infty} \left(\sum_{k=0}^{n} \frac{x^{4k+1}}{(4k+1)!(4(n-k)+2)!} - \sum_{k=0}^{n} \frac{x^{4k+3}}{(4k+3)!(4(n-k))!} \right) (-1)^n y_j^{(2n)}(t).$$

Now let $y_j(t) = \overline{y}_j \phi_j(t)$, where $\phi_j(t)$ is a smooth function evolving from 0 to 1. Then, Equation (4.89) becomes

$$u_j(x, t) = \overline{y}_j \left(\frac{1}{2}x - \frac{1}{6}x^3\right) \phi_j(t) \tag{4.90}$$
$$+ \overline{y}_j \sum_{n=1}^{\infty} \left(\sum_{k=0}^{n} \frac{x^{4k+1}}{(4k+1)!(4(n-k)+2)!} - \sum_{k=0}^{n} \frac{x^{4k+3}}{(4k+3)!(4(n-k))!} \right) (-1)^n \phi_j^{(2n)}(t).$$

The corresponding input can be computed from (4.82c), which is of the form

$$g_j(t) = -\overline{y}_j\phi_j(t) + \overline{y}_j \sum_{n=1}^{\infty} \left(\sum_{k=1}^{n} \frac{1}{(4k-2)!(4(n-k)+2)!} - \sum_{k=0}^{n} \frac{1}{(4k)!(4(n-k))!} \right) (-1)^n \phi_j^{(2n)}(t).$$

(4.91)

For set-point control, we need an appropriate class of trajectories enabling a rest-to-rest evolution of the system. A convenient choice for this purpose is Gevrey functions as introduced in (4.52)

For the convergence of (4.90) and (4.91), we have

Proposition 3 *If $\phi_j(t)$ in the basic output $y^j(t) = \overline{y}^j\phi_j(t)$ is chosen as a Gevrey function of order $1 < \sigma < 2$, then the infinite series (4.90) and (4.91) are convergent.*

Proof. Denote in (4.89):

$$b_n = \left(\sum_{k=0}^{n} \frac{x^{4k+1}}{(4k+1)!(4(n-k)+2)!} \right.$$
$$\left. - \sum_{k=0}^{n} \frac{x^{4k+3}}{(4k+3)!(4(n-k))!} \right) (-1)^n \phi_j^{(2n)}(t).$$

(4.92)

Then, (4.90) converges if $\limsup_{n\to\infty} \sqrt[n]{|b_n|} < 1$. The proof can be proceed similarly to that of Proposition 2.

The convergence of (4.91) then follows easily using the same argument. $\square$

Now let

$$P_j(x) = \frac{1}{2}x - \frac{1}{6}x^3,$$

(4.93a)

$$I_{j,m}(x) = \int_0^x \int_1^z \int_0^y \int_1^t \varphi_m(s-x_j)\mathrm{d}s\mathrm{d}t\mathrm{d}y\mathrm{d}z,$$

(4.93b)

$$\Phi_{j,n}(x) = \left(\sum_{k=0}^{n} \frac{x^{4k+1}}{(4k+1)!(4(n-k)+2)!} - \frac{x^{4k+3}}{(4k+3)!(4(n-k))!} \right)(-1)^n,$$

(4.93c)

$$\Psi_{j,n}(1) = \left(\sum_{k=1}^{n} \frac{1}{(4k-2)!(4(n-k)+2)!} - \sum_{k=0}^{n} \frac{1}{(4k)!(4(n-k))!} \right)(-1)^n.$$

(4.93d)

Set $\sum_{j=1}^{N} \psi_j^m(x,t) = \psi_m(x,t), m > 0$. By the definition of $\psi(x,t)$, we obtain

$$\psi_j^m(x,t) = \overline{y}_j I_{j,m}(x)\phi_j(t) + \overline{y}_j \sum_{n=1}^{\infty} \left(\Phi_{j,n}(x) + \Psi_{j,n}(1)P_j(x) - \Psi_{j,n}(1)I_{j,m}(x) \right)\phi_j^{(2n)}(t). \quad (4.94)$$

To compute $I_{j,m}(x)$, we note that

$$\varphi_m(x - x_j) = \frac{1}{\pi} \sum_{k=1}^{\infty} \frac{(-1)^{k+1} m^{2k-1}}{(2k-1)!} (x - x_j)^{2k-2}.$$

Therefore,

$$
\begin{aligned}
I_{j,m}(x) = &\frac{1}{\pi} \sum_{k=1}^{\infty} \frac{(-1)^{k+1} m^{2k-1}}{(2k-1)} \left(\frac{(x - x_j)^{2k+2}}{(2k+2)!} \right. \\
&- \frac{(1 - x_j)^{2k-1} x^3}{6((2k-1)!)} - \frac{x_j^{2k} x^2}{2(2k)!} - \frac{(1 - x_j)^{2k+1} x}{(2k+1)!} \\
&+ \frac{x_j^{2k} x}{(2k)!} + \frac{(1 - x_j)^{2k-1} x}{2(2k-1)!} - \left. \frac{x_j^{2k+2}}{(2k+2)!} \right).
\end{aligned}
\tag{4.95}
$$

Claim 1 $I_{j,m}(x)$ *given in (4.95) is convergent for all* $x, x_j \in (0,1)$ *with respect to any fixed* m.

   Proof. Consider the first series in (4.95). Fixing $m > 0$, for $x, x_j \in (0,1)$, $j = 1, 2, \ldots, N$, we have

$$\left| \frac{(-1)^{k+1} m^{2k-1}}{(2k-1)} \frac{(x - x_j)^{2k+2}}{(2k+2)!} \right| \leq \frac{m^{2k-1}}{(2k-1)!}.$$

Since $\lim_{n \to \infty} \frac{1}{\sqrt[n]{n!}} = 0$, it follows that for any $a > 0$

$$\lim_{n \to \infty} \sqrt[n]{\frac{a^n}{n!}} = a \lim_{n \to \infty} \frac{1}{\sqrt[n]{n!}} = 0.$$

Thus $\sum_{k=0}^{\infty} \frac{m^{2k-1}}{(2k-1)!}$ is convergent. We conclude that the first series in (4.95) is uniformly convergent. The convergence of the other terms in (4.95) can be proved in the same way.

$\square$

   Based on Claim 1, the series in the right hand side of (4.94) are convergent and $\psi_j^m(x,t)$ can be expanded by (4.94) and (4.95). Moreover, for $g_j(t)$ given in (4.91), $\psi_j^m(x,t)$ tends to $\overline{\psi}_j^m(x) = \overline{y}_j I_{j,m}(x)$ as $t \to \infty$. Note that for fixed x, the radius of convergence of $\overline{\psi}_{j,m}$ on m is ∞. Thus, we can let $m \to +\infty$.

   To complete the control design, we need to determine the amplitude of flat outputs $\overline{y}_j$, $j = 1, \ldots, N$, from the desired shape $\tilde{w}^d(x)$ that may not necessarily be a solution of the steady-state beam equation (4.69). To that end, we use the Green's functions, $G(x, \xi)$, of (4.69), as denoted in (4.17).

Due to the principle of superposition for linear systems, the solution to (4.69), $\overline{w}^d(x)$, can be expressed as

$$\overline{w}^d(x) = \int_0^1 \sum_{j=1}^N G(x,\xi)\overline{\alpha}_j\delta(x-\xi_j)d\xi = \sum_{j=1}^N G(x,\xi_j)\overline{\alpha}_j.$$

Now taking N points on $\widetilde{w}^d(x)$ and letting $\overline{w}^d(x_j) = \widetilde{w}^d(x_i = j)$, $j = 1,\ldots,N$, yield

$$\begin{pmatrix} G(x_1,\xi_1) & \ldots & G(x_N,\xi_1) \\ \vdots & \ddots & \vdots \\ G(x_1,\xi_N) & \ldots & G(x_N,\xi_N) \end{pmatrix} \begin{pmatrix} \overline{\alpha}_1 \\ \vdots \\ \overline{\alpha}_N \end{pmatrix} = \begin{pmatrix} \widetilde{w}^d(x_1) \\ \vdots \\ \widetilde{w}^d(x_N) \end{pmatrix}, \tag{4.96}$$

which represents a steady-state input to output map. Based on Theorem 4.5, the map given in (4.96) is invertible for all $x_j, \xi_j \in (0,1)$, $j = 1,\ldots,N$, and $x_i \neq x_j, \xi_i \neq \xi_j$, if $i \neq j$.

As $\overline{\alpha}_j = -\overline{g}_j$ and $\lim_{t\to\infty} g_j(t) = \overline{g}_j = -\overline{y}_j$ for all $j = 1,\ldots,N$, we obtain from (4.96) that

$$\begin{pmatrix} \overline{y}_1 \\ \vdots \\ \overline{y}_N \end{pmatrix} = \begin{pmatrix} G(x_1,\xi_1) & \ldots & G(x_N,\xi_1) \\ \vdots & \ddots & \vdots \\ G(x_1,\xi_N) & \ldots & G(x_N,\xi_N) \end{pmatrix}^{-1} \begin{pmatrix} \widetilde{w}^d(x_1) \\ \vdots \\ \widetilde{w}^d(x_N) \end{pmatrix}. \tag{4.97}$$

4.5 Summary

In this chapter, we presented two control designs for an Euler-Bernoulli model of the deformable beam.

In the first design, we formally established a map between the in-domain controlled model of the system and a standard boundary-controlled PDE model. Based on that map, we developed a control strategy, which is a combination of feedback stabilization and differential flatness-based feed-forward motion planing. However, since the map holds only for some particular test functions, the original PDE is satisfied in a very weak sense.

To cope with this problem in the second design, we approximate the solution of the original system by that of a target system in the steady state. To do this, we use the technique of lifting to transform the target system to an inhomogeneous PDE driven by sufficiently smooth functions generated by applying blobs. This would allow establishing a relationship between the original system and the target system in a usual weak sense.

In the next chapter, we verify the validity of both designs through numerical simulation studies.

CHAPTER 5

SIMULATION STUDIES OF IN-DOMAIN CONTROLLED EULER-BERNOULLI BEAMS

This chapter presents the simulation results of the designs presented in the previous chapter. We begin the chapter by explaining the numerical implementation and the numerical stability of the simulated model Section 5.1. Then, in Section 5.2, Section 5.3, we present the simulation results for the first and the second design. We conclude the chapter with discussion on results in Section 5.4.

As we will show in the simulation study if the desired curve is not a solution of the corresponding static beam equation, the regulation error with respect to this curve will in general not identically vanish. Therefore, to make the performance evaluation meaningful, we propose in the second set of simulation study to first interpolate the desired curve by the Green's functions of the static beam equation and then to evaluate the regulation error of the controller with respect to the corresponding steady-state solution of the beam.

In the evaluation of interpolation accuracy, we consider 3 setups with different number of actuators and use the L_1-norm as a measure of interpolation errors. We also show the control effort corresponding to different setups to provide a better characterization of the micro-beam efficiency.

5.1 Numerical implementation

In this section, we expain how a beam equation described by a fourth-order in space and second-order in time partial differential equation can be numerically implemented in MATLAB. It is worth mentioning that the unstable dynamics of this equation is one of the most challenging parts in performing the numerical implementation.

We explain the numerical implementation in three folds: first, the approximation of the second-order time derivative operator; then the numerical approximation of the forth-order spatial differentiation operator, or the bi-harmonic operator; and eventually the integration of the nonstandard boundary conditions to the numerical approximation of the bi-harmonic operator.

For the time evolution, we convert the second-order-in-time system in (4.1) into a first-

order-in-time system by introducing a dummy variable, $u(x,t)$, as:

$$w_t(x,t) = u(x,t), \tag{5.1a}$$

$$u_t(x,t) = w_{xxxx}(x,t) + f(x,t). \tag{5.1b}$$

We use a general notation in this part. For instance, we use $f(x,t)$ for inputs instead of showing the exact term. Then, we can rewrite the system in the following matrix form:

$$\dot{X} = AX + P_n \tag{5.2}$$

where $A = \begin{bmatrix} \mathbf{0} & I_{n_x} \\ -DA & \mathbf{0} \end{bmatrix}$, $P_n = \begin{bmatrix} \mathbf{0} \\ F_{n_x} \end{bmatrix}$, and F_{n_x} is nonzero on the location of the point-wise actuators of the system. In these matrices, $\mathbf{0}$ is the null matrix with appropriate dimension, I_{n_x} represents the identity matrix, and DA is the approximation of biharmonic operator.

Now we are dealing with a first-order in time system. Hence, we can use the the leap frog formula for computing time derivative. As stated in Chapter 10 of [103], leap frog approximation of time evolution is numerically stable for first-order in time systems. A method is called numerically unstable in the sense that small errors are amplified unboundedly, in fact, exponentially.

In matrix A, the term DA is the approximation of bi-harmonic operator with associated boundary conditions. For this approximation, we use Chebyshev spectral differentiation [103] to approximate the fourth-order-spatial derivatives of bi-harmonic operator.

The Chebyshev spectral function uses Fast Fourier Transform (FFT) to approximate the derivatives. For the boundary conditions, interpolant method is used. In this method, the additional equations are augmented to the system to enforce the nonstandard boundary conditions. For instance, the term $(1-x^3)$ can be multiplied to enforce the condition $u_{xxx}(1) = 0$, please see Chapter 14 of [103] for more details.

The convergence of the numerical method is checked by varying the time step Δt in the interval $[10^{-3}, 10^{-6}]$ and the mesh-density M for Chebyshev approximation between 40 and 80.

Note that the dynamics of this system are inherently unstable because there is no dampening term in the Euler-Bernoulli PDE equation. Therefore, regardless of numerical stability, one may find the numerical results are growing on time. To harvest the best result, we run the system with stabilizing feedback together.

We first start by implementing System (4.1) with 3 actuators in the domain located at $x = \{0.25, 0.5, 0.75\}$ with initial conditions $h_0(x,0) = -3 \times 10^{-3} e^{-400(x-0.8)^2}$ and $h_1(x,0) = 0$. To comply with the limitation of micro-actuators, we assume downward displacement for the

system. Moreover, for the validation of the linear model of the beam, the displacement is at the order of micro meter for a beam length of a few centimeter. The deflection and the length of the beam, as well as the time, are all represented in normalized coordinates.

As an undamped beam is unstable in open-loop, the controller tuning is started by determining a suitable value of the closed-loop control gain k. Figure 5.1 shows the stabilization of the beam by applying the feedback control derived from (4.37) to g_1 at $x = 0.25$ while g_2 and g_3 are set to 0. As illustrated in Fig. 5.1, the stabilizing feedback damped the beam rapidly.
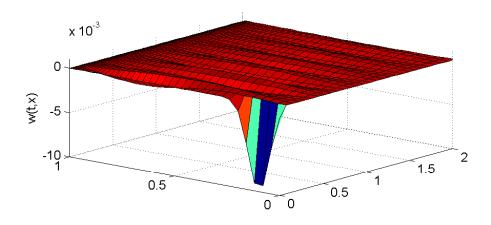

Figure 5.1 Stabilized System.

Then, to try the trajectory tracking behavior, we chose the basic outputs $\phi_j(t)$ as Gevrey functions of the same order. The desired reference trajectory generated from (4.38) is depicted in Fig. 5.2(a). Note that to meet the convergence condition given in Proposition 2, the order is set to $\sigma = 1.11$. g_1, g_2, and g_3 are computed from (4.51) and (4.37), respectively. α_1, α_2, and α_3 are then computed from (4.30) and are illustrated in Fig. 5.3(a). As shown in Fig. 5.2(b), the system is smoothly transferred from the initial profile to the desired one. The error between the system output and the reference trajectory is depicted in Fig. 5.2(c). Figure 5.3(b) shows system outputs at $x = 0.5$ and $x = 0.75$.

The simulation results though far shows the proper numerical implementation. The system stabilized well around the reference trajectories. The numerical computation also shows stable implementation despite initial values and in-domain inputs.

5.2   Numerical Results of the First Design

In this section, we examine the simulation result of the first control scheme presented in Section 4.3.3. The static Green's functions of the system are used for spacial decomposing
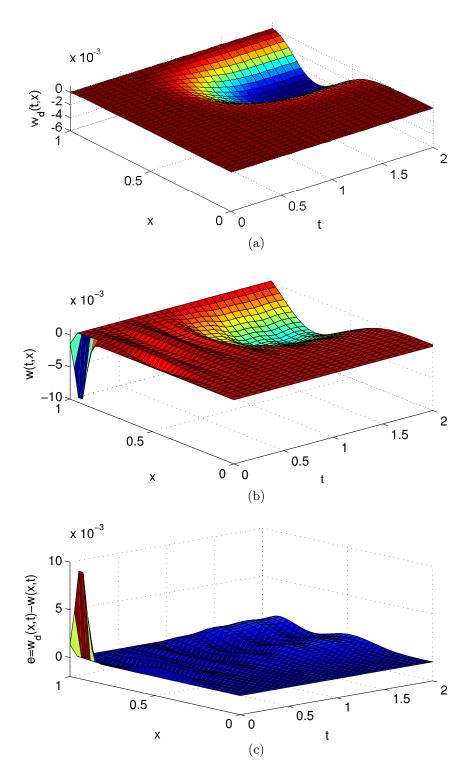
Figure 5.2 Deformation control: (a) reference trajectory; (b) beam deflection; (c) tracking error.
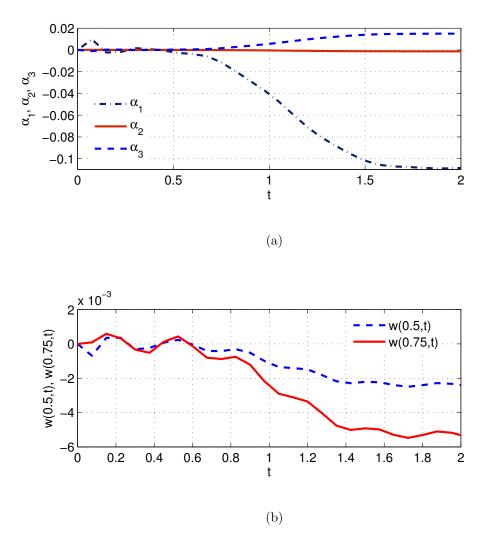
(a)

(b)

Figure 5.3 Simulation results: (a) control signals $\alpha_1, \alpha_2,$ and α_3; (b) transversal deflection of the beam at $x = 0.5$ and $x = 0.75$.

of the reference trajectories. Figure 5.4 shows the Green's function $G(x, \xi)$ for $\xi = \{0.1, 0.2, \cdots, 0.9\}$ as a basis to decompose the given reference trajectories. The lowest curve is the Green's function for $\xi = 0.1$ and the others correspond to ξ in increasing order.

We considered a system with 10 actuators uniformly distributed in the domain.

In the simulation study, we consider the deformation control in which the desired shape is given by

$$w_d(x, t) = -10^{-3} \phi(t) \left(e^{-100(x-0.4)^2} + 2e^{-100(x-0.6)^2} + 3e^{-400(x-0.7)^2} \right), \; x \in (0, 1), \qquad (5.3)$$

where $\phi_j(t)$ is the Gevrey function of order $\sigma = 1.11$ as derived from the convergence study of the controller. The desired shape is depicted in Fig. 5.5(a).

The feedforward controls are computed from (4.51) and the feedback law is given in (4.37). Accordingly, the in-domain control signals, $\alpha_1, \cdots, \alpha_{10}$, are derived from (4.30), illustrated in Fig. 5.6(a) and Fig. 5.6(b). As shown in Fig. 5.5(b) and Fig. 5.5(c), these control signals steer the deflection of the beam along the given reference trajectory with reasonable tracking errors. Nevertheless, we can observe that the steady-state error in the interval $[0.5, 0.7]$ is significantly bigger than that of the other positions. The reason is that the reference trajectory has an important peak at the position 0.8 that draws the beam downward. This is due to the physical constraint of the device and indicates that for improving the overall tracking accuracy, more actuators are desirable.
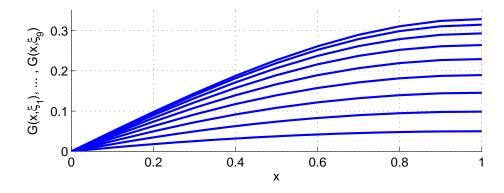

Figure 5.4 Green's function of the beam for $\xi = \{0.1, 0.2, \cdots, 0.9\}$.

5.3 Simulation Results for the Second Design

In this section we evaluate the performance of the second design from Section 4.4.

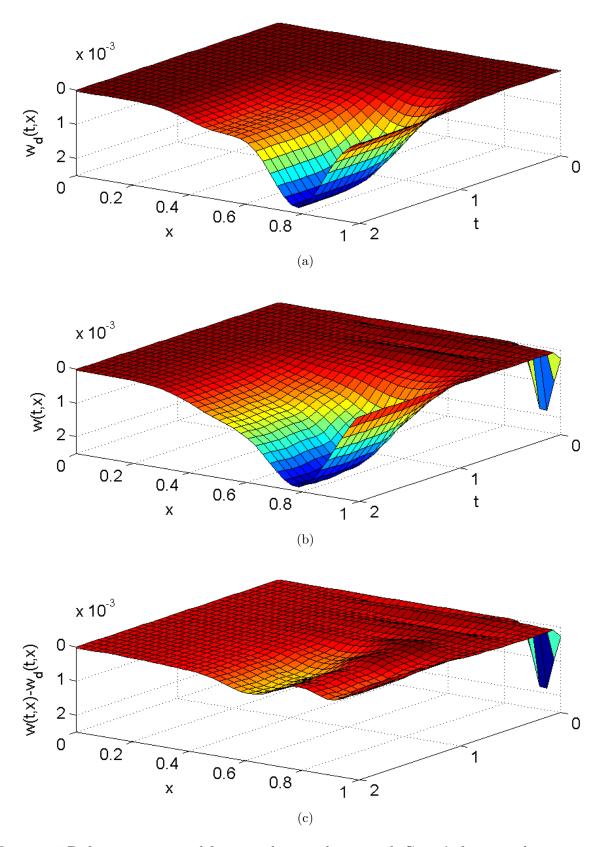In this study, we consider the deformation control in which the desired shape is given in

Figure 5.5 Deformation control for time-domain design with Green's function decomposition: (a) desired shape; (b) beam deflection; (c) tracking error;
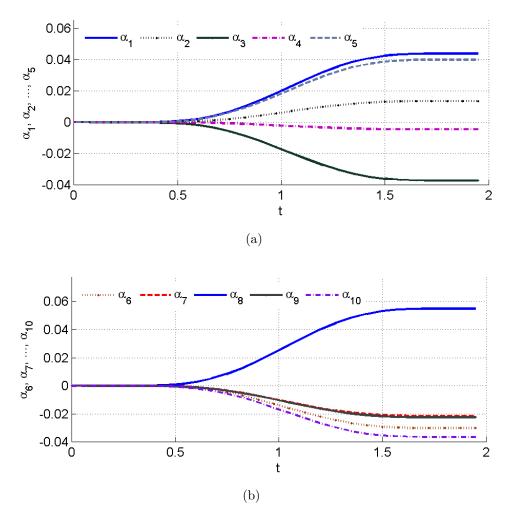
Figure 5.6 Control signals: (a) α_1-α_5; (b) α_6-α_{10}.

steady-state form by:

$$\widetilde{w}^d(x) = -10^{-3}\left(e^{-100(x-0.4)^2} + 2e^{-100(x-0.6)^2} + 3e^{-400(x-0.7)^2}\right),\ x \in (0,1),\qquad (5.4)$$

as shown in Fig. 5.7(a).

In order to obtain an exponential closed-loop convergence, the actuator for feedback stabilization is located at the position $x_{N+1} = 1$. To evaluate the effect of the number of actuators to interpolation accuracy, measured by $\|\widetilde{w}^d(x) - \overline{w}^d(x)\|_{L^1(0,1)}$, and control effort, we considered 3 setups with, respectively, 8, 12, and 16 actuators evenly distributed in the domain. It can be seen from Fig. 5.7 that the setup with 8 actuators exhibits an important interpolation error and the one with 16 actuators requires a high control effort in spite of a high interpolation accuracy. The setup with 12 actuators provides an appropriate trade-off between the interpolation accuracy and the required control effort, which is used in control algorithm validation.

For this simulation study, we use a MATLAB Toolbox for dynamic Euler-Bernoulli beams simulation provided in Chapter 14 of [110]. With this Toolbox, the simulation accuracy can be adjusted by choosing the number of modes used in implementation. In the simulation, we implement System (4.59) The corresponding feedforward control signals with $\alpha_1, \ldots, \alpha_{12}$, that steer the beam to deform are illustrated in Fig. 5.8. The evolution of beam shapes and the regulation error are depicted in Fig. 5.9. It can be seen that the beam is deformed to the desired shape and the regulation error vanishes along the whole beam, which confirms the expected performance of the developed control scheme.

5.4 Discussion

The simulation results demonstrate the validity of the designs. In both designs, the controller was able to steer the system along prescribed trajectories with a feasible control effort for the MEMS actuators and with a acceptable range of tracking errors. However, since the first design is valid in a very weak sense, in real implementation the outcome might not match that of the simulation study. Nonetheless, this caveat is rectified in the second design.

As we realized from simulation study, if the desired curve is not a solution of the corresponding static beam equation, the regulation error with respect to this curve will in general not identically vanish. Therefore, to make the performance evaluation meaningful, we have proposed in the second set of simulation study to first interpolate the desired curve by the Green's functions of the static beam equation and then to evaluate the regulation error of the controller with respect to the corresponding steady-state solution of the beam.

In the evaluation of interpolation accuracy, we have considered 3 setups with different
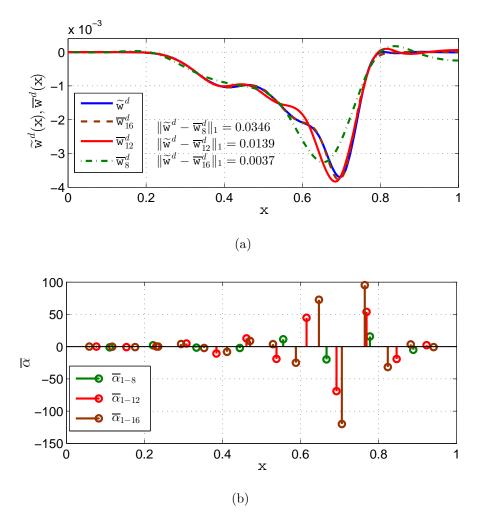
(a)

(b)

Figure 5.7 Effect of number of actuators: (a) interpolation accuracy ($\tilde{w}^d(x)$: desired shape; $\overline{w}_n^d(x)$: solution of the steady-state beam equation with $n = 8$, 12, and 16 in-domain actuators); (b) amplitude of steady-state control signals for different setups.
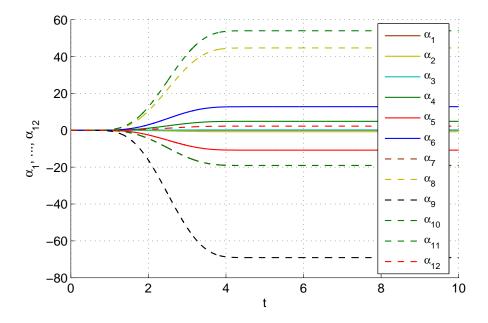
Figure 5.8 Feedforward control signals: $\overline{\alpha}_1, \ldots, \overline{\alpha}_{12}$.

number of actuators and have adopted the L_1-norm of interpolation errors. We also have shown the control effort corresponding to different setups to provide a better characterization of the micro-beam efficiency.

Eventually, using the Green's function not only makes the algorithm computationally traceable but also is a very promising choice for real time implementation. As the static Green's function used in trajectory planning can be computed off-line, the developed scheme facilitates real-time implementations. As a result, the basic flat output for differential flatness method can be computed directly by an inverse static matrix calculation. This complexity reduction will have an important impact on the real time implementation for large scale deformable mirrors.
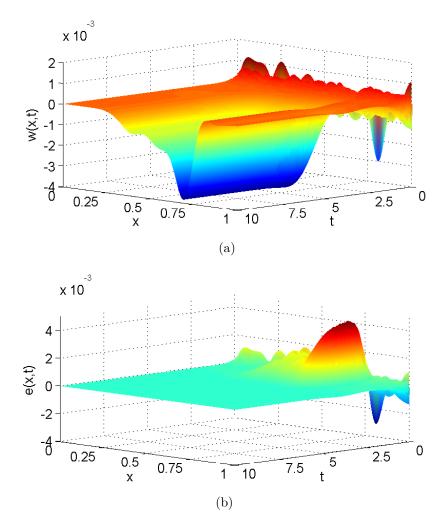
(a)

(b)

Figure 5.9 Set-point control: (b) system response; (c) regulation error.

CHAPTER 6

CONCLUSION AND RECOMMENDATION

High precision and real time control of deformable mirrors is an enabling key of forth-coming extremely large ground-based telescopes. In this regards, this thesis addressed a systematic deformation control scheme for MEMS-actuated deformable mirrors in the context of astronomical telescopes.

To meet the high precision requirement, the design is directly carried out using the partial differential equation model of the system. To avoid early lumping in the motion planning, we use the properties of the Green's function of the system to represent the reference trajectories. A finite set of these functions is considered to establish a one-to-one map between the input space and output space. This allows an implementable scheme for real-time applications. The only truncation is at the level of implementation of the controller. As a result, there are no neglected dynamics to compromise the performance of the controller. To account for instability, model uncertainties, and disturbances, a stabilizing feedback is designed to stabilize the system around the reference trajectories. The presented control scheme is a combination of differential flatness for feedforward motion planning and stabilizing feedback controllers, leading to a simple structure requiring only one measurement point on the boundary. Nonetheless, the feedforward control is inherently unrobust due the method of open-loop trajectory planning, which depends heavily on the model. Adding more sensors is a way to improve the robustness. However, this is not a viable option for current state-of-the-art microsystems.

The presented scheme is particularly suitable for micro-systems for which the design, fabrication, and operation with a high number of on-chip sensors represent a serious technological challenge.

Below, we summarize the main contributions of this work.

6.1 Main Contributions

The objective of this dissertation was to develop a high-precision and real-time implementable control structure in order to mitigate the complexity introduced by closed-loop control at the level of every actuator in MEMS deformable mirrors.

We approached the problem as follow: first, we introduced the dynamics of a MEMS-actuated deformable mirror described by a set of partial differential equations with un-

bounded control operators in the domain of the system. Then, for the deformation control of this device we developed two control designs. In the first design, we established a map between the in-domain controlled system and a standard boundary controlled model. Based on that, we developed a control strategy, which is a combination of feedback stabilization and differential flatness-based feed-forward motion planing. This scheme shows a way to deal with the tracking control problem of in-domain PDE systems. However, the map holds only for some particular test functions. Thus, the original PDE is satisfied in a very weak sense. To cope with this caveat, in the second design instead of trying to establish such an equivalence, we approximated the solution of the original system by that of a target system in the steady-state mode. To this end, we used the technique of lifting to transform the target system, which is controlled by boundary actuators, to an inhomogeneous PDE driven by sufficiently smooth functions generated by applying blobs. This would allow establishing a relationship between the original system and the target system in a usual weak sense.

The control schemes developed in this work require just one displacement feedback data from a boundary point for one-row-actuator mirror. The feedback loop can be directly provided using an interferometer sensor on an inactive actuator of the mirror.

The benefits of this approach can be listed as:

First, this work addresses a systematic scheme for the control of deformable mirrors. That is the scheme can be directly generalized for different boundary condition configurations of the system. The system architecture and the procedure for feed-forward control design remain the same, but only the feedback stabilization law should be reconsidered according to new boundary conditions.

Second, the proposed control scheme requires only to close few feedback control loops, typically one for 1D devices. Consequently, the implementation and operation of such devices will be drastically simplified.

Third, the design is directly performed with the partial differential equation model of the system. Hence, there is no neglected dynamics to sacrifice the performance. The only truncation requires at the level of the controller implementation.

Fourth, the presented scheme can be considered as an extension of the flat systems to a system controlled by multiple actuators, which is essentially a multiple-input multiple-output (MIMO) problem. To the best of the author's knowledge, a treatment without requiring early truncations for tracking control of this type of PDE systems has not yet been reported In the context of PDE-based control designs.

Finally, we introduced a Green's function-based decomposition scheme that enables a simple and computationally tractable implementation of the proposed control. As the static Green's function used in trajectory planning can be computed offline, the developed scheme

facilitates real-time implementations. This will have an important impact on the operation of large-scale deformable mirrors.

6.2 Recommendations and Future Work

The next step of this research work may be to examine the performance of the purposed method on a physical set-up. A simple way of testing the approach is to use a segmented deformable mirror between a light source and a continuous deformable mirror to introduce a distortion. Then, using a wavefront sensor, e.g. Shack-Hartmann sensor, one is able to validate the performance of the control scheme on the continuous mirror to correct the distortion.

The mentioned devices are all tested individually in the laboratory of Adaptive Optics during this PhD research. The remaining part is to establish the adaptive optic loop as explained in Chapter 2. A real time communication protocol such as TCP/IP requires to establish the realtime data exchange in electronic loop. For the optic loop, identifying the feasible distance between the devices requires an optics expert's insight.

Further perspectives of the theory presented in this work is to extend this control scheme to a plate equation, or in other words to a case of more than one row of actuators. One may consider this extension, similarly to Chapter 9 of [17], by decomposing the plate into two different beam equations. Then, for each set of equations the proposed control scheme may be applicable.

Deformation control of deformable mirrors has many different applications and a list of those applications is provided in the introduction of this manuscript. Since the proposed control is a systematic design, it can directly be exploited for other applications with a good insight to requirements associated to that particular application.

The proposed control scheme may concern other in-domain controlled PDE systems. For instance, one initial generalization example could be the well-known case of heating up and cooling down certain materials along a specific profile that requires multiple actuators acting in different temperatures at different instance of time.

BIBLIOGRAPHY

[1] M. Abramowitz and I. A. Stegun. *Handbook of Mathematical Functions.* Dover Publications, New York, 1972.

[2] R. A. Adams and J. F. Fournier. *Sobolev Spaces.* Academic press, New York, 2nd edition, 2003.

[3] K. Ammari and M. Mehrenberger. Study of the nodal feedback stabilization of a string-beams network. *J. Appl Math Comput*, 36:441–458, 2011.

[4] K. Ammari, D. Mercier, V. Regnier, and J. Valein. Spectral analysis and stabilization of a chain of serially connected Euler-Bernoulli beam and strings. *Communications on Pure and Applied Analysis*, 11(2):785–807, 2012.

[5] K. Ammari and M. Tucsnak. Stabilization of Bernoulli-Euler beams by means of a pointwise feedback force. *SIAM J. Control Optimal*, 39(4):1160–1181, 2000.

[6] T. Anderson, O. Garpinger, M. Owner-Petersen, F. Svahn, and A. Ardegerg. Vovel concept for large deformable mirrors. *Optical Engineering*, 45(7):73001–1–13, 2006.

[7] A. Badkoubeh, J. Zheng, and G. Zhu. Flatness-based deformation control of an Euler-Bernoulli beam with in-domain actuation. *Submitted to Automatica*, 2014.

[8] A. Badkoubeh and G. Zhu. Tracking control of a linear parabolic PDE with in-domain point actuators. *International Journal of Electrical and Electronics Engineering*, 5(11):11–25, 2011.

[9] A. Badkoubeh and G. Zhu. Deformation control of a 1-dimensional microbeam with in-domain actuation. In *IEEE 51st Annual Conference on Decision and Control, CDC*, Maui, Hawaii, Dec. 2012.

[10] A. Badkoubeh and G. Zhu. Flatness-based deformation control of a 1-dimensional microbeam with in-domain actuation. In *Annual Conference of the IEEE Industrial Electronics Society*, Montreal, QC, Canada, Oct. 2012.

[11] A. Badkoubeh and G. Zhu. A Green's function-based design for deformation control of a microbeam with in-domain actuation. *Journal of Dynamic Systems, Measurment, and Control*, 136(11), Oct 2013.

[12] A. Badkoubeh and G. Zhu. A Green's function-based design for deformation control of a microbeam with in-domain actuation. In *American Control Conference, ACC*, Washington, DC, USA, June 2013. IEEE. Awarded the best paper of the session.

[13] A. Badkoubeh, G. Zhu, and R. Beguenane. Open-loop adapive opics wih closed-loop conrol of deformable mirror. In *International Symposium on Optomechatronic Technologies, ISOT*, pages 1–6, Toronto, ON, Canada, Oct 2010. IEEE.

[14] M.J. Balas. Finite-dimentional control of disturbuted parameter systems by galerkin approximation of infinite dimentional controllers. *Journal of Mathematical Analysis and Applications*, 114:17–36, 1986.

[15] H. T. Banks, R. C. H. Del Rosario, and R. C. Smith. Reduced order model feedback control design: Numerical implementation in a thin shell model. *IEEE Trans. Auto. Contr*, 45(7):1312–1324, 2000.

[16] H. T. Banks, R. C. H. del Rosario, and H. T. Tran. Proper orthogonal decomposition-based control of transverse beam vibration: Experimental implementation. *IEEE Trans. Contr. Syst. Technol.*, 10(5):717–726, 2012.

[17] H. T. Banks, R. C. Smith, and Y. Wang. *Smart Material Structures: Modeling, Estimation and Control.* John Wiley & Sons, Chichester, 1996.

[18] H. T. Banks, Ralph C. Smith, D. E. Brown, R. J. Silcox, and Vern L. Metcalf. Experimental confirmation of a PDE-based approach to design of feedback controls. *SIAM J. Control and Optimization*, 35(4):1263–1296, 1997.

[19] A. Bensoussan, G. Da Prato, M. Delfour, and S. K. Mitter. *Representation and Control of Infinite-Dimensional Systems.* Birkhauser, Boston, 2006.

[20] T. G. Bifano, R. K. Mali, J. K. Dorton, J. Perreault, N. Vandelli, M. N. Horenstein, and D. A. Castanon. Continuous-membrane surface-micromachined silicon deformable mirror. *J. of Opt. Eng.*, 36(5):1354–1360, 1997.

[21] T. G. Bifano, R. K. Mali, J. K. Dorton, J. Perreault, N. Vandelli, M. N. Horenstein, and D. A. Castanon. Continuous-membrane surface-micromachined silicon deformable mirror. *J. of Opt. Eng.*, 36(5):1354–1360, 1997.

[22] C. Blain, O. Guyon, C. Bradley, and O. Lardière. Fast iterative algorithm (FIA) for controlling MEMS deformable mirrors: principle and laboratory demonstration. *Optics Express*, 19(22):21271–21294, 2011.

[23] C. Bonato, S. Bonora, A. Chiuri, P. Mataloni, G. Milani, G. Vallone, and P. Villoresi. Phase control of a path-entangled photon state by a deformable membrane mirror. *J. Opt. Soc. Am. B*, 27(6):A175–A180, 2010.

[24] J. Borggaard, J. Burns, E. Cliff, and S. Schreck (ed.). *Computational Methods for Optimal Design and Control.* Birkhauser, Boston, 1998.

[25] G. Chen, M. C. Delfour, A.M. Krall, and G. Payre. Modeling, stabilization and control of serially connected beams. *SIAM J. Control and Optimization*, 25(3):526–546, 1987.

[26] G. Chen, S G. Krantz, D. L. Russell, C. E. Wayne, H. H. West, and M. P. Coleman. Analysis, designs, and behavior of dissipative joints for coupled beam. *SIAM J. Appl. Math.*, 49(6):1665–1693, 1989.

[27] J. M. Coron. *Control and Nonlinearity*. American Mathematical Society, 2007.

[28] R. Cortez. Numerical methods based on regularized -distributions. Technical report, The University of North Carolina, 2005.

[29] R. F. Curtain and H. J. Zwart. *An Introduction to Infinite-Dimensional Linear System Theory*, volume 12 of *Texts in Applied Mathematics*. Springer-Verlag, NY, 1995.

[30] C. Dafermos and M. Slemrod. Asymptotic behavior of solutions of nonlinear contraction semigroups. *J. Funct. Anal.*, 13(3):97–106, 1973.

[31] R. G. Dekany, M. C. Britton, D. T. Gavel, B. L. Ellerbroek, G. Herriot, C. E. Max, and J.-P. Veran. Adaptive optics requirements definition for tmt. *Proceedings of the SPIE: Conference on Advancements in Adaptive Optics*, 5490:879–890, 2004.

[32] A. Diouf, A. P. Legendre, J. B. Stewart, T. G. Bifano, and Y. Lu. Open-loop shape control for continuous microelectromechanical system deformable mirror. *App. Opt.*, pages 148–154, 2010.

[33] N. Doble and D. R. Williams. The application of MEMS technology for adaptive optics in vision science. *IEEE Journal of Selected topics in Quantum Electronics*, 10(3):629–636, 2004.

[34] N. Doble and D. R. Williams. The application of MEMS technology for adaptive optics in vision science. *IEEE Journal of Selected topics in Quantum Electronics*, 10(3):629–636, 2004.

[35] W. B. Dunbar, N. Petit, P. Rouchon, and Ph. Martin. Motion planning for a nonlinear Stefan problem. *ESAIM: Control, Optimisation and Calculus of Variations*, 9:275–296, August 2003.

[36] B. L. Ellerbroek and C. R. Vogel. Inverse problems in astronomical adaptive optics. *Inverse Problems*, 25(063001):1–41, 2009.

[37] E. J. Fernandez and P. Artal. Membrane deformable mirror for adaptive optics: Performance limits in visual optics. *Optic Express*, 11(9):1056–1069, 2003.

[38] A. Ferreira and S. S. Aphale. A survey of modeling and control techniques for micro- and nanoelectromechanical systems. *IEEE Trans. Syst., Man, Cybern., C*, 41:350–364, 2011.

[39] M. Fliess, Rouchon H., and Rudolph P. A distributed parameter approach to the control of a tubular reactor: a multi variable case. In *Proc. of the 37th Conference on Decision and Control*, 1998.

[40] M. Fliess, J. Lévine, P. Martin, and P. Rouchon. Flatness and defect of nonlinear system introductory theory and examples. *International Journal of Control*, 61:1327–1361, 1995.

[41] M. Fliess, J. Lévine, P. Martin, and P. Rouchon. Flatness and defect of nonlinear systems: Introductory theory and examples. *Int. J. of Control*, 61:1327–1361, 1995.

[42] M. Fliess, J. Lévine, P. Martin, and P. Rouchon. A Lie-Bäcklund approach to equivalence and flatness of nonlinear systems. 44(5):922–937, 1999.

[43] M. Fliess, Ph. Martin, N. Petit, and P. Rouchon. Active restoration of a signal by precompensation technique. In *the 38th IEEE Conf. on Decision and Control*, pages 1007–1011, Phoenix, AZ, Dec. 1999.

[44] R. Fraanje, P. Massioni, and M. Verhaejen. A decomposition approach to distributed control of dynamic deformable mirrors. *Int. J. of Optomechatronics*, 4(3):269–284, September 2010.

[45] R. Fraanje, P. Massioni, and M. Verhaejen. A decomposition approach to distributed control of dynamic deformable mirrors. *Int. J. of Optomechatronics*, 4(3):269–284, 2010.

[46] B. Z. Guo and Y. H. Luo. Controllability and stability of a second-order hyperbolic system with collocated sensor actuator. *System and Control Letters*, 46(5):45–65, 2002.

[47] B. Z. Guo and G. Q. Xu. Riesz bases and exact controllability of c_0-groups with one dimensional input operators. *System and Control Letters*, 52:221–232, 2004.

[48] W. Han and B. D. Reddy. *Plasticity: Mathematical Theory and Numerical Analysis.* Springer, New York, 1999.

[49] B. Jacob and H. Zwart. *Linear Port-Hamiltonian Systems on Infinite-dimensional Spaces.* Birkhauser, 2012.

[50] B. Jocob and H. Zwart. Equivalent conditions for stabilizability of in6nite-dimensional systems with admissible control operators. *SIAM Journal of Control Optim.*, 37:1419–1455, 1999.

[51] B. Jocob and H. Zwart. Exact controllability of $c_0$groups with one dimensional input operators. *Advance in Mathematical Systems Theory*, Basel:221–242, 2001.

[52] A. Kharitonov and O. Sawodny. Optimal flatness based control for heating processes in the glass industry. In *Proc. of the 43rd IEEE Conference on Decision and Control*, pages 2435–2440, Atlantis, Bahamas, 2004.

[53] D. E. Kirk. *Optimal Control Theory: an Introduction.* Prentice-Hall, New Jersey, 1970.

[54] G. T. A. Kovacs. *Micromachined Transducers Sourcebook.* McGraw-Hill, New York, 1998.

[55] M. Krstić. *Delay Compensation for Nonlinear, Adaptive, and PDE Systems.* Birkhuser, 2009.

[56] M. Krstic, B. Guo, A. Balogh, and A. Smyshlyev. Control of a tip-force destablized shear beam by observer-based boundary feedback. *SIAM J. Control Optim*, 47(2):553–574, 2008.

[57] M. Krstić, I. Kanellakopoulos, and P.V. Kokotović. *Nonlinear and Adaptative Control Design.* John Wiley & Sons Ltd, New York, 1995.

[58] M. Krstić and A. Smyshlyaev. *Boundary Control of PDEs: A Course on Backstepping Designs.* SIAM, 2008.

[59] J. Kulakarni, R. D'Andrea, and B. Brandl. Application of disturbuted control techniques to the adaptive secondary mirror of cornell's large atacama telescope. In *Proc. SPIE*, volume 750, Hi, USA, 2003.

[60] J.E. Lagnese, G. Leugering, and E.J.P.G. Schmidt. *Modelling and Controllability of networks of Thin Beam, System Modelling and Optimization.* Lecture Notes in COntrol and Information Science. Springer, 1992.

[61] J.E. Lagnese, G. Leugering, and E.J.P.G. Schmidt. Control of plannar networks of timoshenko beams. *SIAM J. Control Optim.*, 31:780–811, 1993.

[62] J.E. Lagnese, G. Leugering, and E.J.P.G. Schmidt. Modelling of dynamic networks of thin thermoelastic beams. *Math. Methods Applied Science*, 16:327–358, 1993.

[63] G. L. Lamb. *Introductory Application of Partial Differential Equations.* John Wiley and Sons, Inc., New York, 1995.

[64] B. Laroche, Ph. Martin, and P. Rouchon. Motion planning for a class of partial differential equations with boundary control. In *Proc. of the 37th IEEE Conference on Decision and Control*, pages 3494–3497, Tampa, FL, USA, 1998.

[65] B. Laroche, Ph. Martin, and P. Rouchon. Motion planning for the heat equation. *International Journal of Robust Nonlinear Control*, 10:629–643, 2000.

[66] I. Lasiecka. *Mathematical Control Theory of Coupled PDEs.* SIAM, Philadelpia, 2002.

[67] I. Lasiecka and R. Triggiani. *Control Theory for Partial Differential Equations: Volume 1 and Volume 2.* Cambridge Universioty Press, Cambridge, UK, 2000.

[68] P. Le Gall, C. Prieur, and L. Rosier. Output feedback stabilization of a clamped-free beam. *International Jouranal of Control*, 80(8):1201–1216, 2007.

[69] R. J. LeVeque. *Finite Difference Method for Ordinary and Partial Differential Equations Steady-state and Time-Dependent Problems.* SIAM, Philadelphia, 1955.

[70] Jean Lévine. *Analysis and Control of Nonlinear Systems: A Flatness-based Approach.* Springer-Verlag, Berlin, 2009.

[71] Z. Luo, B. Guo, and O. Morgul. *Stability and Stabilization of Infinite Dimensional Systems with Applications.* Springer, London, 1999.

[72] Z. H. Luo, N. Kitamura, and B. Z. Guo. Shear force feedback control of flexible robot arms. *IEEE Trans. on Robot. Auto.*, 11(5):760–765, 1995.

[73] A. F. Lynch and J. Rudolph. Flatness-based boundary control of a class of quasilinear parabolic distributed parameter systems. *Int. J. of Control*, 75(15), 2005.

[74] A. F. Lynch and J. Rudolph. Flatness-based boundary control of a class of quasilinear parabolic distributed parameter systems. *International Journal of Control*, 75(15), 2005.

[75] D. H. S. Maithripala, J. M. Berg, and W. P. Dayawansa. Control of an electrostatic MEMS using static and dynamic output feedback. *ASME J. of Dyn. Syst., Meas. and Contr.*, 127:443–450, 2005.

[76] Ph. Martin, R. M. Murray, and P. Rouchon. Flat systems, equivalence and trajectory generation. Cds technical report, CDS, Caltech, CA, 2003.

[77] P. Massioni and M. Vehaegen. Disturbiuted control for identical dynamically coupled systems: A decomposition approach. *IEEE Trans. on Automatic Control*, 54(4):124–135, 2009.

[78] T. Meurer. *Control of Higher-Dimensional PDEs: Flatness and Backstepping Designs.* Springer, Berlin, 2013.

[79] T. Meurer and A. Kugi. Tracking control for boundary controlled parabolic PDEs with varying parameters: Combining backstepping and differential flatness. *Automatica*, 45(5):1182–1194, 2009.

[80] T. Meurer and A. Kugi. Motion planning for piezo-actuated flexible structures: Modeling, design, and experiment. *IEEE Trans. Contr. Syst. Technol.*, 2012.

[81] T. Meurer, D. Thull, and A. Kugi. Flatness-based tracking control of a piezoactuated Euler-Bernoulli beam with non-collocated output feedback: Theory and experiments. *International Journal of Control*, 81(3):473–491, 2008.

[82] T. Meurer and M. Zeitz. Feedforward and feedback tracking control of nonlinear diffusion-convection-reaction systems using summability methods. *Ind. Eng. Chem. Res.*, 44(8):2532–2548, 2005.

[83] D. Miller and S. Grocott. Robust control of the multiple mirror telescope adaptive secondary mirror. *Opt. Eng.*, 38(8):1267–1287, 1999.

[84] K. Morris. Control of systems governed by partial differential equations. In William S. Levine, editor, *The Control Systems Handbook: Control System Advanced Methods, Chapter 67*, pages 1–37. CRC Press, 2nd edition, 2010.

[85] K. Morzinski, K. Harpsoe, D. Gavel, and S. Ammons. The open-loop control of MEMS: Modeling and experimental results. In *Proc.of SPIE Conf. on MEMS Adaptive Optics*, volume 6467, pages 645–654, CA, USA, 2007.

[86] K. Morzinski, K. Harpsoe, D. Gavel, and S. Ammons. The open-loop control of MEMS: Modeling and experimental results. In *Proc. of SPIE Conf. on MEMS Adaptive Optics*, volume 6467, pages 645–654, CA, USA, 2007.

[87] M. E. Motamedi (editor). *MOEMS: Micro-Opto-Electro-Mechanical Systems*. SPIE Press, 2005.

[88] A. Pazy. *Semigroups of Linear Operators and Applications to Partial Differential Equations*. Applied Mathematical Sciences. 1983.

[89] M. Pederson. *Functional Analysis in Applied Mathematics and Engineering*. Chapman and Hall CRC, 2000.

[90] N. Petit, P. Rouchon, J. M. Boueih, F. Guerin, and P. Pinvidic. Control of an industrial polymerization reactor using flatness. *International Journal of Control*, 12(5):659–665, 2002.

[91] Andrei D. Polyanin. *Handbook of Linear Partial Differential Equations for Engineers and Scientists*. Chapman & Hall/CRC, New York, 2002.

[92] R. Rebarber. Exponential stability of coupled beam with dissipative joints: A frequency domain approach. *SIAM J. Control and Optimization*, 33(1):1–28, 1995.

[93] L. Rodino. *Linear Partial Differential Operators in Gevrey Spaces*. World Scientific, River Edge, NJ, 1993.

[94] J. Rudolph. *Flatness Based Control of Distributed Parameter Systems*. Shaker-Verlag, Aachen, 2003.

[95] S. D. Senturia. *Microsystem Design*. Kluwer Academic Publishers, Norwell, MA, 2002.

[96] L. Sherman, J. Y. Ye, O. Albert, and T. B. Norris. Adaptive correction of depth-induced aberrations in multiphoton scanning microscopy using a deformable mirror. *Journal of Microscopy*, 206(1):65–71, 2002.

[97] H. Sira-Ramirez and S. K. Agrawal. *Differential Flat Systems*. Marcel Dekker Inc., NY, 2004.

[98] J. B. Stewart, A. Diouf, Y. Zhou, and T. G. Bifano. Open-loop control of a MEMS deformable mirror for large-amplitude wavefront control. *J. of the Optical Society of America*, 24(12):3827–3833, 2007.

[99] J. B. Stewart, A. Diouf, Y. Zhou, and T. G. Bifano. Open-loop control of a MEMS deformable mirror for large-amplitude wavefront control. *J. Opt. Soc. Am. A*, 24:3827–3833, 2007.

[100] R. R. A. Syms. Principles of free-space optical microelectromechanical systems. *Proc. of the I MECH E Part C J. of Mech. Eng. Science*, 222(1):1–18, 2008.

[101] S. Timoshenko and S. Woinowsky. *Theory of Plates and Shells*. MacGraw-Hill, NY, 2nd edition, 1959.

[102] S. Timoshenko and S. Woinowsky. *Theory of Plates and Shells*. MacGraw-Hill Book Company, NY, 2nd edition, 1959.

[103] L. N. Trefethen. *Spectral Method in MATLAB*. SIAM, Philadelphia, 2000.

[104] M. Tucsnak and G. Weiss. *Observation and Control for Operator Semigroups*. Birkhauser Verlag AG, Basel, 2009.

[105] R. K. Tyson. *Adaptive Optic Engineering Handbook*. Marcel Dekker, NY, 2000.

[106] E. Ventsel and T. Krauthammer. *Thin Plate and Shells: Theory, Analysis, and Applications*. Marcel Dekker, 2001.

[107] C. R. Vogel and Q. Yang. Modelling, simulation, and open-loop control of a continous facesheet MEMS deformable mirror. *J. of Opt. Soc. Am.*, 23(5):1074–1081, 2006.

[108] C. R. Vogel and Q. Yang. Modelling, simulation, and open-loop control of a continous facesheet MEMS deformable mirror. *J. of Opt. Soc. Am.*, 24(12):3827–3833, 2007.

[109] C. R. Vogel and Q. Yang. Modelling, simulation, and open-loop control of a continous facesheet MEMS deformable mirror. *J. of Opt. Soc. Am.*, 24(12):3827–3833, 2007.

[110] B. Yang. *Stress, Strain, and Structural Dynamics: an Interactive Handbook of Formulas, Solutions, and MATLAB Toolboxes*. Elsevier Academic Press, Burlington, 2005.

[111] G. Zhu. Electrostatic MEMS: Modelling, control, and applications. In J. Lévine and Ph. Mullhaupt, editors, *Advances in the Theory of Control, Signals and Systems with Physical Modeling*, volume 407 of *Lecture Notes in Control and Information Sciences*, pages 113–123. Springer-Verlag, Berlin, 2011.